5-1999

Cenozoic Structural and Stratigraphic Evolution of the Southeastern Salmon Basin, East-Central Idaho

James J. Blankenau
Utah State University

CENOZOIC STRUCTURAL AND STRATIGRAPHIC EVOLUTION OF THE SOUTHEASTERN SALMON BASIN, EAST-CENTRAL IDAHO

by

James J. Blankenau

A thesis submitted in partial fulfillment
of the requirements for the degree

of

MASTER OF SCIENCE

in

Geology

Approved:

UTAH STATE UNIVERSITY
Logan, Utah

1999

ABSTRACT

Cenozoic Structural and Stratigraphic Evolution of the Southeastern Salmon Basin, East-Central Idaho

by

James J. Blankenau, Master of Science

Utah State University, 1999

Major Professor: Dr. Susanne Janecke
Department: Geology

The southeastern Salmon basin (SB) of east-central Idaho is a complex east-dipping half graben containing four unconformity-bounded sequences of Tertiary volcanic, alluvial fan, lacustrine, and fluvial deposits. From oldest to youngest these are the Challis volcanic group, sedimentary rocks of Tendoy (new name), sedimentary rocks of Sacajaweja (new name), and Quaternary-Tertiary deposits. The thick sequence of volcanic rocks was deposited in a southeast-trending paleovalley. New mapping, cross-cutting relationships, $^{40}Ar/^{39}Ar$ age determinations, and angular unconformities show that the SB has experienced at least four episodes of extension, and that it lies in the core of an Eocene to Oligocene rift zone.

The largest episodes of extension in the SB were the second and third episodes of extension. These were responsible for the deposition of the sedimentary rocks of Tendoy and sedimentary rocks of Sacajaweja, respectively. Episode 2 occurred along the west southwest-dipping Agency-

Yearian fault, and can be attributed to gravitational collapse of the Sevier fold and thrust belt between the late middle Eocene and Oligocene (?). Several southwest-dipping low-angle normal faults were active during the third episode and may have been active into early Miocene time. The third episode of extension reflects continued gravitational collapse. Also active during episode 3 was the Salmon basin detachment fault, which is interpreted as a regional detachment based on its lateral extent and low dip angle (11°).

Extensional folds are common in the southeastern Salmon basin and represent at least two generations of folds. Interference between north-northeast and southeast-trending folds locally produced dome and basin features. The folds are typically open to gentle, and have a maximum fold height of 2.2 km. Most of the folds are fault-bend folds, and some are associated with growth strata. The development of the Tendoy anticline and Pattee Creek syncline in the hanging wall of the Agency-Yearian fault produced two depositional basins during the deposition of the sedimentary rocks of Tendoy. Facies patterns and megabreccia deposits in the subbasins indicate that there was considerable topography along the margins of the subbasins. (153 pages)

ACKNOWLEDGMENTS

I would like to thank Jim Evan and Don Fiesinger for their valuable insights and suggestions into this project and for serving as committee members. I thank the Muleshoe ranch, Mark and Ginger Myers, Leroy Bird, Joe Caywood, Gail Andrews, and R. J. Smith for graciously allowing me access to their property, and the Salmon District of the Bureau of Land Management for providing aerial photography of the study area. I also thank Daniel Axelrod (University of California-Davis) for providing unpublished data. Additional thanks to Kim Robeson, Jonathan Lim, Piper Goessel, Colby VanDenburg, Kelly Keighley, and Jeff Evans for their helpful comments. Finally, and most of all I would like to thank Susanne Janecke for her patience, support, and insights into this project. This study was supported by NSF grant EAR93-17395 to Susanne Janecke.

James J. Blankenau

CONTENTS

LIST OF TABLES

LIST OF FIGURES

LIST OF PLATES
(in pocket)

INTRODUCTION AND OBJECTIVES

The Salmon basin is located in east-central Idaho and is bounded by the Beaverhead Range to the northeast, the Salmon River Mountains to the northwest, and Lemhi Range to the south and west (Figure 1). This study focuses on the southeastern portion of the Salmon basin around the town of Tendoy, Idaho. Detailed geologic mapping was conducted in parts of five 7.5 minute quadrangles (Lemhi Pass, Agency Creek, Tendoy, Baker, and Goldstone Mountain quadrangles). Geological mapping and basin analysis were used to determination the structure and Tertiary deformational history of the basin.

The Salmon basin is north of the Snake River Plain, in the Rocky Mountain Basin and Range province, and in the Sevier fold and thrust belt. The basin is in the footwall of the Hawley Creek thrust (Skipp, 1987, 1988), and in the hanging wall of the Miner-Beaverhead Divide reverse or thrust fault, which has since been correlated with the Medicine Lodge thrust (Ruppel, 1978, 1982; Ruppel and Lopez, 1984) and the Cabin thrust (Skipp, 1988). Janecke et al. (in press) argue against correlation with either thrust. Work in progress by Karl Evans of the U.S. Geological Survey may clarify these correlations.

The Salmon basin is superimposed on a large structural culmination that brings Middle Proterozoic metasedimentary rocks of the Belt basin and its equivalents to the surface. The culmination has been interpreted as a paleohigh dating back to Precambrian and Early Paleozoic times (Armstrong, 1975; Ruppel, 1975; Burchfiel et al., 1992) and as a single (Skipp, 1987) or

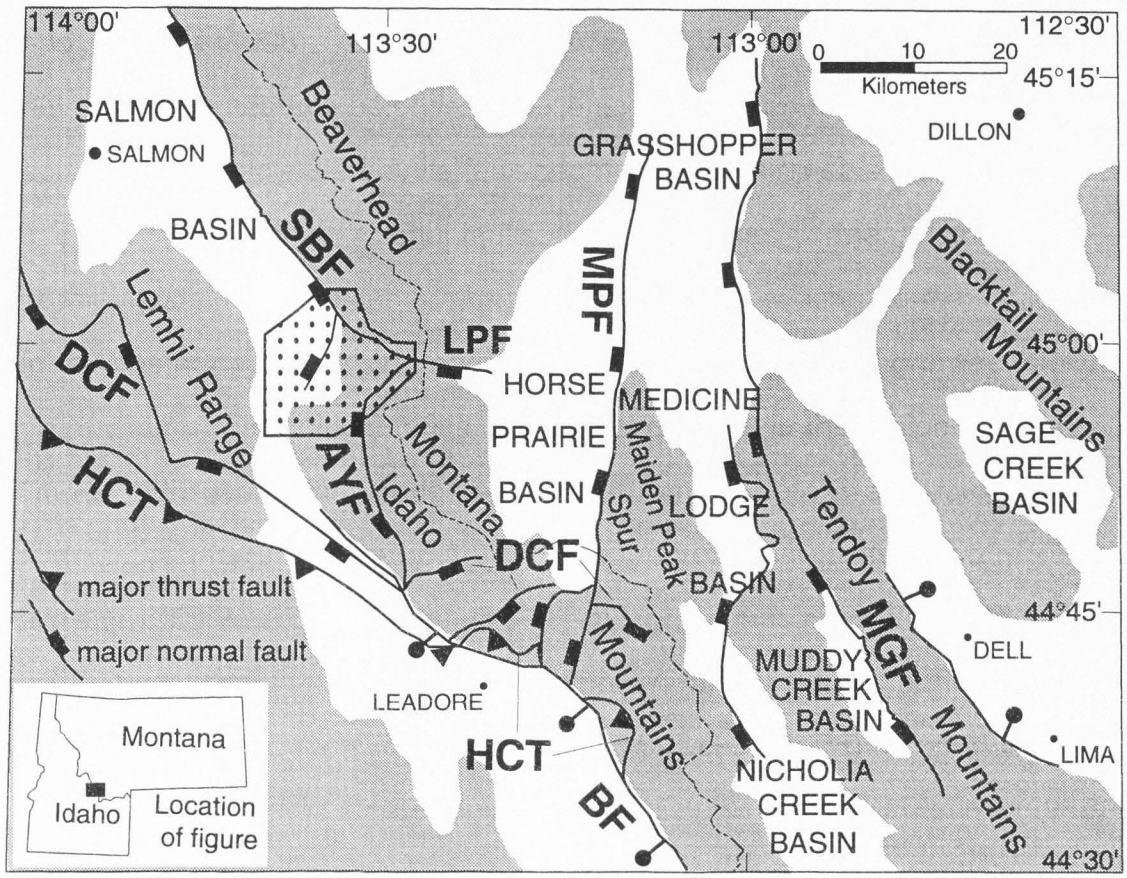

Figure 1. Location map of the southeastern Salmon basin, Idaho. The study area is in the outlined stippled area, and was conducted in parts of the Lemhi Pass, Agency Creek, Tendoy, Baker, and Goldstone Mountain 7.5' quadrangles. SBF=Salmon basin detachment fault, AYF=Agency-Yearian fault, DCF=Divide Creek fault, HCT=Hawey Creek thrust fault, BF=Beaverhead fault, MPF=Maiden Peak fault, MGF=Muddy-Grasshopper fault. Shaded areas are mountain ranges.

multiple (Janecke, unpublished data) structural culmination(s) of the Sevier fold and thrust belt. Paleozoic rocks are preserved only on the flanks of the paleohigh, and are exposed 4.5 km south of the study area along Hayden Creek (Anderson, 1956) and along Reese Creek (Staatz, 1979).

The Salmon basin is east of the Cretaceous Idaho batholith, but a small outlier of the batholith occurs north of the study area in the Beaverhead Range. This outlier, the Carmen stock, is a granodiorite intrusion exposed at the head of Carmen Creek. It has a radiometric ($^{40}Ar/^{39}Ar$) date of 82.4 ± 1.2 Ma and 80.9 ± 1.9 Ma (Kilroy, 1984). The Carmen stock and a rapakivi granite exposed in the Salmon River Mountains northwest of the study area are the area's two most distinctive rock types. The rapakivi granites intrude Precambrian quartzites of the Lemhi Group (Anderson, 1956) and the Yellowjacket Formation (Ruppel, 1975; Ruppel et al., 1993) and are 1370 Ma (Evans, 1981; Evans and Zartman, 1988). Clasts derived from the rapakivi granite occur locally in the study area, and help delineate part of a paleovalley of late Mesozoic to middle Eocene age (Janecke et al., in press).

The Salmon basin is a structurally complex half-graben that contains middle Eocene volcanic rocks that have been correlated with the Challis volcanic group, and younger sedimentary rocks (Anderson, 1956; Tucker, 1975; Staatz, 1979; Fritz and Harrison, 1985; Harrison, 1985). Previous mapping showed that the Salmon basin has a triangular shape in plan view, due to basinward dipping normal faults on its western and northeastern sides, and that few faults repeat units within the basin (Anderson, 1956, 1957, 1959, 1961; Harrison, 1985; Ruppel et al., 1993).

The basin-bounding faults have exposed gray Middle Proterozoic feldspathic quartzites, pure quartzites, and argillites of the Yellowjacket Formation and the Lemhi Group (Anderson 1956, 1957, 1959, 1961; Ruppel, 1975; Staatz, 1979). Middle Proterozoic rocks have been estimated to be over 12,000 meters thick in the Beaverhead Mountains (Hansen, 1983), and these were mapped as the Gunsight, Apple Creek , and Yellowjacket formations in the field area (Staatz, 1979).

The basin fill includes volcanic and sedimentary rocks. The volcanic sequence in the southeastern Salmon basin is very complex and was erupted at the northeastern margin of the Challis volcanic field (Anderson, 1956; Tucker, 1975; Staatz, 1979; Harrison, 1985). Challis volcanism occurred between 51 and 45 Ma in the region (Fisher et al., 1992; Janecke and Snee, 1993; M'Gonigle and Dalrymple, 1996), and a proposed modern analogy for the Challis volcanic field and topography is Mt. St. Helens, Washington (Fritz and Harrison, 1985). This analogy has been disputed by Janecke and Snee (1993), who suggested that there was subdued paleotopography at the end of peak volcanism. Janecke et al. (in press), however, argue that preexisting erosional topography influenced the distribution of volcanic rocks early during Challis volcanism.

Anderson (1956) initially described the volcanic and sedimentary sequences of the Salmon basin, but his descriptions were incomplete and very generalized. Staatz (1979) improved upon Anderson's (1956) descriptions, and was the first to describe and map the many different types of volcanic rocks within the area. Staatz (1979) also described a major

angular unconformity between older and younger Challis volcanic rocks. VanDenburg (1997) confirmed many aspects of Staatz's (1979) descriptions of volcanic rocks but described some additional units, including a lithic-rich tuff and a volcaniclastic sandstone. This paper builds upon Staatz's (1979) descriptions. Ruppel et al. (1993) discovered a caldera to the northwest of the study area in the Withington Creek area of the northern Lemhi Mountains, but mapped all the volcanic rocks inside and outside the caldera as undifferentiated Challis volcanic rocks. M'Gonigle and Dalrymple (1996) dated several key tuffs in the sequence using $^{40}Ar/^{39}Ar$ single crystal laser methods.

The nature and significance of the sedimentary rocks in the Salmon basin have been controversial despite 40 years of study. Anderson (1956, 1957, 1959, 1961) interpreted the sedimentary basin fill deposits to have been deposited in four distinct depositional episodes and to lie in angular unconformity on Challis volcanic rocks. Harrison (1985), like Ross (1962, 1963), challenged this interpretation and instead concluded that the Tertiary sedimentary rocks in the basin were deposited as one continuous sequence during a single episode of extension that was contemporaneous with the end of Middle Eocene volcanism. Staatz (1979) lumped all sedimentary rocks together in the eastern part of the present study area and stated that these sedimentary rock were separated from the underlying Challis volcanic rocks by an angular unconformity. Staatz (1979) inferred an Oligocene age for the fine-grained sedimentary rocks along Cow Creek southeast of the study area, but stated that these sedimentary rocks could range in age from late Eocene

to Pliocene. Tucker and Birdseye (1989) described a thick sequence of conglomerates along Kenney Creek and concluded that these deposits were synvolcanic alluvial fan deposits that predated formation of the Salmon rift basin. Like Harrison, Tucker and Birdseye (1989) thought the sedimentary rocks were middle Eocene.

To the north of the study area Harrison (1985) interpreted the Salmon basin as a full-gaben that resulted from the superposition of an east-northeast tilted half-graben on a slightly older west-dipping half-gaben. Faulting continued along the eastern margin long after faulting stopped along the western margin. Unlike Tucker and Birdseye (1989), Harrison (1985) interpreted conglomerates on the northeast and west sides of the Salmon basin as syntectonic to normal faulting. Previous workers have made three observations in the southeastern Salmon basin: 1) rock units in the basin generally get younger to the northeast, 2) rocks have an overall dip to the east-northeast, and 3) the basin is bounded on its northeastern side by a major fault (Anderson, 1956, 1957, 1959, 1961; Tucker, 1975; Staatz, 1979). These observations indicate a half-graben rather than a full-graben geometry. We will demonstrate that Harrison's (1985) model of a full-graben is inaccurate for the southeastern Salmon basin using structural and sedimentological data.

Because previous studies have had a lack of emphasis on the structure of the basin, a true understanding of the basin's evolution has not been achieved. Anderson (1956, 1957, 1959, 1961) identified very few faults in his studies, but did note other structural features. One of the most unusual

is the presence of folded Cenozoic sedimentary and volcanic rocks in the Salmon basin. Because folds are generally considered to be rare in extensional settings, they are a particular focus of this study. This paper will examine some of the largest folds in the basin, determine the mechanisms which allowed for their formation during extension, and discuss the importance of the folds in the basin's evolution.

Although many of the early workers in the Salmon basin interpreted the basin-bounding faults as high-angle normal faults (Anderson, 1956, 1957, 1959, 1961; Tucker, 1975; Harrison, 1985), their descriptions of the faults suggest a low-angle geometry. Tucker (1983) described a small portion of the basin-bounding fault as having a southwesterly dip of only 10-20° and as reactivating a preexisting thrust fault. Tucker and Birdseye (1989) also described mylonitic fault rocks along this fault surface. Tucker (1975) mapped other parts of the basin-bounding fault as a series of northwest-striking, southwest-dipping, high-angle normal faults offset by right-lateral northeast-striking, strike-slip faults. This study presents field evidence that the basin-bounding fault (the Salmon basin detachment fault) is instead a continuous and regionally extensive low-angle normal fault and that many of the area's other normal faults also have a low dip angle.

Other workers have documented multiple episodes of Cenozoic extension in the adjacent areas (Janecke, 1992, 1994, 1995; Fritz and Sears, 1993; VanDenburg et al., 1996; VanDenburg, 1997), and it is likely that the Salmon basin has experienced a similar complex deformational history. Janecke (1992, 1994, 1995), Fritz and Sears (1993), VanDenburg

and Janecke (1996), VanDenburg (1997), and VanDenburg et al., (1998) have documented five episodes of extension in surrounding basins. Each episode is characterized by its fault geometry. The first episode of extension has southwest-dipping normal faults, the second has northeast-striking normal faults, the third has north to north-northwest-striking normal faults, the fourth has northeast-striking normal faults, and the fifth has northwest-striking normal faults. The oldest faults (southwest-dipping) in the region are pre-Challis faults which may have been active from the Late Cretaceous to middle Eocene (VanDenburg, 1997), and the youngest faults in the region are active Basin and Range faults. A similar history is possible in the Salmon basin, because Staatz (1979) mapped both northwest- and northeast-striking faults along Agency and Pattee Creeks, and Tucker (1975) mapped them along Wimpey Creek and Kenney Creek. This study tests Harrison's (1985) model to determine whether the basin has undergone one or multiple episodes of extension, by examining the sedimentary basin fill and structural relationships in the southeast part of the Salmon basin.

This study incorporates new $^{40}Ar/^{39}Ar$ age determinations and previously obtained dates from the volcanic and sedimentary sequence with structural data to help constrain the timing of volcanism and extensional deformation. Discontinuous exposures, and a lack of dateable material or datable fossils in the sedimentary sequence provided obstacles in dating, so structural information was key in the reconstruction of the Tertiary deformational history of the southeastern Salmon basin.

The age of volcanism and sedimentation in the Salmon basin has been debated recently, and prior to this study only four K/Ar and four $^{40}Ar/^{39}Ar$ age determinations constrained the age of the Tertiary rocks there (Axelrod, 1968, unpublished data; Staatz, 1979; Harrison, 1985; Tucker and Birdseye, 1989; Table 1). Of these dates, three are from rocks of the volcanic sequence and five are described as being from tuffs interbedded in the sedimentary sequence. The validity of most of these age determinations is in question, however, because 1) sample localities are only approximately given, 2) dates are in apparent conflict with more recent isotopic age determinations, and/or 3) rocks or minerals of the Challis Volcanic Group were inadvertently used to date the overlying sedimentary rocks (Table 1). Table 1 summarizes the previous age determinations. Table 2 contains $^{40}Ar/^{39}Ar$ dates obtained from correlative ash-flow tuffs in adjacent basins (M'Gonigle and Dalrymple, 1993; VanDenburg, 1997). Along with radiometric dates, ages obtained from fossil flora in the basin-fill sedimentary rocks were used to determine the age of sedimentation in the southeastern Salmon basin (Wolfe and Wehr, 1987; Axelrod unpublished data).

The Salmon basin was chosen as a study area because it lies at the core of a proposed Eocene to Oligocene rift zone of Janecke (1994; Figure 2) and west of the complexly deformed Horse Prairie half-graben (VanDenburg, 1997; VanDenburg et al., 1998). The Paleogene rift zone was well studied to the south (Janecke, 1994) and east (VanDenburg, 1997), but not in the Salmon basin where the age and geometry of extension were incompletely known prior to this study. The proposed rift zone is characterized by

TABLE 1. AGE DETERMINATIONS FROM PREVIOUS WORKERS IN THE SALMON BASIN

Sample from	Age (Ma)	Location (latitude / longitude	Reference	Reliable ?
Undifferentiated Challis rocks	46.7±1.4*	4 miles south of Salmon	Axelrod, 1968	Maybe, 1
Brecciated rhyolite tuff at the base of sedimentary rocks of Tendoy	41.1±1.6*	McDevitt Creek (44°56'00" / 113°38'15")	Harrison, 1985	No, 1, 2, 3b
Thin tuff interbedded in shales along Cow Creek	46.5†	Road cut along Cow Creek (44°55'33" / 113°33'00")	Axelrod, written comm.	No, 1, 3a, 4
Tuff of Curtis Ranch	42*	3500 ft northeast of the mouth of Sharky Creek (44°57'33" / 113°32'35")	Staatz, 1979	No, 2
Thin tuff interbedded in sedimentary rocks of Sacajaweja	44.2±1.7*	Kenney Creek (45°2'20" / 113°37'15")	Tucker and Birdseye, 1989	No, 2, 3a
Thin tuff interbedded in bentonite shales in the Snook bentonite quarry at the mouth of Haynes Creek (sedimentary rocks of Tendoy ?)	30.60 ± 0.07†	Haynes Creek (45°1'12" / 113°40'45")	Axelrod, 1998	Yes, 5
White tuff in undifferentiated Challis rocks	46.5†	West of Salmon	Axelrod, written comm.	Maybe, 4, 1

Notes: * = K/Ar age determination

† = $^{40}Ar/^{39}Ar$ age determination

1 = Sample locality is only approximately given.

2 = Date is in apparent conflict with more recent isotopic age determinations.

3 = rocks or minerals of the Challis Volcanic Group may have been used to date the overlying sedimentary rocks. Reworked material (3a) or volcanic material in a younger megabreccia deposit (3b) may have been dated.

4 = Unpublished data

5 = Sample from same sedimentary unit as previous age determination. Source of 5.3 my discrepancy is uncertain.

TABLE 2. AGE DETERMINATIONS FROM PREVIOUS WORKERS IN ADJACENT BASINS

Rock unit	Age (Ma)	Method	Source	Sample number
Quartzite-bearing ash-flow tuff (Tqt)	48.64 ± 0.33	$^{40}Ar/^{39}Ar$ single crystal, sanidine	M'Gonigle and Dalrymple, 1996	5 (Tcq)†
Vitric tuff of Lemhi Pass (Tcvt)	48.04 ± 0.43	$^{40}Ar/^{39}Ar$ single crystal, sanidine	M'Gonigle and Dalrymple, 1996	8 (Tcl)†
Lithic-rich tuff (Tclt)	49.37 ± 0.66	$^{40}Ar/^{39}Ar$ single crystal, sanidine	VanDenburg et al., 1998	3*
Biotite tuff (Tcbt)	48.94 ± 0.17	$^{40}Ar/^{39}Ar$ single crystal, sanidine	VanDenburg et al., 1998	4*
Quartz-sanidine ash-flow tuff (Tqs)	46.01 ± 0.39	$^{40}Ar/^{39}Ar$ single crystal, sanidine	M'Gonigle and Dalrymple, 1996	11 (88-59)†
Rock slide deposit derived from lavas of Challis volcanic Group	47.56 ± 0.59	$^{40}Ar/^{39}Ar$ whole rock	VanDenburg et al., 1998	7*
Tuff of Curtis ranch (Tcr)	47.53 ± 0.13	$^{40}Ar/^{39}Ar$ single crystal, sanidine	VanDenburg et al., 1998	5*
Tertiary intrusion (Tbi)	47.51 ± 0.42	$^{40}Ar/^{39}Ar$ single crystal, sanidine	VanDenburg et al., 1998	8*

Notes: * = Sample numbers from VanDenburg et al.,1998.
† = Sample numbers from M'Gonigle and Dalrymple, 1996.

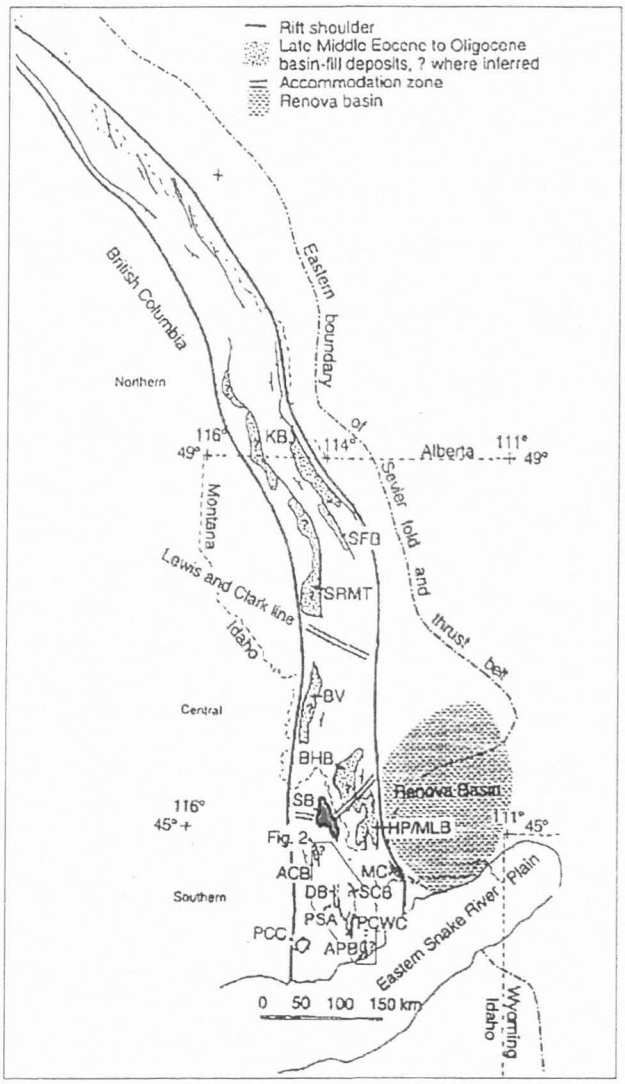

Figure 2. Elements of a hypothesized Eocene to Oligocene rift zone (Janecke, 1994). Salmon basin is outlined in red and denoted by SB. Abbreviations are: ABC = Allison Creek; APB = Arco Pass basin; BHB = Big Hole basin; BV = Bitterroot Valley; DB = Donkey Hills; HP/MLB = Horse Prairie and Medicine Lodge basin; KB = Kishenehn basin; MC = Muddy Creek; PCC = Pioneer core complex; PCWC = Pass Creek/Wet Creek; SB = Salmon basin; SC = Sawmill Canyon; SFB = South Fork basin; SRMT = southern Rocky Mountain Trench.

dominantly east-tilted half-grabens and extension that continued after volcanism (Janecke, 1994). The driving force for this phase of extension is thought to be the gravitational collapse of the Sevier fold and thrust belt (Janecke, 1992, 1994). If the rift model is correct, then gravitational collapse was contemporaneous from British Columbia to Nevada. The examination of the Tertiary extensional history, paleogeographical data, and structural and spatial relationships in the Salmon basin will be used to test and further refine the rift hypothesis (see also VanDenburg, 1997).

Constenius (1996), in an analysis of initial Cenozoic extension in the Cordilleran foreland fold and thrust belt, supported the theory that extension was driven by gravitational collapse, argued that the onset of extension began shortly after the end of contraction, and that most normal faults reactivate preexisting thrust faults. Constenius (1996) implied that the first normal faulting to affect the region after contraction was the north to north-northwest striking rift-bounding faults including those in Figure 2, but other workers have documented an earlier episode of northwest-southeast extension during Challis time (middle Eocene) in southwestern Montana and east-central Idaho (McIntyre et al., 1982; Fisher et al., 1992; Janecke, 1992; Snider, 1995). Recently an even older episode of extension was documented along the Divide Creek fault (VanDenburg, 1997; VanDenburg et al., 1998) and along southwest-dipping normal faults in the northern Lemhi Range (Tysdal, 1996a, 1996b; Tysdal and Moye, 1996). This study will lend insight to the timing of initial extension in the region.

This thesis addresses five poorly understood tectonic issues concerning the Salmon basin. The goals of this study were to document the geometry and lateral extent of normal faulting, to investigate the causes and significance of folds during extension, clarify the timing and episodicity of extension, and to apply models of sedimentation in rift basins to better understand how sedimentation occurs in rift basins. The fifth goal was to test whether the Salmon basin was formed in a rift zone of Eocene to Oligocene age, as predicted by Janecke's rift model, and to determine whether extension in the region was driven by gravitational collapse or by thermally driven extension. These five goals were addressed using structural and sedimentological evidence gathered from detailed field work and from them a clearer picture of the Cenozoic deformational history of the Salmon basin was drawn.

STRATIGRAPHY

The southeastern Salmon basin contains four unconformity-bounded sequences of Tertiary rocks, which overlie a thick sequence of Middle Proterozoic quartzites (Figure 3). This study focuses on the Tertiary stratigraphy, so descriptions of pre-Tertiary rock will not be emphasized. The Tertiary rocks are subdivided into 1) middle Eocene Challis volcanic rocks and 2) younger sedimentary rocks. The younger sedimentary rocks can be subdivided into three unconformity-bounded sequences. Because the Tertiary rocks are extremely variable in thickness and lithology from place to place, several correlation charts are presented to describe the stratigraphy in each subregion of the study area (Figure 3). In order to determine the structural evolution of the Salmon basin, it is critical to examine its statigraphy. In the following I describe the stratigraphy of the southeastern Salmon based on contact mapping and field descriptions.

METHODS

Contact mapping and field descriptions was the primary data collected in the field. Field descriptions of rocks included recording rock type, crystal content, crystal size, fresh color, degree of welding, clast content, clast size, clast shape, sorting, presence of sedimentary structures, and nature of contacts. Each of the different rock types was sampled for further compositional and thin section analysis, and for $^{40}Ar/^{39}Ar$ age determinations by William McIntosh of the New Mexico Geochronology laboratory, Socorro, New Mexico.

Figure 3. Stratigraphic correlation columns of Cenozoic rocks in the southeast Salmon basin. Columns represent different regions of the study area. Relative thickness of the different rock units are shown. QTg = Quaternary Tertiary gravel; Tcg4 = Sedimentary rocks of Sacajaweja; Tss = Tertiary sandstone; Tsh = Tertiary shale; Tcg3 = conglomerate facies of the sedimentary rocks of Tendoy; Ts = sedimentary rocks of Sharky Creek; Ti = intrusion; Tmb = megabreccia deposits, parentheses indicate source of the deposits; Tqs2 = younger quartz-sanidine ash-flow tuff; Tcr = tuff of Curtis Ranch; Tl = Challis lava; Tcs = Challis sandstone; Tt = white tuff; Tgt = green tuff; Tqs1 = older quartz-sanidine ash-flow tuff; Tldac= dacite lava; Tlt = lithic rich tuff; Tcg2 = granite-clast conglomerate; Taf = airfall tuff; Tcto = Challis older undifferentiated tuff; Tqt = quartzite-bearing ash-flow tuff; Tcg1 = basal conglomerate; Y = middle Proterozoic quartzite

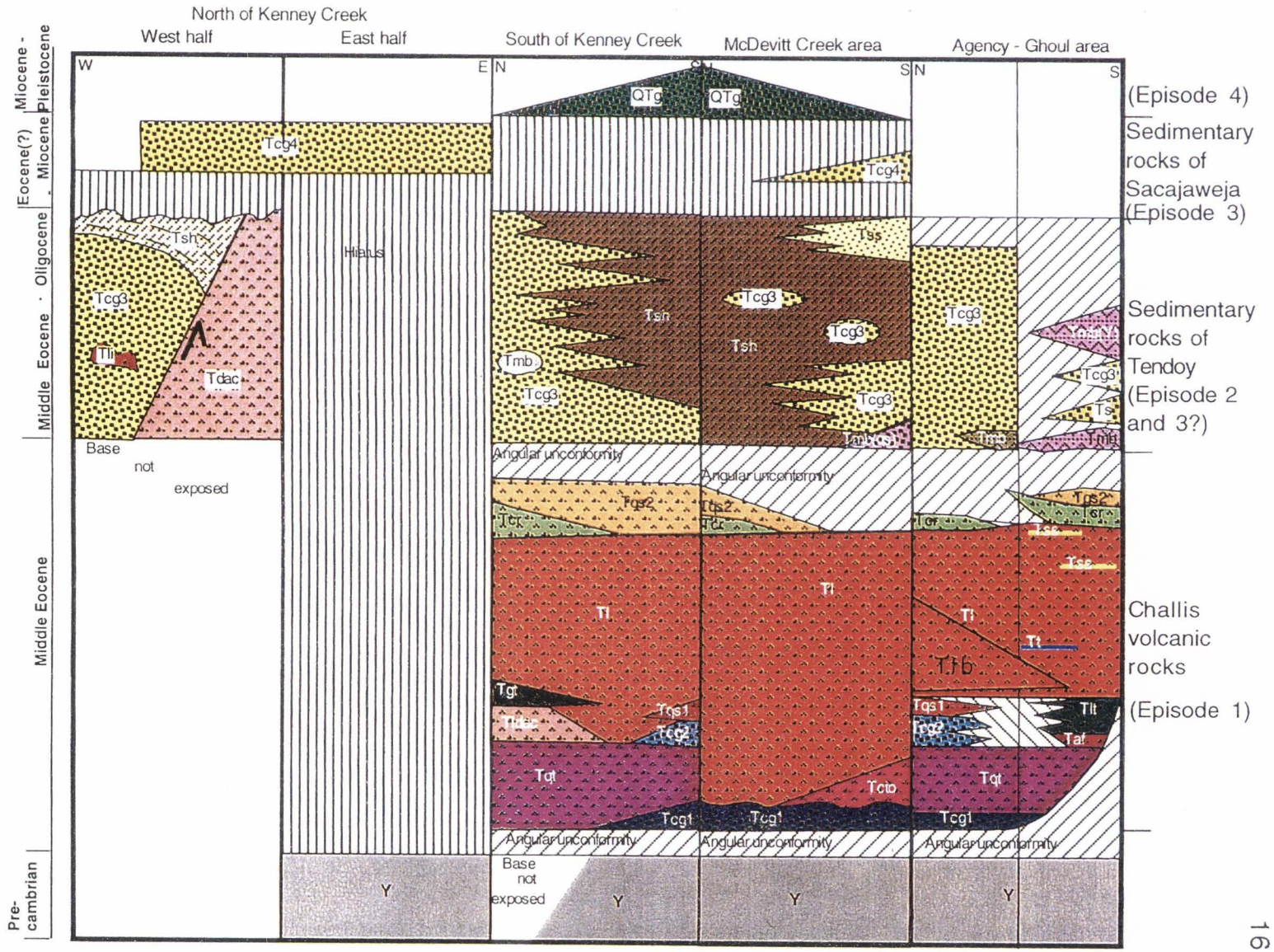
North of Kenney Creek
West half
East half
South of Kenney Creek
McDevitt Creek area
Agency - Ghoul area
W
E
N
S
N
S
Miocene - Pleistocene
Eocene(?) - Miocene
Middle Eocene - Oligocene
Middle Eocene
Pre-cambrian
(Episode 4)
Sedimentary rocks of Sacajaweja (Episode 3)
Sedimentary rocks of Tendoy (Episode 2 and 3?)
Challis volcanic rocks
(Episode 1)
QTg
Tcg4
Tsh
Tcg3
Tli
Tdac
Base not exposed
Hiatus
Tss
Tmb
Angular unconformity
Tqs2
Tcr
Tsic
Tl
Tlb
Tqt
Tqs1
Tcg2
Tcg1
Tlt
Taf
Tcto
Base not exposed
Y

Map data, lithologic descriptions, and the previous stratigraphic work of Staatz (1979) and VanDenburg (1997) were used to construct four stratigraphic columns for the southeast Salmon basin (Figure 4). Common lithological units [quartzite-bearing ash-flow tuff (Tqt), lava flows (Tl), tuff of Curtis Ranch (Tcr), and younger quartz-sanidine ash-flow tuff (Tqs2)] can be correlated between the three columns.

MIDDLE PROTEROZOIC QUARTZITES (Y)

The oldest rocks in the region are Precambrian micaceous and feldspathic quartzites, argillites, and some interbedded siltites (Staatz, 1979). These slightly metamorphosed sedimentary rocks have been mapped as the Yellowjacket, Gunsight, Apple Creek, and Big Creek Formations in the region (Anderson, 1956; Staatz, 1979; Hansen, 1983). The dominate unit in the study area is the Apple Creek Formation according to correlations of Link et al., 1993; P. K. Link, pers. comm., 1997. It is characterized by a light gray micaceous, fine to medium grained, thinly bedded quartzite, but further work is need to accurately map and differentiate the Precambrian rock units. Middle Proterozoic sedimentary rocks were not differentiated in this study.

CENOZOIC ROCKS

Challis volcanic rocks

The Challis volcanic rocks in the Salmon basin are dominantly rhyolitic ash-flow and ash-fall tuffs, and andesitic lavas flows, with interbedded conglomerates, sandstones, and breccia deposits. Lava flows

Figure 4. Distribution of Challis volcanic rocks in the southeast Salmon basin. Simplified map of plate 1.

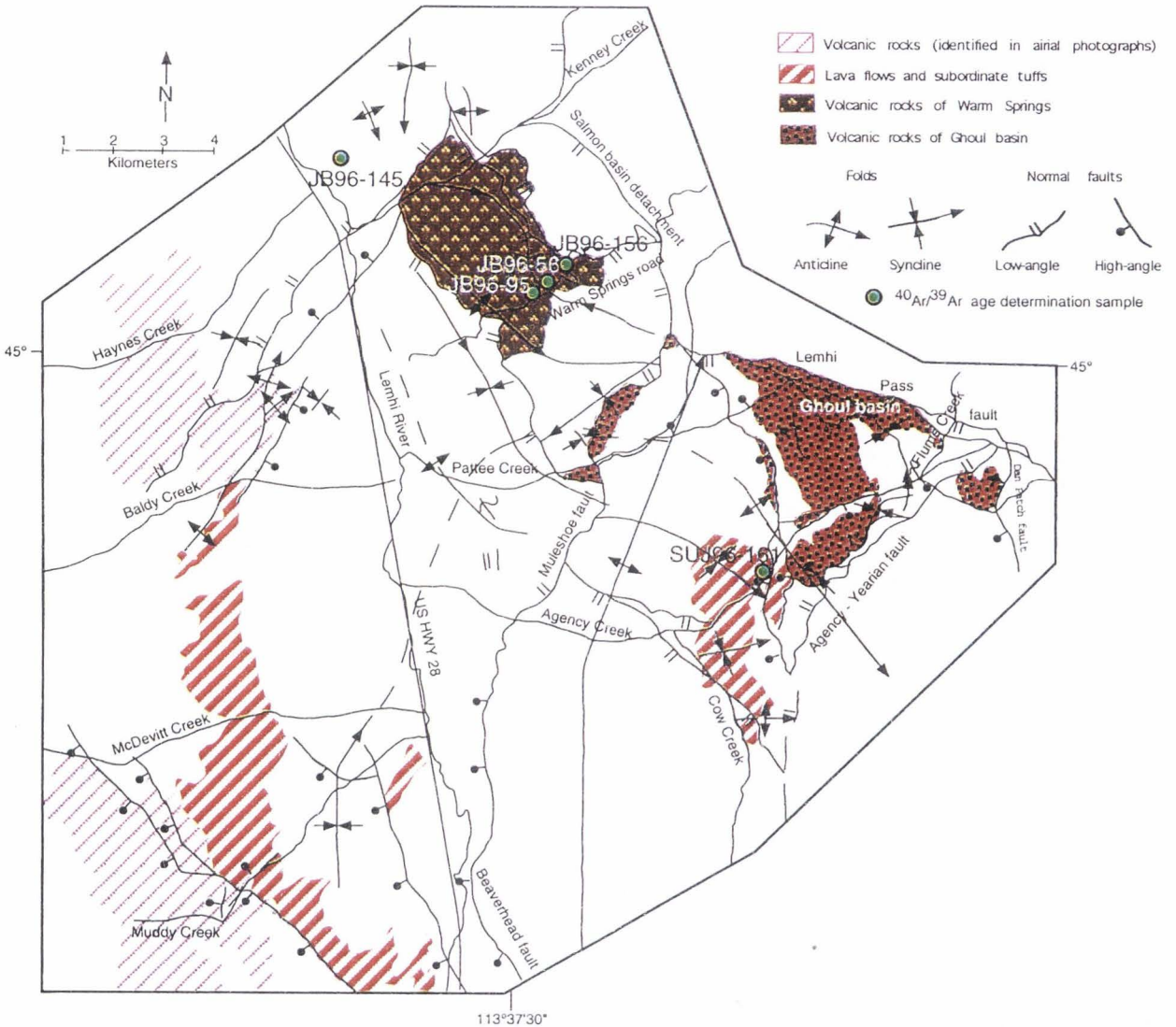
Volcanic rocks (identified in airial photographs)
Lava flows and subordinate tuffs
Volcanic rocks of Warm Springs
Volcanic rocks of Ghoul basin
Folds
Normal faults
Anticline
Syncline
Low-angle
High-angle
40Ar/39Ar age determination sample
N
1 2 3 4
Kilometers
JB96-145
JB96-156
JB96-56
JB96-95
SU96-161
Kenney Creek
Salmon basin detachment
Warm Springs road
Haynes Creek
Baldy Creek
Lemhi River
Pattee Creek
Muleshoe fault
Lemhi Pass
Ghoul basin
fault
Agency Creek
US HWY 28
Agency - Yearian fault
Cow Creek
McDevitt Creek
Muddy Creek
Beaverhead fault
45°
45°
113°37'30"

dominate the southwest portion of the study area from Baldy Creek to south of Muddy Creek (Figure 4). In the area between Kenney Creek and Ghoul basin, thick continuous sections of volcanic rocks are exposed. The volcanic rocks pinch out to the south of Agency Creek and are faulted out to the north by the Lemhi Pass fault. The Challis volcanic rocks in the study area display great thickness and lithologic variability. Because of this variability, the study area has been divided into three subregions for descriptive purposes. The three subregions are around Ghoul basin, McDevitt Creek, and south of Kenney Creek (Figure 4). The volcanic rocks represent a continuous sequence, and the angular unconformity described by Staatz (1979) in the volcanic rocks was not present.

Basal conglomerate (Tcg1). The oldest Tertiary rocks occurring in the study area are the basal conglomerates which unconformably overly Precambrian quartzites. This unit is probably middle Eocene in age, and has been previously described by Anderson (1956), Staatz (1979), and VanDenburg (1997). The basal conglomerate contains subrounded to rounded pebbles and cobbles, in a fine white to gray ash matrix. This clast-supported conglomerate contains 100% quartzite clasts, averaging 25 cm in diameter, and rare boulders up to 2 m in diameter are also present. The unit varies from strong to poorly cemented, and its base is typically more strongly cemented than the top. This unit is very thin (15 m thick) and only occurs in scattered outcrops between Baldy Creek and McDevitt Creek; to the south of

Muddy Creek; in section 11 of T19N, R24E; and in section 7 of T19N, R25E (Plate 1). On the eastern side of the field area the unit is typically present beneath the overlying quartzite-bearing ash-flow tuff, but this is not the case on the western and southwestern sides of the field area where it locally underlies lava flows. The basal conglomerate weathers to a distinctive red color on the western and southwestern side of the field area.

Quartzite-bearing ash-flow tuff (Tqt). The basal conglomerate is conformably overlain by the quartzite-bearing ash-flow tuff. This tuff is white, pinkish red, white gray, or pink gray, and contains abundant black quartzite clasts, and lesser amounts of smoky quartz, sanidine, and plagioclase in a white ash matrix. Typical quartzite lithics resemble the Apple Creek and Yellowjacket formations, and are dark gray to black, angular, micaceous, and 2-4 cm across, but are locally up to 20 cm across. The quartzite-bearing ash-flow tuff is typically poorly welded, but may be densely welded typically of pinker color in these regions. It has a maximum thickness of 430 m along section C-C' (Plate 2). The spatial distribution of the quartzite-bearing ash-flow tuff indicates that it was confined to an east southeast-trending paleovalley. The quartzite-bearing ash-flow tuff pinches out to the south and is cut to the north by the Lemhi Pass fault. It crops out between Kenney Creek and Warm Springs road in sections 21, 28, 29, 32, 33, and 38 of T 20 N, R 24 E; near Pattee Creek in sections 1, 2, 10, and 11; and near Agency Creek in sections 7, 15, 16, 18, and 19 of T 19 N, R 25 E (Plate 1). An

$^{40}Ar/^{39}Ar$ age determination on single sanidine crystals yielded a mean age of 48.64 ± 0.33 Ma for the quartzite-bearing ash-flow tuff near Lemhi Pass (Table 2; M'Gonigle and Dalrymple 1993, 1996). A caldera in the northern Lemhi Range (Ruppel et al., 1993) was probably the source for this tuff. The distinctive quartzite lithics in this unit support a source caldera in the northern Lemhi Range where the widely exposed Yellowjacket Formation could have provided the black lithics. An $^{40}Ar/^{39}Ar$ age obtained from a quartzite-bearing ash-flow tuff in the caldera along Withington Creek yielded an age of 49.51±0.14 Ma (sample SUJ96-131, Table 3; Figure A1). This age is somewhat older than other dates obtained from the quartzite bearing ash-flow tuff by M'Gonigle and Dalrymple (1996).

Granite-clast conglomerate (Tcg2). The granite-clast conglomerate correlates with the Conglomerate of Flume Creek of Staatz (1979), but has been renamed for this study, because Staatz (1979) included a younger, unrelated conglomerate (Tcg3 of this study) along Flume Creek in the unit. The new name, granite-clast conglomerate, was selected because the conglomerate contains distinctive clasts of Proterozoic porphyritic rapakivi granite derived from approximately 20 km to the north-northwest of the study area in the Salmon River Mountains (VanDenburg et al., 1998; Evans and Zartman, 1990). The granite-clast conglomerate is a poorly sorted, well rounded, cobble and boulder gravel directly overlying the quartzite-bearing ash-flow tuff. Middle Proterozoic quartzite clasts are the

TABLE 3. NEW AGE DETERMINATIONS FROM THE SOUTHEASTERN SALMON BASIN

Sample number	Rock type	Location (latitude / longitude)	Method	Age Ma	Comments
JB96-156	lava flow or shallow intrusive	Sect. 34; R24E; T20N (45°1'17" / 113°35'51")	$^{40}Ar/^{39}Ar$ step-heating of a groundmass concentrate	36.85 ±0.16	highly disturbed; unreliable
JB96-95	tuff of Curtis Ranch (Tcr)	Sect. 34; R24E; T20N (45°0'21" / 113°36'25")	$^{40}Ar/^{39}Ar$ single sanidine crystals	47.58 ±0.14	excellent age determination
JB96-56	quartz sanidine ash-flow tuff 2 (Tqs2)	Sect. 34; R24E; T20N (45°0'26" / 113°39'32")	$^{40}Ar/^{39}Ar$ single sanidine crystals	46.13 ±0.19	reliable; same unit as SUJ96-161
JB96-145	intrusion (Ti) into Tcg3	Sect. 30; R24E; T20N (45°1'58" / 113°39'32")	$^{40}Ar/^{39}Ar$ step-heating of a groundmass concentrate	37.08 ±0.21	intrudes Tcg3; highly disturbed spectrum; unreliable
SUJ96-161	quartz sanidine ash-flow tuff 2 (Tqs2)	Sect. 19; R25E; T19N (44°57'33" / 113°32'30")	$^{40}Ar/^{39}Ar$ single sanidine crystals	45.95 ±0.12	reliable; same unit as JB96-56
SUJ96-131	Densely welded rhyolite tuff*	Sect. 19; R23; T20N (45°2'35" / 113°47'24")	$^{40}Ar/^{39}Ar$ single sanidine crystals	49.51 ±0.14	in Withington Creek caldera; excellent age determination

Notes: Age spectrum graphs of the age determinations are shown in Appendix A.

* = Ash-flow tuff with lithics of Yellowjacket Formation which may correlate wtih the quartzite-bearing ash-flow tuff (Tqt).

dominate clast type, and well rounded granite clasts are present, some being greater than 2.5 m in diameter. Bands of the older quartz-sanidine ash-flow tuff (Tqs1) are interbedded with the granite-clast conglomerate. These bands may represent small intermittent eruptions from the same caldera responsible for the deposition of the overlying older quartz-sanidine ash-flow tuff, or megabreccias derived from a quartz-sanidine ash-flow tuff that was deposited after the quartzite-bearing ash-flow tuff and has since been eroded. The granite-clast conglomerate has a maximum thickness of 170 m along section D-D' (Plate 2). It is exposed only in the eastern portion of the field area (sections 7, 18, and 15 of T 19 N, R 25 E, and section 11 of T 19 N, R 24 E; Plate 1), and is absent from the equivalent stratigraphic position in a thick sequence of the Challis volcanic group south of Kenney Creek. The granite-clast conglomerate is exposed to the east, east of Lemhi Pass (Staatz, 1979), and in the Horse Prairie basin (VanDenburg, 1997).

Air-fall tuff (Taf). The air-fall tuff is one of the tuffs present south of the pinch-out of the granite-clast conglomerate. This is a white, light gray, and light pink, air fall, fine-grained, moderately welded tuff. It contains crystals of biotite (< 2 mm) and plagioclase (< 1 mm). The air-fall tuff is only exposed in section 18 of T 19 N, R 25 E, and has a thickness of 21 m at this location (Plate 1). This tuff may correspond to Staatz's (1979) rhyolitic tuff beds (Tct), and is probably an air-fall deposit related to the overlying lithic-rich tuff.

Lithic-rich tuff (Tlt). The lithic-rich tuff lies directly over the air-fall tuff (Taf), and it is white to pinkish white, poorly to moderately welded ash-flow tuff. It contains volcanic and quartzite lithics along with biotite, and smoky quartz. The lithic-rich tuff is distinguished from the quartzite-bearing ash-flow tuff by the dominance of dark crystal-rich, rhyolitic lithic fragments over quartzite lithics, and the presence of biotite (VanDenburg, 1997). This unit was mapped incorrectly as the quartzite-bearing ash-flow tuff by Staatz (1979). The lithic-rich tuff has a limited distribution and occurs only in section 18 of T 19 N, R25 E, where it has a thickness of 110 m (Plate 1). This unit was first mapped and described by VanDenburg (1997) on the east side of the Beaverhead Range, where it has a maximum thickness of 1250 m.

Older quartz-sanidine ash-flow tuff (Tqs1). The older quartz-sanidine welded tuff is a tan-orange to light pink welded tuff containing euhedral to subhedral crystals of sanidine (< 3 mm), and smoky quartz (< 3 mm), along with pumice fragments in a fine crystalline matrix. Quartzite lithics are also present in minor amounts, and it has a maximum thickness of 120 m. The older quartz-sanidine welded-tuff differs from the younger quartz-sanidine ash-flow tuff in that it is typically more densely welded, and is more tan to orange in color, but the two are otherwise lithologically similar. The older quartz-sanidine ash-flow tuff occurs in sporadic outcrops in the east side of the study area in the Ghoul basin-Agency Creek area (sections 7, 15, and 17 of T 19 N, R 25 E) and near Pattee Creek in section 11 of T 19 N, R 24 E (Plate 1). The vitric tuff of Lemhi Pass of Staatz (1979) is at the same stratigraphic position and has roughly the same mineralogy as the older

quartz-sanidine ash-flow tuff. An $^{40}Ar/^{39}Ar$ age determination obtained from the vitric tuff of Lemhi Pass yielded an age of 47.95 ± 0.12 Ma (M'Gonigle and Dalrymple, 1996). Staatz (1979) originally mapped the older and younger quartz-sanidine ash-flow tuffs as a single unit.

Dacite lava flows (Tldac). The quartzite-bearing ash-flow tuff is directly overlain by purple to purple gray, or brown dacite lava flows, between Kenney Creek and Warm Springs road. The dacite lava flows contain phenocrysts of euhedral biotite, hornblende, and plagioclase (< 4mm) along with minor amounts of quartz and augite (?) in a fine crystalline matrix. Near the top of the sequence of dacite, lava flows are aphanitic lavas like those of the lava sequence (Tl). The dacite lava flows are exposed in sections 20, 28, 29, 32, 33, and 34 of T 20 N, R 24 E, and have a maximum thickness of 95 m in section 32 (Plate 1). This unit is similar to the dacite lava flows (Tcdl) of VanDenburg (1997) that are exposed in the west-central Bannock Pass and east-central Goat Mountain quadrangles, both above and below a quartz-sanidine ash-flow tuff (older Tqs (?)).

Green tuff (Tgt). The green tuff is a new unit not described previously which directly overlies the dacite lava. This unit has a maximum thickness of 120 m, and is not present outside the Kenney Creek area. It is a green to light green biotite tuff, containing abundant biotite (euhedral, < 2 mm), and smoky quartz, minor sanidine (subhedral), and pumice in a white to light green ash matrix. This unit consists of 1 to 10 m thick beds of massive ash-flow tuff, but also contains some rhythmically layered beds. Coarse sections also contains lithics of volcanic clasts (3 mm) and a few quartzite

clasts. It is exposed at Kenney Creek and to the south in sections 29, 28, and 33 of T 20 N, R 24 E (Plate 1).

Lava flows (Tl). Intermediate lava flows of the Challis volcanic group are widespread in the study area. The western portion of the study area between Haynes and Muddy Creeks is dominanted by the intermediate lava flows where they unconformably overlie Middle Proterozoic quartzites. The lava flows are typically black to dark gray green, or dark brown black, and vary from being aphanitic to porphyritic, and dense to vesicular. Sometimes the lava flows display a platy appearance. Plagioclase is the most common crystal (< 1.5 mm), but the porphyritic flows may contain olivine. Interbedded with the flows are thin biotitic tuffs and volcaniclastic sandstones. These two units are typically too thin to map at the scale of 1:24,000. Secondary chalcedony and calcite also occur in many of the flows. The lava flows have a maximum thickness of 490 m along section C-C'. Intermediate lava flows crop out throughout the southwest portion of the study area as well as in sections 4, 11, 15, 22, 24, 25, and 36 of T 19 N, R 24 E; sections 27, 28, and 29 of T 20 N, R 24 E; and sections 7, 8, 9, 15 - 20, and 30 of T 19 N, R 25 E (Plate 1).

Challis breccia (Tcb). The Challis breccia unit is locally interbedded with the sequence of intermediate lava flows. In places only the Challis breccia unit occurs and the lava sequence is absent. Where the lava sequence is absent, the Challis breccia unit has a maximum thickness of 365 m along section E-E'. These flows are hematitic red to green, consisting of subangular lava clasts (< 75 cm), in an angular lapilli and red ash matrix.

This unit also contains pumice fragments and secondary veins of calcite. The Challis breccia unit is exposed along Agency Creek in section 17 of T 19 N, R 25 E (Plate 1).

White tuff (Tt). A white biotite tuff is locally interbedded in the lava sequence. This tuff is dominated by glass shards, and the dominant crystal is biotite (< 2 mm) with minor amounts of quartz and plagioclase. This unit is has a maximum thickness of 15 m, and may correlate with VanDenburg's (1997) biotite tuff.

Challis sandstone (Tcs). Locally interbedded with and overlying the lava sequence is a tan, poorly cemented, moderately to well sorted, subrounded, coarse sand to pebbly volcaniclastic sandstone. Clasts in this sandstone are of the underlying lavas and tuffs. The Challis sandstone typically occurs in thin interbeds (> 10 m) in the lava sequence and directly overlies the lava sequence. The limited exposure and its irregular distribution indicate that this unit was deposited in topographic lows on top of and within the lava sequence. The thickest (50 m) and best exposed section of the Challis sandstone is exposed in section 8 of T19N, R25E (Plate 1).

Tuff of Curtis Ranch (Tcr). The tuff of Curtis Ranch is perhaps the most widely distributed tuff in the study area. It is a white to greenish white ash-flow tuff containing abundant biotite, and lesser amounts of smoky quartz, sanidine, plagioclase, and angular volcanic and quartzite lithics. Pumice is abundant to rare, and typically concentrated at the top of the unit. The tuff is typically poorly welded, but is densely welded in places. This tuff conformably overlies the lava sequence, and has marked thickness

variations, with the thickest section (365 m) in sections 25 and 36 of T19N, R24E. The tuff of Curtis Ranch is exposed in a number of scattered outcrops in sections 28, 29, 33, and 34 of T 20 N, R 24 E; sections 25 and 36 of T 19 N, R 24 E; sections 9, 13, and 31 of T 19 N, R 25 E; sections 13 and 12 of T 18 N, R 23 E; and sections 25 and 36 of T 19 N, R 23 E (Plate 1). This unit was first mapped and described by Staatz (1979), and partly remapped by VanDenburg (1997) east of the study area. A K-Ar age of 42 Ma was reported by Staatz (1979) from the tuff of Curtis Ranch, but this is an anomalously young age for a Challis volcanic rock (Janecke and Snee, 1993; Fisher et al., 1992; M'Gonigle and Dalrymple, 1996). A new $^{40}Ar/^{39}Ar$ age of 47.58 ± 0.14 Ma for the tuff of Curtis Ranch from section 34 of T20N R24E was determined in this study (sample SUJ96-131, Table 3; Figure A2; Figure 4). VanDenburg et al. (1998) reported a similar date of 47.53 ± 0.13 Ma ($^{40}Ar/^{39}Ar$ single crystal date on sanidines) from the tuff of Curtis Ranch in the Horse Prairie basin (Table 2).

Younger quartz-sanidine ash-flow tuff (Tqs2). At the top of the Challis volcanic sequence is the younger quartz-sanidine ash-flow tuff. This tuff is typically white to white green, or gray green, and contains euhedral chatoyant sanidine and smoky quartz in a fine ash matrix. Occasional red glass shards are also locally present. The degree of welding is usually less than that in the older quartz-sanidine ash-flow tuff, but can locally be just as dense. The younger quartz sanidine welded tuff has a maximum thickness of 75 m along sections C-C' and H-H' (Plate 2). Because the younger quartz-sanidine ash-flow tuff and the older quartz-sanidine ash-flow tuff are

lithologically similar, their stratigraphic positions are used to distinguish them. Their striking similarity may indicate that they were erupted from a common caldera. Two $^{40}Ar/^{39}Ar$ age determinations from single crystals of sanidine in the younger quartz-sanidine ash-flow tuff yielded ages of 46.13 ± 0.19 from section 34 of T20N, R24E and 45.95 ± 0.12 Ma from section 19 of T19N, R25E (samples 96-56 and SUJ96-161, Table 3; Figure A3; Figure A4; Figure 4). The younger quartz-sanidine ash-flow tuff is exposed in sections 3 and 4 of T19N, R24E; sections 28, 33, and 34 of T20N, R24E; sections 9, 10, 15, 16, 17, and 19 of T19N, R25E; section 24 of T19N, R24E; sections 1 and 12 of T18N, R23E; and sections 25 and 36 of T19N, R23E (Plate 1). The younger quartz-sanidine ash-flow tuff has variable thickness and discontinuous distribution that may in part reflect subsequent erosion. Many of the megabreccias of the overlying sedimentary rocks of Tendoy were derived from the younger quartz-sanidine ash-flow tuff.

Challis tuff undifferentiated (**Tcto/Tcty**). The Tcto classification was used to designate undifferentiated older tuffs, and the Tcty was used to designate undifferentiated younger tuffs identified on aerial photographs north of Baldy Creek in the northwest portion of the study area. These underlie (Tcto) and overlie (Tcty) a thick sequence of lava flows exposed in the Haynes Creek area. These tuffs could be separated from one another on the basis of their stratigraphic position. In cross-section (E-E') the possible correlation between the undifferentiated older tuffs and the quartzite-bearing ash-flow tuff is shown (Plate 2).

Post-Challis sedimentary rocks

Post-Challis sedimentary rocks are comprised of syntectonic conglomerates, sandstones, and shales. Anderson (1956, 1957, 1959, 1961) and Harrison (1985) have accurate lithologic descriptions of the basin-filling sedimentary rocks of the Salmon basin, but their stratigraphic subdivisions were incorrect. Harrison (1985) did not recognize angular unconformities in the basin-fill sequence during her research north of the present study area, so her sedimentation model was oversimplified. Anderson (1956, 1957, 1959, 1961) did recognize angular unconformities in the sedimentary sequence, but failed to accurately describe the sedimentary rocks and their facies relationships. Staatz (1979) mistook conglomerates in the post-Challis sedimentary rocks for the syn-Challis granite-clast conglomerate. His descriptions thus overemphasized the fine-grained units of the post-Challis sedimentary rocks. This study proposes three new divisions for the sedimentary rocks of the southeastern Salmon basin based on angular unconformities.

The oldest and most widespread package of sedimentary rocks is here named the sedimentary rocks of Tendoy. These lie in angular unconformity over Challis volcanic rocks (18°) and Middle Proterozoic metasedimentary rocks. The sedimentary rocks of Tendoy are overlain in angular unconformity (13°) by the sedimentary rocks of Sacajaweja. The youngest sedimentary rocks in the southeastern Salmon basin are Quaternary-Tertiary sediments. The clasts in the syntectonic conglomerates range from 100% Middle

Proterozoic metasedimentary rock clasts to 100% volcanic clasts. The clast compositions are interpreted as resulting from structural control during sedimentation so the conglomerates have been separated based on their age and not on their composition. A full analysis of compositional variations in the conglomerates and their relationship with structures in the study area is presented in the Basin Evolution section.

Sedimentary rocks of Tendoy

The sedimentary rocks of Tendoy are the most widespread and voluminous of all the sedimentary rocks in the southeastern Salmon basin (Figure 5). They lie in angular unconformity on Challis volcanic rocks. This angular relationship is most pronounced along Muddy Creek where there is a 18° angular discordance, but the sedimentary rocks are conformable at the nose of the Warm Springs anticline. This package of sedimentary rocks contains three fine-grained facies, megabreccias, and five conglomerate facies. The three fine-grained facies are the shale facies, sandstone facies, and the sedimentary rocks of Sharky Creek. The sedimentary rocks of Sharky Creek are transitional between the fine-grained and conglomeratic facies. Megabreccias differ from one another in composition. The five conglomerate facies are the Pattee Creek northeast, Pattee Creek west, Sandy Creek, Haynes Creek, and Flume Creek facies, and they differ from one another by geographic location and clast compositions. The conglomerate facies and the shale facies are the thickest and most wide-spread units of the sedimentary rocks of Tendoy. The coarse conglomerate

Figure 5. Simplified map of the study area showing the distribution of the different ages of sedimentary rocks.

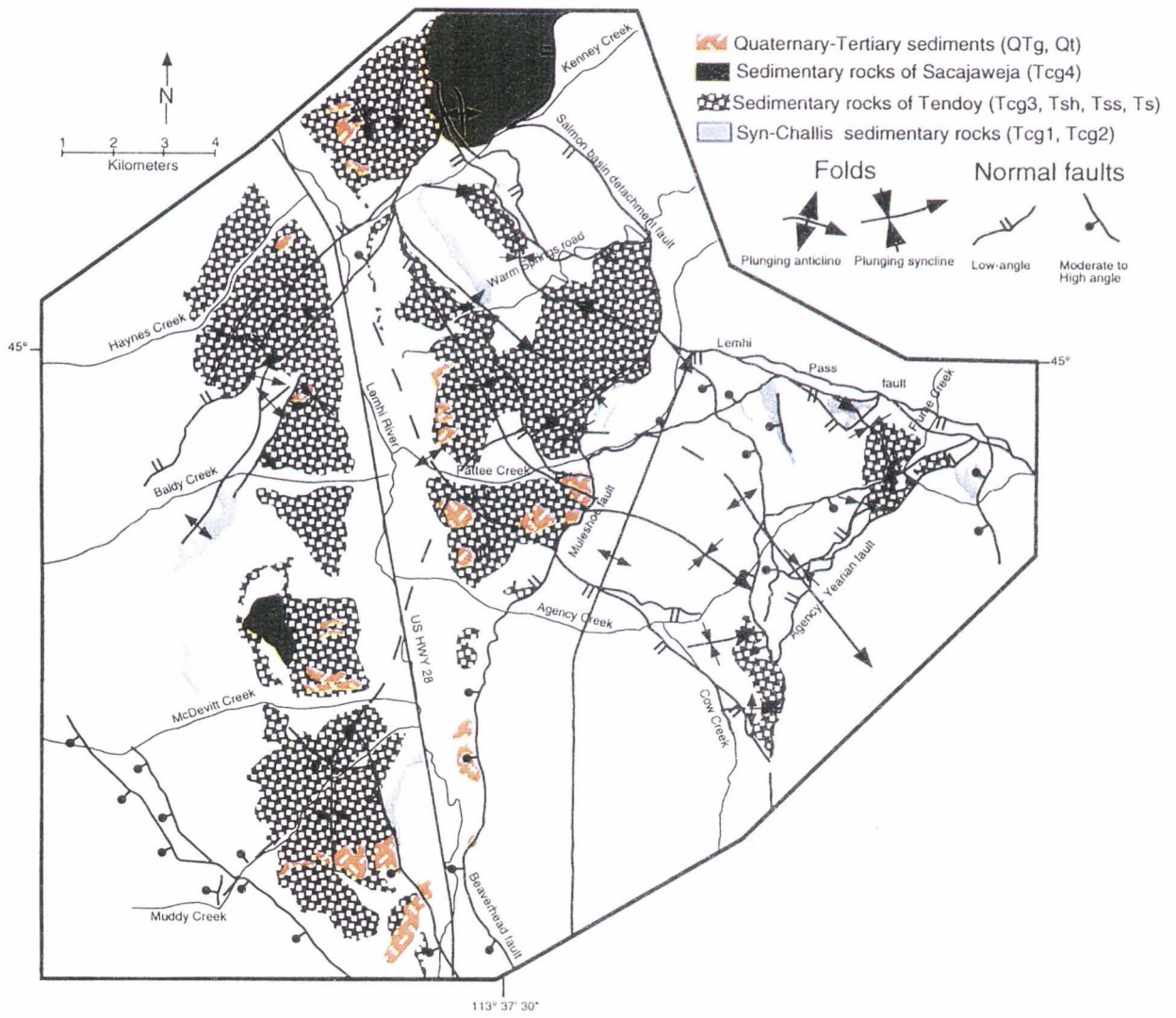
Quaternary-Tertiary sediments (QTg, Qt)
Sedimentary rocks of Sacajaweja (Tcg4)
Sedimentary rocks of Tendoy (Tcg3, Tsh, Tss, Ts)
Syn-Challis sedimentary rocks (Tcg1, Tcg2)
Folds
Normal faults
Plunging anticline
Plunging syncline
Low-angle
Moderate to High angle
N
1 2 3 4
Kilometers
45°
45°
113° 37' 30"
Kenney Creek
Salmon basin detachment fault
Haynes Creek
Lemhi Pass fault
Lemhi
Lemhi River
Baldy Creek
Pattee Creek
Mulkey Creek fault
Agency Creek
Yearian fault
US HWY 28
McDevitt Creek
Cow Creek
Muddy Creek
Beaverhead fault

facies interfinger with the finer grained facies. The intermediate facies (sandstones) are subordinate to the shale and conglomeratic facies, and the total thickness of the sedimentary rocks of Tendoy is 1440 m along section C-C' (Plate 2).

Middle conglomerate (Tcg3). The middle conglomerate overlies the Challis volcanic sequence and Middle Proterozoic quartzites in angular unconformity. It interfingers with the shale unit, and is probably middle Eocene to Oligocene in age. The middle conglomerate has a maximum thickness of 900 m along cross-section C-C' (Plate 2). This is the most widespread type of sedimentary rock in the study area, and it also has the greatest variation in composition. The depositional environments of the five facies in the middle conglomerate (Pattee Creek northeast, Pattee Creek west, Haynes Creek, Sandy Creek, and Flume Creek facies) will be discussed in greater detail in the Basin Evolution chapter.

The Sandy Creek facies is located on the west side of the area between Kenney Creek and Sandy Creek (Plate 1). Here the middle conglomerate consists of interbedded conglomerates (~ 40%) and sandstones (~ 60%). The sandstones are tan, fine-grained, well-rounded, well-sorted, well-cemented quartz arenites. The conglomerates vary from being clast-supported conglomerates to pebbly sandstones and have a matrix of sand. They contain subrounded, poorly sorted, quartzite clasts. Maximum clast size is 15 cm in diameter, but typical clast size is 8 cm. The conglomerates are interpreted as representing fluvial or beach deposits in a near-shore/beach environment.

The Pattee Creek northeast facies extends from south of Kenney Creek, west of the Salmon basin detachment fault, and east of the Lemhi River to Agency Creek (Plate 1). The conglomerate here is very angular to subangular, matrix to clast supported, with a tan tuffaceous matrix. Clasts range from pebbles to cobbles with a maximum grain size of 20 cm. The conglomerate is typically dominated by quartzite clasts, except within ~ 100 m of its base where it contains mostly volcanic clasts. It ranges from being well to poorly cemented. Where the conglomerate is well cemented it forms resistant fins. Interbeds of lithic arenites are also present. The conglomerate facies interfingers with the shale unit in this region, and sandstone beds are rare.

The Pattee Creek west facies is located in the southwestern portion of the study area west of the Lemhi River, and south of McDevitt Creek (Plate 1). Here the middle conglomerate commonly contains 100% volcanic clasts. The volcanic clasts are typically derived from lavas flows, but occasional tuffaceous clasts are present. It is a matrix-supported conglomerate with subrounded clasts that have a maximum size of 1 m. Its matrix has a tan to brown tuffaceous clay and sand matrix. Petrified wood is common, making up 1 to 2% of the unit. The middle conglomerate overlies Challis volcanic rocks (Tl, Tcr, Tqs2) in angular unconformity in the McDevitt Creek region.

The Haynes Creek facies occurs in the northwestern corner of the study area north of Baldy Creek, and has been mapped on aerial photographs and during field reconnaisance (Plate 1). This is a well-cemented volcanic-clast-dominated boulder conglomerate and sedimentary

breccia. The Haynes Creek facies may be related to the Pattee Creek west facies, but further work is needed to confirm that they are the same.

The Flume Creek facies crops out at the confluence of Flume and Agency Creeks, in the eastern portion of the study area (Plate 1). Staatz (1979) incorrectly mapped the conglomerate at this location as a conglomerate interbedded with the Challis volcanic rocks (Tcg2 of this study). The Flume Creek facies contains cobble- to pebble-sized (2 to 17 cm in diameter) clasts that are well to moderately well rounded. It is clast-supported in a white tuffaceous clay and medium to coarse sand matrix. Clasts consist of both Middle Proterozoic quartzites (~ 40%) and volcanic rocks (~ 60%), but compositions vary and some beds contain only volcanic clasts. Volcanic clasts are derived almost entirely from lavas flows, but occasional tuffaceous clasts are present. The most common tuffaceous clasts are clasts of the quartz-sanidine ash-flow tuff. Lenses of tan fine- to medium-grained volcaniclastic sandstonesare interbedded with the conglomerates. The sand grains are well to moderately well rounded, and well to moderately sorted.

Shale unit (Tsh). The finest grained units in the sedimentary rocks of Tendoy are a white to tan very finely laminated to massive, non-calcareous, tuffaceous shales. The shale unit often contains abundant woody debris, occasional debris-flow deposits, and volcaniclastic sandstone lenses. Individual beds in the shale are thinly bedded tuffaceous silt, massive bentonite, and thick- to thinly-bedded dark brown to black lignite. Individual beds of tuffaceous silt and bentonite may be stained a hematitic

red, or contain spherical calcite nodules. The bentonitic beds often display popcorn weathering. The debris flow deposits comprise a small fraction of this unit, and can be up to 2.3 m thick, but are typically less (1 to 1.5 m thick). The maximum grain size of clasts in the debris flow deposits is 20 cm, and clasts are typically sub- to well-rounded Middle Proterozoic quartzite clasts. West of the Lemhi River, the debris flow deposits also contain clasts of quartzite-bearing ash-flow tuffs and 1 to 2% lava clasts.

The shale unit is widely distributed throughout the center of the basin, and is well exposed along gullies and stream cuts. Excellent outcrops occur west of the Lemhi River along Muddy Creek, tributaries of McDevitt Creek, Baldy Creek, and at the mouth of Haynes Creek, and east of the Lemhi River along Agency, Pattee, and Kenney Creeks (Figure 6, Plate 1). This unit has a maximum thickness of 1150 m along section C-C' (Plate 2), but may be thicker because the base of this unit is not exposed in its thickest section. This unit represents a lake that formed after Challis volcanism.

Sedimentary rocks of Sharky Creek (Ts). The sedimentary rocks of Sharky Creek are composed of undifferentiated matrix-supported conglomerate, bentonite, limestone, and white biotite tuff. Because the four members were too thin to map separately at a scale of 1:24,000, they were grouped and mapped as the sedimentary rocks of Sharky Creek. The conglomerate is composed of subangular volcanic clasts less than 50 cm in diameter (typically 5-10 cm) floating in a white tuffaceous matrix containing abundant biotite crystals. The limestone is light gray, massive, and contains light green nodules. The white tuff contains pumice fragments along with

Figure 6. Simplified map showing the distribution of different types of sedimentary rocks in the study area.

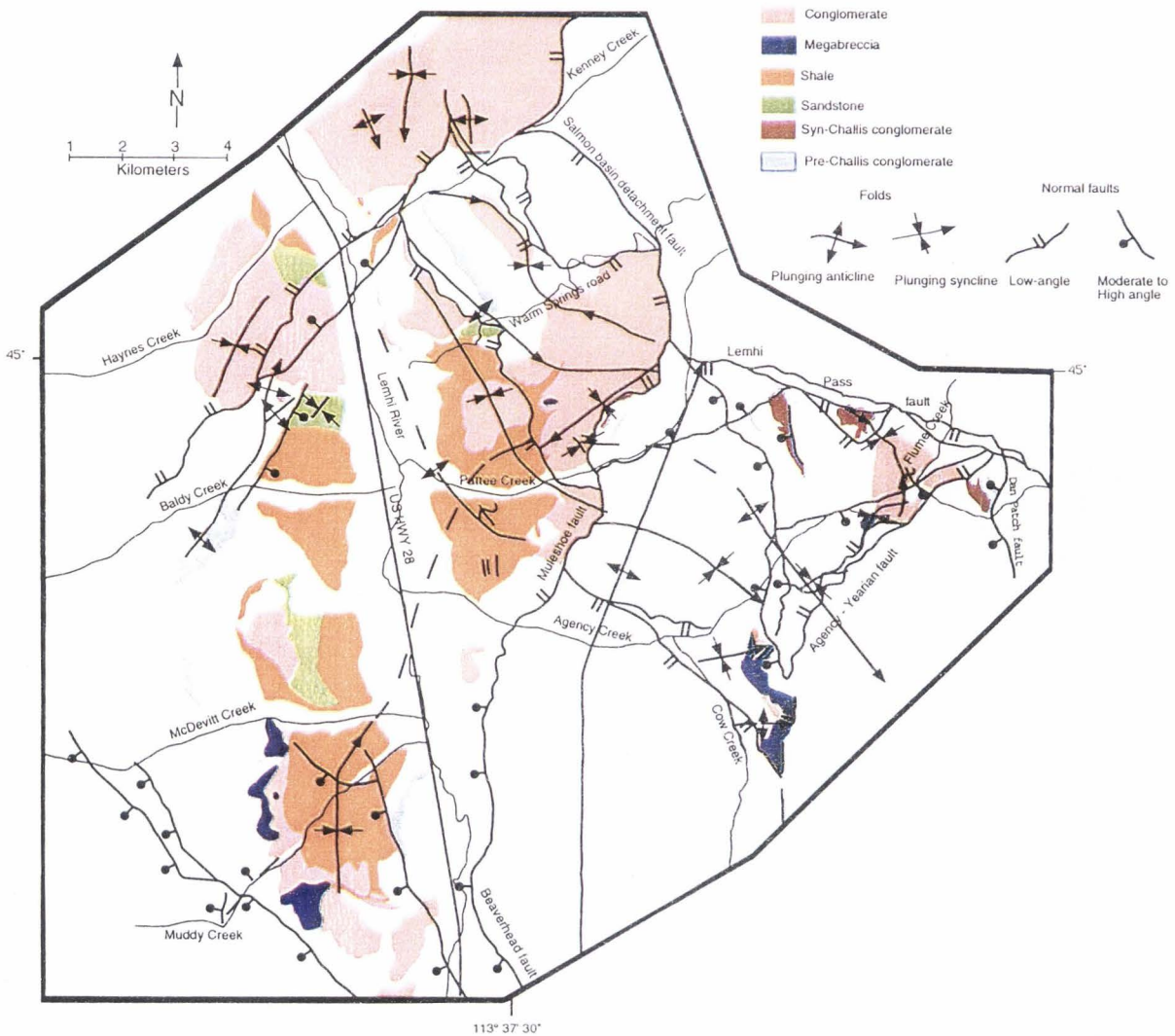
Conglomerate
Megabreccia
Shale
Sandstone
Syn-Challis conglomerate
Pre-Challis conglomerate
Folds
Plunging anticline
Plunging syncline
Normal faults
Low-angle
Moderate to High angle
N
1 2 3 4
Kilometers
Kenney Creek
Salmon basin detachment fault
Warm Springs road
Haynes Creek
Lemhi River
Lemhi Pass fault
Flume Creek
Dan Patch fault
Baldy Creek
Pattee Creek
US HWY 28
Muleshoe fault
Agency Creek
Agency - Yearian fault
McDevitt Creek
Cow Creek
Beaverhead fault
Muddy Creek
45°
45°
113° 37' 30"

crystals of biotite, smoky quartz, and sanidine. The tuff has a maximum thickness of 30 cm. Bentonitic beds are white and display popcorn weathering. The sedimentary rocks of Sharky Creek are only exposed along Sharky Creek in section 30 of T19N, R 25E (Plate 1), and have a maximum thickness here of 120 m. Staatz (1979) mapped fine-grained tuffaceous sedimentary rocks which interfinger with thick megabreccias (S. U. Janecke, unpublished mapping) along strike to the south. These fine-grained tuffaceous sedimentary rocks are probably correlative to the sedimentary rocks of Sharky Creek. The sedimentary rocks of Sharky Creek have been mapped separately from other fine-grained facies because of their lithology, and they are interpreted as being deposited in a subbasin separate from the other sedimentary rocks of Tendoy. The presence of both a thick sequence of conglomerates, and a large volume of fine-grained sedimentary rocks (bentonites, limestone, and a tuff) in the sedimentary rocks of Sharky Creek leads to the interpretation that this unit represents a transition between fine-grained and conglomeratic facies.

Tertiary sandstone (Tss). This unit is interbedded with the shale unit and its distribution is limited to section 25 of T19N, R23E, and sections 4 and 30 of T19N, R24E (Plate 1). This unit is a coarse- to fine-grained, well-rounded, well-sorted, moderately- to well-cemented lithic arenite. Some small-scale cross-bedding is present, and in places bedding has been disrupted by bioturbation. This unit may represent a near-shore facies of a lake in which the shale unit was deposited.

Monolithologic breccia (Tmb(qs)/Tmb(l)/Tmb(y)). Locally overlying the Challis volcanic sequence and interbedded in the sedimentary rocks of Tendoy are monolithologic megabreccias. The compositions and degree of brecciation vary between the deposits. **Tmb(qs)** denotes a megabreccia containing clasts of the quartz-sanidine ash-flow tuff. Outcrops of Tmb(qs) occur in sections 1, 7, 12, 13, and 18 of T18N, R23E (Plate 1). **Tmb(cr)** denotes a megabreccia containing clasts of the tuff of Curtis Ranch. The only megabreccia containing clasts of the tuff of Curtis Ranch is a small pod in section 10 of R24E T19N (Plate 1). **Tmb(l)** denotes megablocks containing fragments of lava flows. There is only one outcrop of Tmb(l) in the study area and this unit is a large 275-m thick coherent block of lava south of the Pattee Creek northeast facies and north of sandstone outcrops. This deposit is in section 22 of T19N, R24E (Plate 1). **Tmb(y)** denotes a clast-supported megabreccia consisting of angular clasts up to 15 cm in diameter of Middle Proterozoic quartzites. This unit typically outcrops poorly, but may be (where good outcrops occur) well cemented. The quartzite-clast megabreccia has a maximum thickness of 170 m, in sections 30 and 31 of T19N, R25E, east of the confluence of Agency and Cow Creeks (Plate 1). Similar deposits occur along strike to the south in the hanging wall of the Yearian segment of the Agency-Yearian fault (S. U. Janecke, unpublished mapping). The presence of megabreccias is important because they provide information on relief, proximity, and composition of nearby highlands.

Intrusions (Ti). Hematitic red, or dark gray andesitic intrusions occur in both the sedimentary rock sequence and the Challis volcanic

sequence. The intrusions typically appear brecciated and highly altered. The edges of intrusions are typically aphanitic and not altered, whereas the cores are porphyritic and very altered. These masses are interpreted as intrusions because they have highly irregular contacts with fingers extending out from a main core outcrop that can be traced in the field. Outcrops occur in the sedimentary rocks in sections 19 and 30 of R24E T20N (Plate 1). An intrusion in Challis volcanic rocks is interpreted from aerial photographs in sections 13 and 14 of T19N, R23E (Plate 1). An $^{40}Ar/^{39}Ar$ whole-rock age determination from the intrusion into the Sandy Creek facies of the sedimentary rocks of Tendoy yielded an age of 37.08 ± 0.21 Ma. The spectrum was highly disturbed and the spectrum indicates that the age is unreliable (Sample JB96- 145, Table 3; Figure A5).

Age of the sedimentary rocks of Tendoy

The sedimentary rocks of Tendoy have yielded three fossil flora (Cow Creek flora, Haynes Creek flora, and Salmon flora), which have been described by Staatz (1979) and Axelrod (1998). The Cow Creek flora collected in small scattered outcrops along Cow Creek are described as being from deciduous hardwood forests in cool temperate upland areas at an elevation of 1220 m (Axelrod, 1998). Wolfe and Wehr (1987) assigned a late Eocene age to the Salmon flora collected from sedimentary rocks where the Lemhi River Valley narrows and joins the Salmon River, which may correlate with the tuffaceous sedimentary rocks along Cow Creek, because they both lack species that are considered diagnostic of a middle Eocene age. The

sedimentary rocks containing the Cow Creek flora appear to overlie the tuff of Curtis Ranch and megabreccias derived from the 46 Ma younger quartz-sanidine ash-flow tuff (S. U. Janecke, unpublished mapping). A rhyolitic tuff interbedded in the sedimentary rocks along Cow Creek was dated by Axelrod (unpublished data) and yielded an $^{40}Ar/^{39}Ar$ age of 46.5 Ma. This date was probably obtained from a bed that has been reworked from the underlying volcanic rocks because the date is older than the underlying volcanic rocks. The Haynes Creek flora were collected from the Snook bentonite quarry north of Haynes Creek. The Haynes Creek flora have yielded an $^{40}Ar/^{39}Ar$ age determination of 30.6±0.7 Ma (Axelrod, 1998). Overall, the fossil flora of the Salmon basin are poorly dated, but are probably of late Eocene age.

The sedimentary rocks of Tendoy were deposited after the younger quartz-sanidine ash-flow tuff (Tqs2), which has been dated at 46.13 ± 0.19 Ma and 45.95 ± 0.12 Ma ($^{40}Ar/^{39}Ar$ age determinations on single crystals of sanidine; Table 3; Figure A3; Figure A4). The sedimentary rocks of Tendoy are probably the same age as the sedimentary rocks of Bear Creek in the Horse Prairie basin of southwest Montana, because both were deposited during correlative episodes of extension (episode 2 of this study, and phase 3 of VanDenburg, 1997). Also both deposits contain megabreccias derived from the underlying Challis volcanic rocks. The sedimentary rocks of Bear Creek have middle- to late-Eocene mollusks in limestones near the base of the section, and are overlapped by late early Arikareean (~ 30-25 Ma) sedimentary rocks of Everson Creek (VanDenburg, 1997; VanDenburg et al.,

1998). The sedimentary rocks of Tendoy were deposited before slip on the Lemhi Pass fault which was active between approximately 46 Ma and 27 Ma (VanDenburg, 1997).

The $^{40}Ar/^{39}Ar$ age determination obtained from an intrusion into the sedimentary rocks of Tendoy between Kenney Creek and Sandy Creek (Sample JB96-145, Table 3; Figure A5), was an inconclusive date because of its disturbed spectrum (Figure A5), but shows that volcanic activity was still continuing at a low level during the deposition of the sedimentary rocks of Tendoy. The 31 Ma $^{40}Ar/^{39}Ar$ age determination obtained by Axelrod (1998) from Haynes Creek appears to be reliable (Table 1), because this is a reasonable age for post-Challis sedimentary rocks and is from probable sedimentary rocks of Tendoy. Also, all 15 crystals analyzed for the 31 Ma age determination were with in the two sigma confidence level of each other. Further work is needed to confirm the preliminary correlations between the sedimentary rocks around Haynes Creek and sedimentary rocks of Tendoy. The available data also permit a correlation between the sedimentary rocks around Haynes Creek and the sedimentary rocks of Sacajaweja. In either case, the bulk of the sedimentary rocks of Tendoy are older than the 31 Ma tuff interbedded in bentonites at the mouth of Haynes Creek. Overall the sedimentary rocks are not well dated, but most of this sequence was deposited between 46 and 31 Ma (late middle Eocene to early Oligocene). The upper part of the section may be younger.

Sedimentary rocks of Sacajaweja

The sedimentary rocks of Sacajaweja consist of quartzite-clast-dominated conglomerates. These conglomerates lie in angular unconformity over the sedimentary rocks of Tendoy and Middle Proterozoic metasedimentary rocks. The sedimentary rocks of Sacajaweja are very thick (maximum thickness 1940 m), but subsequent erosion has limited their distribution to the northeast corner of the study area, and possibly to a small area north of McDevitt Creek (Figure 5; Plate 1).

Conglomerate of Kenney Creek (Tcg4). The conglomerate of Kenney Creek is a thick sequence of syntectonic conglomerates with excellent outcrops (Figure 7A, 7B), which have been described in detail by Tucker and Birdseye (1989). Tucker and Birdseye (1989) divided this package of conglomerates into five subunits based on lithologic characteristics and geomorphic expression. In general the assemblage of conglomerates was described as matrix-rich immature sedimentary rocks containing mixed volcanic and nonvolcanic clast conglomerates and interbedded fine-grained sandstones, deposited as debris flows (Tucker and Birdseye, 1989). This study agrees with Tucker and Birdseye's (1989) descriptions, as generally consisting of well-rounded, well-sorted, Middle Proterozoic quartzites clasts (volcanic clasts are rare) in a sandy matrix, but also identifies a unit not documented in their study. The conglomerates are typically clast supported, but may be matrix supported. Interbeds of lithic arenites are present, which are white to tan or gray, fine- to medium-grained, and thinly laminated, and in places contain abundant woody debris. The

A)

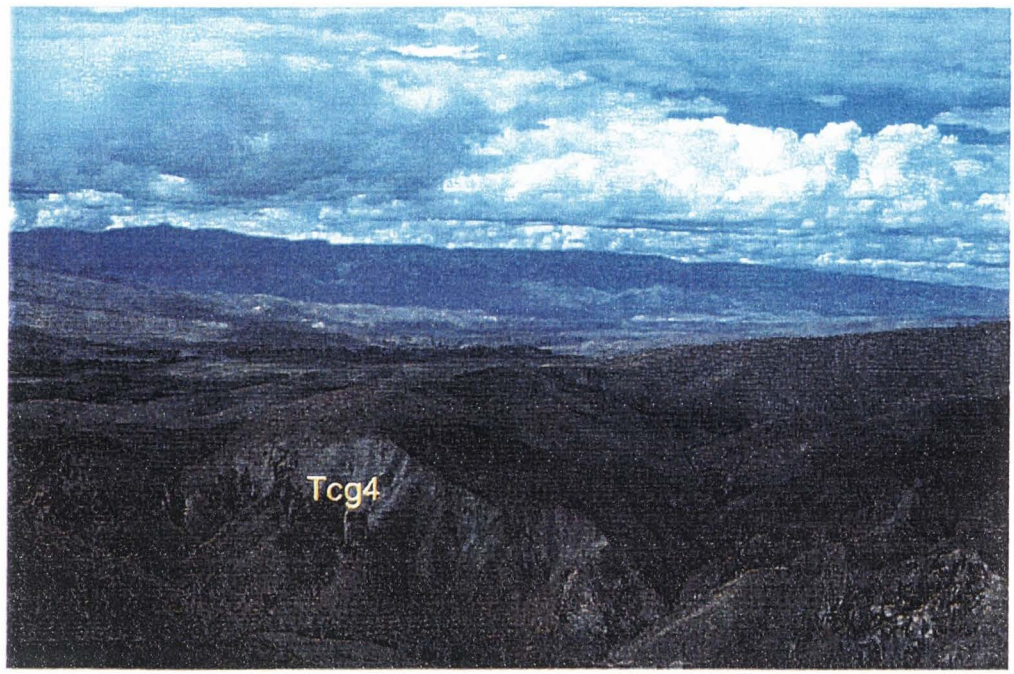

B)

Figure 7. Photographs of the excellent outcrops of conglomerates of the sedimentary rocks of Sacajaweja (Tcg4) looking north across Kenney Creek. Figure 7B is a closeup of the outcrops on the right side of Figure 7A.

base of the unit is a sedimentary breccia deposit (25 m thick) that was previously not identified. The breccia consists of clast-supported angular clasts (6 cm) of Middle Proterozoic quartzite. The striking similarity of this unit to modern talus slopes leads to the interpretation of this unit as a paleotalus deposit. The conglomerate of Kenney Creek (Tcg4) has a 13° angular discordance with the underlying middle conglomerate (Tcg3) west of faults D, E, and C. The conglomerate of Kenney Creek is located between Kenney and Sandy Creeks in the northern portion of the field area, in sections 15, 16, 21, 22 of T20N, R24E (Plate 1), and has a maximum thickness of 1940 m north of section A-A' (Plate 2). Tucker and Birdeye (1989) assigned a late middle Eocene age to the conglomerate based on a K-Ar age of 43.1 ± 1.7 Ma from a thin andesitic crystal tuff collected from the upper half of their Unit 2. This study was unable to locate the tuff to confirm its primary volcanic character. The anomalously old age of the tuff suggests that the dated material was reworked from the Challis volcanic sequence.

The sedimentary rocks of Sacajaweja may be the same age as gravels at the base of VanDenburg's (1997) sedimentary rocks of Everson Creek (his unit Tg2). Both units directly overlie the Lemhi Pass fault, and are tilted east to northeast toward a younger detachment fault (the Salmon basin detachment fault and the Maiden Peak fault, respectively). This correlation suggest an age between late Eocene to early Miocene for the sedimentary rocks of Sacajaweja.

Fault breccia (Tmb). A breccia occurs in poor outcrops in the hanging wall of the Salmon basin detachment fault and in the footwall of fault

E between Kenney Creek and the Warm Springs road (Plate 1). This clast-supported breccia consists of 1 to 8 cm long, angular clasts of Middle Proterozoic metasedimentary rocks, and is probably a fault breccia related to movement along the Salmon basin detachment fault. Alternatively this deposit might be a thick sedimentary breccia of the sedimentary rocks of Tendoy, or sedimentary rocks of Sacajaweja. This is unlikely because it would make faults D and E thrust faults that place older on younger sedimentary rocks. Since faults D and E are subparallel to other unequivocal normal faults in the area, this possibility seems unlikely.

Quaternary-Tertiary deposits

Quartzite clast gravel (QTg). This subhorizontal gravel occurs in sporadic outcrops in the study area and horizontally overlies the shale and sandstone units in angular unconformity (28°). It represents the third sedimentary sequence in the study area. The quartzite clast gravel is a well-rounded, cobble to boulder (maximum clast size 50 cm) gravel containing abundant clasts of Middle Proterozoic quartzites, with rare clasts of rapakivi granite. It has a maximum thickness of 60 m and outcrops in sections 7, 8, 17 of T18N, R24E; section 25 of T19N, R23E; and sections 21 and 22 of T19N, R24E (Plate 1). Outcrops of QTg typically occur approximately 500 ft (150 m) above the Lemhi River. Some of these deposits may preserve a relic depositonal surface, and may represent ancient river terraces of the Lemhi River. These deposits are undated.

Quaternary deposits (Qal, Qc, Qt2, Qt1, Qls, Qaf). Six different Quaternary deposits were mapped in the study area. The deposits mapped were alluvium (Qal), colluvium (Qc), older terrace deposits (Qt1), younger terrace deposits (Qt2), landslide deposits (Qls), and alluvial fan deposits (Qaf). Alluvial deposits occur along the Lemhi River and its tributaries and consist of unconsolidated stream deposits. Colluvial deposits consist of unconsolidated gravel, sand, and silt, which occur on hill sides. Terrace deposits are located on both the eastern and western sides of the Lemhi River and represent two different stages of down cutting. Landslide deposits are common thoughout the study area in all rock types, but are most abundant in the shale unit (Tsh). Alluvial fan deposits are present at the mouth of several canyons in the southern portion of the study area.

SUMMARY OF TERTIARY STRATIGRAPHY

A thick sequence (up to 1.4 km) of Challis volcanic rocks accumulated in the southeastern Salmon basin between 48.64 ± 0.33 Ma and 45.95 ± 0.12 Ma (M'Gonigle and Dalrymple, 1993; VanDenburg, 1997; this study; Tables 2 and 3). The distribution of Challis volcanic rocks defines an east southeast-trending paleovalley and rugged topography. Following Challis volcanism during the late middle Eocene to Oligocene (?), three thick sequences of syntectonic sedimentary rocks were deposited in angular unconformity over the volcanic rocks. The sedimentary rocks of Tendoy, which are dominated by conglomerates and tuffaceous shales, are the most widespread and voluminous sedimentary rocks in the study area, and were

deposited between late middle Eocene and Oligocene time (46 to 23.7 Ma). They are overlain in angular unconformity by the poorly dated sedimentary rocks of Sacajaweja, which were probably deposited after 30.7 Ma during the Oligocene and early Miocene. Erosional processes have dominated during the Quaternary.

STRUCTURAL GEOLOGY

The southeastern Salmon basin is a structurally complex east-dipping half-graben that has experienced at least four temporally distinct episodes of extension. The east side of the basin is bounded by the large northwest-striking Salmon basin detachment fault, and the southeast side is bounded by the north-northwest-striking Agency-Yearian fault. Associated with many of the faults are extensional folds. The extensional folds in the southeast Salmon basin have the dominant trends of northeast-southwest, northwest-southeast, and north-south. This section will first give a description of the methods used to obtain structural data in the field and the laboratory, then give a general description of the folds and faults, followed by a detailed description of the faults and folds arranged from the oldest to youngest. The section will conclude with a discussion of the relationships between the folds and faults in the study area.

METHODS

Structural data were obtained during field mapping and by using a variety of laboratory methods. Field data included recording the strike and dip of beds and faults. Where possible, slip vectors on faults were measured. Folds were examined for their hingelines and relations to faults.

Geologic mapping of the different rock types and structures in the area was conducted over the course of 15.5 weeks of field work in the southeastern Salmon basin. This was done with the aid of color (1:23,000) and black and white (1:40,000) aerial photographs and 7.5 minute

topographic maps (Appendex B1). Aerial photographs were used to determine the preliminary locations of geologic features, and then using this information, the contacts were walked to confirm their location and plotted on the topographic maps.

In the laboratory, aerial photographs were used to determine possible problem areas to examine in more detail in the field. The aerial photographs were also used to locate geologic features that could not be located in the field.

Once mapping was completed, all map data were compiled onto a topographic base map at the scale of 1:24,000 (Plate 1). Strike and dip measurements and some fault data from the original mapping of Staatz (1979), and reconnaissance and photo geologic mapping of Janecke (unpublished data, 1996-1997) between Baldy and Haynes Creeks and along the western margin of the study area, were simplified and compiled onto the base map (Plate 2). Mapping by Staatz (1979) was simplified by taking out small faults and lumping the pre-Tertiary rock units into a single unit. Once a geologic map was completed, further analysis of the basin could be done.

Faults were grouped by age, using cross-cutting relationships and fault strikes. These relationships were most apparent when simplified maps of the study area showing only the faults were constructed (Figure 8). Three-point problems were done on the map traces of the faults where field data did not provide direct measurements of the strike and dip of faults. A slip vector stereogram was constructed for the Salmon basin detachment fault from

Figure 8. Simplified map of normal faults in the study. Faults of the same color are the same age.

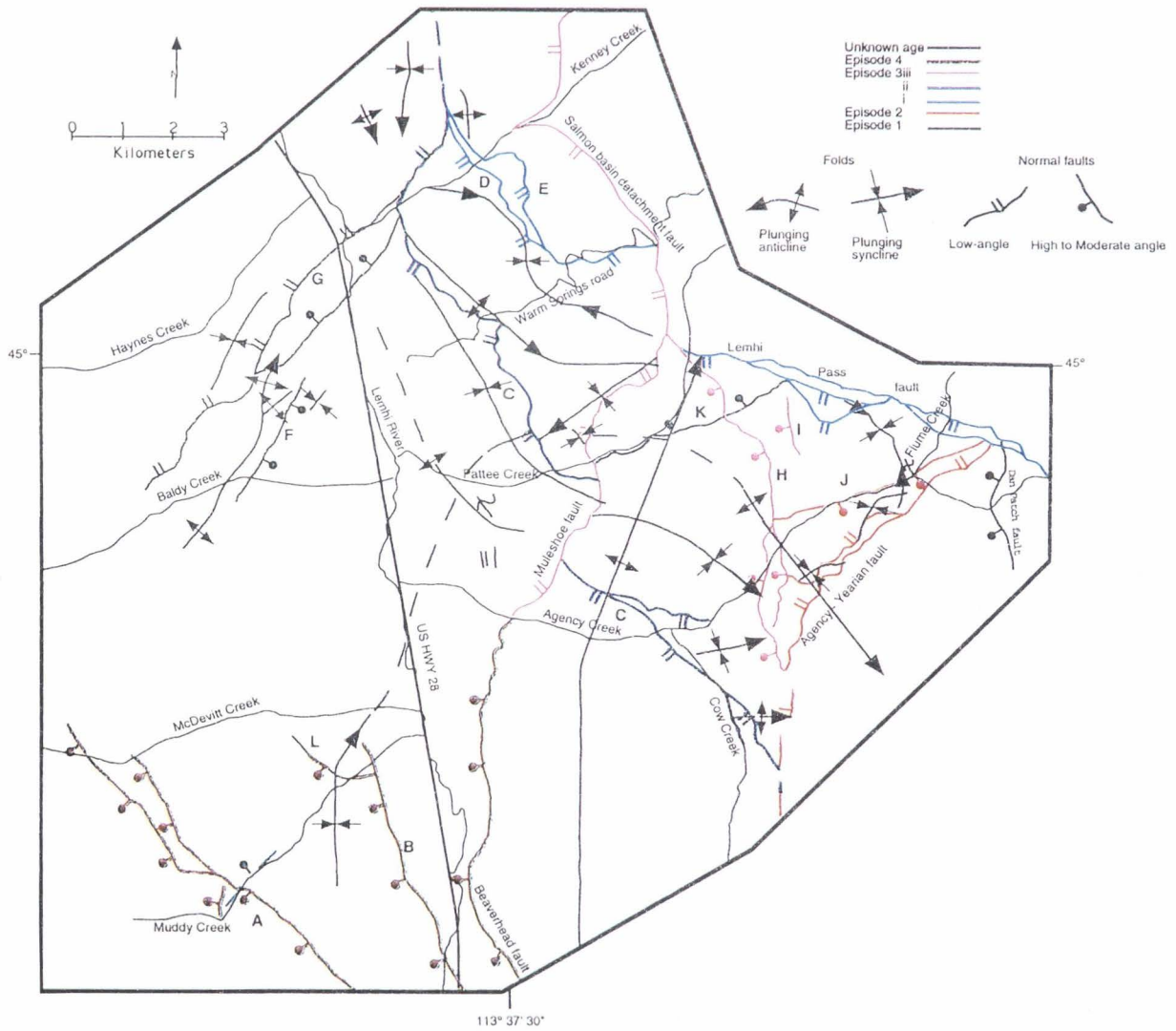
Kilometers
0 1 2 3
Unknown age
Episode 4
Episode 3iii
ii
i
Episode 2
Episode 1
Folds
Plunging anticline
Plunging syncline
Normal faults
Low-angle
High to Moderate angle
Kenney Creek
Salmon basin detachment fault
Warm Springs road
Haynes Creek
Baldy Creek
Lemhi River
Pattee Creek
Lemhi Pass fault
Flume Creek
Mulkshoe fault
Agency Creek
Agency Yearian fault
Dan Patch fault
US HWY 28
McDevitt Creek
Cow Creek
Muddy Creek
Beaverhead fault
A
B
C
D
E
F
G
H
I
J
K
L
45°
45°
113° 37' 30"

slicken-line data obtained from small subsidiary faults in the footwall of the fault along Kenney Creek.

Nine cross sections were constructed from map data and provided information on fault geometries at depth, basin geometry, and fault and fold relationships (Plate 2). Cross sections were constructed assuming dip-slip deformation along the fault surfaces, and because many of the folds in the study area are interpreted as fault-bend folds fault geometries were determined by the presence or absence of folds in the hanging wall of faults. Stereogram data were used for the axial surfaces of the folds.

Because many of the structures in the Salmon basin have experienced multiple deformational events, typical vertical cross-section profiles of folds do not display the true fold geometry. As a result a down-plunge projection of the Warm Springs anticline was constructed to show a more realistic geometry of this plunging structure (cross-section I-I', Plate 2). The down-plunge projection was constructed using the method outlined by Ramsay and Huber (1987). This down-plunge projection gives an accurate view of the Warm Springs anticline, but the adjacent structures are distorted because their fold axes do not parallel that of the Warm Springs anticline.

Folds were also analyzed by comparing the cross sections with sandbox models of extensional folds in McClay (1989). This comparison lent insights into the origin of growth strata on the flanks of the Tendoy anticline and Pattee Creek syncline.

Folds were further analyzed by stereograms. Poles to bedding for each limb of a fold were plotted, and from this, the mean vector and alpha 95

confidence cone for each limb were calculated. This was then used to determine the trend and plunge, interlimb angle, and bisecting surface for each fold, assuming a cylindrical fold. Fault orientations were also plotted and the angle between the bisecting surface and fault plane was determined (Table 4; Figure 9).

Faults

Faults of different episodes and phases are distinguished on the basis of 1) orientation and 2) cross-cutting relationships. The first episode of extension is characterized by faults with northeast strikes, the second by north north-west strikes, the third by west-northwest then northwest strikes, and the final episode by north-south to northwest strikes (Figure 8). Sense of slip is only know for the Salmon basin detachment fault. Because slip vectors were absent from most of the faults in the study area, dominantly dip-slip deformation was assumed. This assumption is consistent with the younger-on-older geometry of all the faults, the presence of thick sections of basin-fill sedimentary rocks in the hanging walls of many of the faults, and with kinematic data for dip-slip on correlative normal faults (Janecke, 1992). Folds related to individual faults were used to determine whether fault geometries were planer, listric, or flat and ramp. The major normal faults of the southeast Salmon basin will be discussed from oldest to youngest.

Folds

Folds are common in the southeastern Salmon basin, and their presence was first documented by Anderson (1956, 1957, 1959, 1961), and

TABLE 4. DESCRIPTION OF EXTENSIONAL FOLDS IN THE SOUTHEASTERN SALMON BASIN

Fold	Orientation (plunge and trend)	Bisecting surface (strike and dip)	Interlimb angle (0, C, G)	Mean fold spacing	N	Episode of extension	Associated normal fault*	Angle between trend of fold axis and strike of fault	Angle between axial plane and fault plane
Tendoy anticline north of Agency Creek	02°/022°	016° 86°W	106° O	4.0 km	14	2	Agency-Yearian	16.6°	68°
Pattee Creek syncline N	21°/239°	234° 76°W	117.3° O	4.0 km	20	2	Agency-Yearian	18°	50°
Pattee Creek syncline S	10°/010°	189° 87°W	137° G	5.9 km	31	2	Agency-Yearian, or Beaverhead	21.9° 18.5°	65° 55.5°
Campground syncline	35°/121°	309° 82°E	140° G	3.0 km	16	2 or 3i	Agency-Yearian, or Lemhi Pass fault	83.9° 16°	87° 65°
Muddy monocline	11°/292°	127° 48°W	129° G	isolated	11	?			
Flume Creek syncline	27°/153°	319° 84°E	141° G	3.0 km	17	2 or 3i	Lemhi Pass, Agency-Yearian, and/or Dan Patch	38.1° 82.8° 8°	71° 87° 60°
Warm Springs anticline south of Kenney Creek	35°/123°	308° 88°E	122° G	1.8 km	35	3i	Faults D and E, and Lemhi Pass	14°	71.2°
Alkali syncline	18°/128°	313° 75°E	142.2° G	1 km	12	3ii	Fault C	18°	78.6°
Alkali anticline	05°/179°	358° 89°E	169.9° G	____	7	3ii	Fault C	0°	62°

Notes: O = Open, C = Closed, G = Gentle

* More than one fault is listed if there is uncertainty about the identity of the controlling normal fault.

Figure 9. Stereograms of poles to bedding for extensional folds of the southeastern Salmon basin. Folds are typically open to gentle with interlimb angles between 106° and 170°. The angle between the axial plane of the folds and their associated normal fault ranges from 50° to 87°. Janecke et al. (1998) provides more descriptive information.

Tendoy anticline north nose

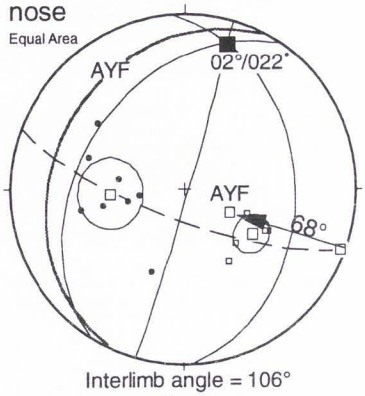

Interlimb angle = 106°
N=14

Pattee Creek syncline north

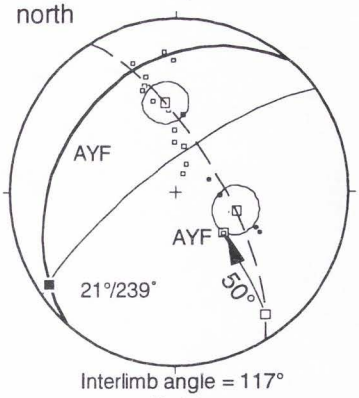

Interlimb angle = 117°
N=20

Pattee Creek syncline south

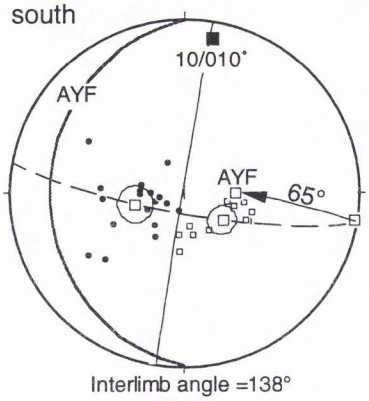

Interlimb angle =138°
N=33

Campground syncline

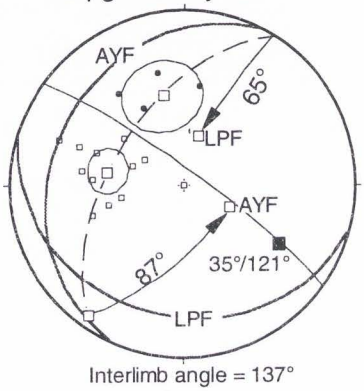

Interlimb angle = 137°
N=18

Muddy monocline

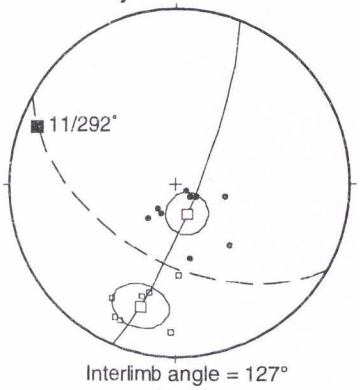

Interlimb angle = 127°
N=17

Flume Creek syncline

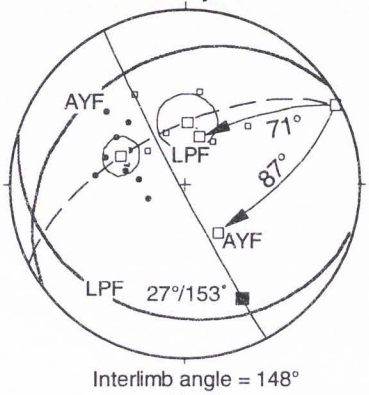

Interlimb angle = 148°
N=17

Warm Springs anticline NW of Pattee Creek syncline

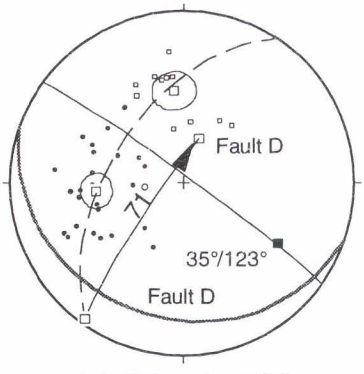

Interlimb angle = 122°
N=35

Alkali syncline

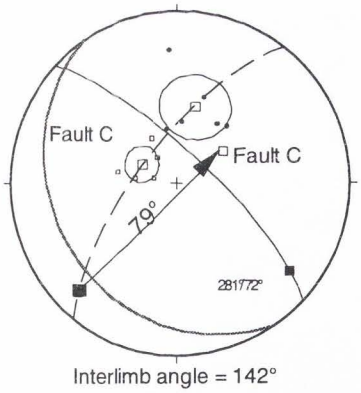

Interlimb angle = 142°
N=11

Alkali anticline

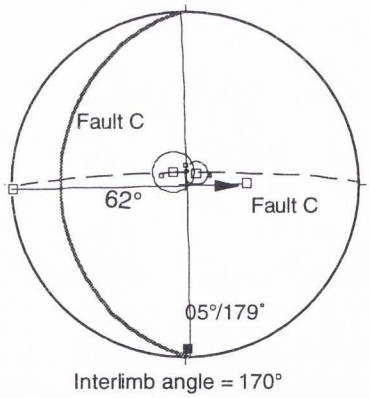

Interlimb angle = 170°
N=7

Explanation

- • ▫ Pole to bedding
- □ Pole to bisecting surface
- ■ Fold axis
- Pole to average orintation of each limb and alpha 95
- AYF □ Pole to normal fault
- 35° Angle between fault plane and bisecting surface
- Fault plane
- Bisecting surface
- Cylindrical best fit

later by Staatz (1979). Because Eocene and younger volcanic and sedimentary rocks are folded, and they postdate the Late Cretaceous to early Eocene contractional deformation of the area (Harlan et al., 1988), the folds must be related to the middle Eocene to recent extensionof the area. Extensional folds have been documented in a variety of settings, and many different mechanisms are responsible for their formation (Schlische, 1996; Janecke et al., 1998). This study documented seven major and nine minor folds in the study area with the three general trends of northwest-southeast, northeast-southwest, and north-south (Figure 10). The northeast-southwest trending folds are generally associated with episode 2, and the northwest-southeast trending folds with phases 3i and 3ii. The north-south trending folds are typically small and of uncertain origin so they can not be assigned an age. This section describes the major folds in the study area together with the genetically related normal fault, whenever it has been identified. To describe the folds, I use nomenclature defined by Janecke et al. (1998; Table 4). After each description, possible mechanisms for the formation of each fold are discussed.

Before the folds of the southeastern Salmon basin are discussed, a brief overview of the mechanisms, responsible for the formation of some types of extensional folds will be given. For a more thorough discussion of extensional folds and their mechanisms, see Schlische (1996) and Janecke et al. (1998).

The most commonly recognized extension-related fold is the rollover anticline. Xiao and Suppe (1992) described this type of fold as the bending

Figure 10. Map of extensional folds in the study. Folds with similar trends have the same color.

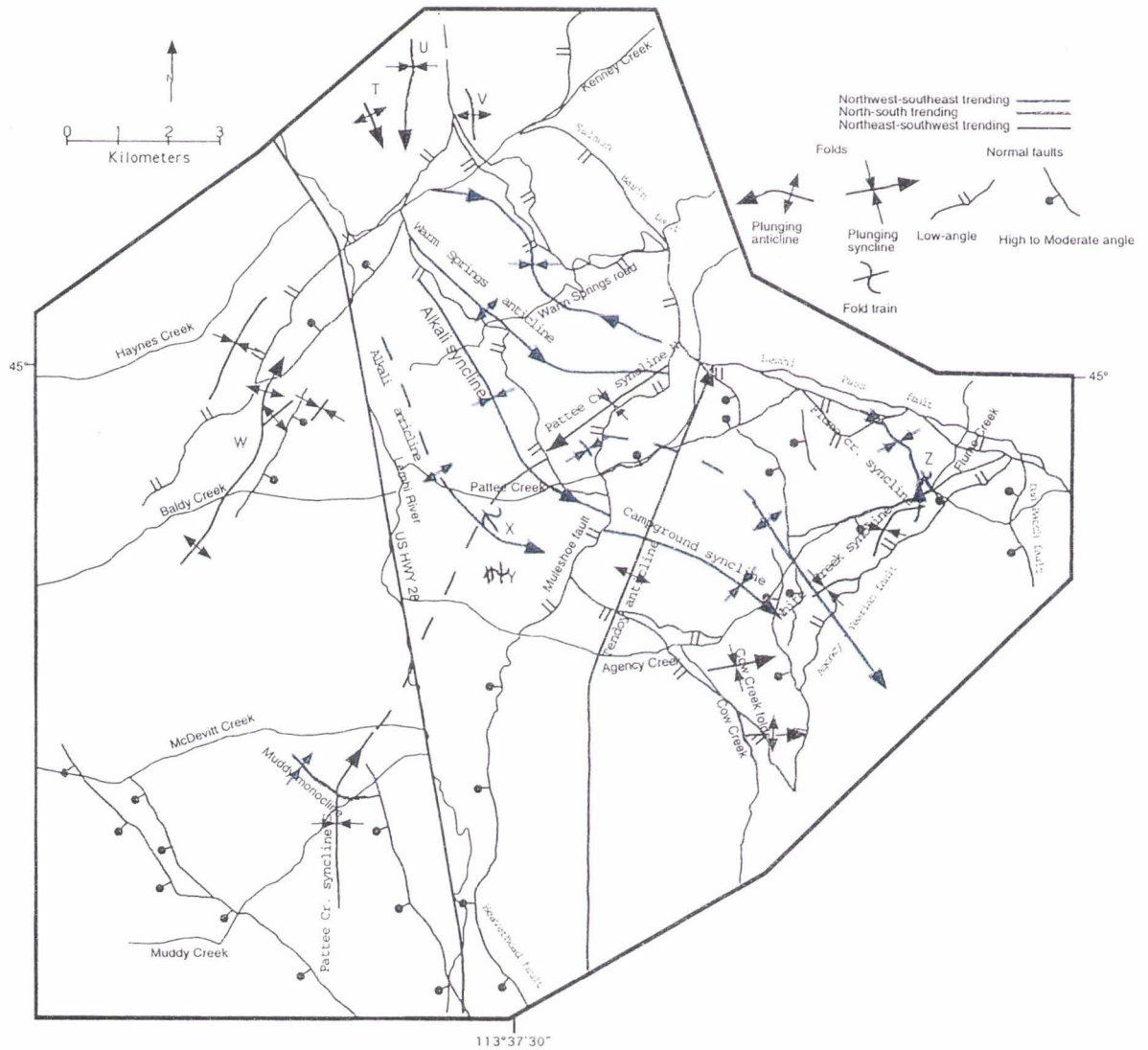
N
0 1 2 3
Kilometers
Northwest-southeast trending
North-south trending
Northeast-southwest trending
Folds
Normal faults
Plunging anticline
Plunging syncline
Low-angle
High to Moderate angle
Fold train
Kenney Creek
Warm Springs
Warm Springs anticline
Warm Springs fold
Alkali syncline
Alkali anticline
Haynes Creek
Baldy Creek
Pattee Creek
Pattee Cr. syncline
Muleshoe fault
Campground syncline
Fender anticline
Agency Creek
Cow Creek fold
Cow Creek
Fluke Creek
Pattee Cr. syncline
Muddy Creek
Muddy monocline
Pattee Cr. syncline
McDevitt Creek
US HWY 28
Lemhi River
45°
113°37'30"

or collapse of hanging wall fault blocks in response to slip on non-planar normal faults. The factors controlling the geometry of the folds are 1) the shape of the fault, 2) post-depositional slip along the fault, 3) the direction of relative partial motion in hanging wall collapse, 4) deposition rate relative to slip rate, and 5) compaction (Xiao and Suppe, 1992). A critical factor in controlling fold geometry in many extensional folds is the shape of the underlying fault.

Twiss and Moores (1992) described how ramp-flat geometries in normal faults can produce both anticlines and synclines in the hanging wall. In one of their models (their figure 5.5), a syncline is produced by the slipping of the hanging wall over a ramp connecting two gently dipping segments of a fault. The resulting fold is called a fault-ramp syncline. A fault-bend anticline is produced if the hanging wall slips over a flat that connects two segments of the fault that are dipping steeply.

Fault-bend folding produces rollover folds and flat-ramp folds that are parallel to the fault strike, but it is also possible to form folds which are oriented perpendicular to a fault. Fault-bend folds may be perpendicular to the strike of faults and coincide with bends in faults (John, 1987). This type of fold may be present in the Salmon basin where the northwest-striking Salmon basin detachment fault, which bounds the northeastern edge of the basin, joins the west-northwest striking Lemhi Pass fault.

Fault propagation folds form above normal faults that have not cut through to the surface. The normal faults associated with fault propagation folds project toward or up dip of the anticlinal flexure (Patton, 1984; Patton

and Fletcher, 1995; Cooke and Pollard, 1997; Janecke et al., 1998). These folds are difficult to identify, because often the controlling fault is not seen, so they may be mistaken for fault-bend folds (Janecke et al., 1998).

Fault drag folds are produced in rocks adjacent to fault planes by frictional resistance (Twiss and Moores, 1992; Davis and Reynolds, 1996). These folds are localized and occur only close to the associated normal fault (Janecke et al., in press).

EPISODE 1 OF EXTENSION

The earliest episode of extension in the southeast Salmon basin is characterized by one northeast-striking normal fault (Figure 8). The fault in the study area associated with this early episode of extension is fault K (Figure 8; Table 5).

Fault K has a trace that extends east-northeast along the southern edge of Pattee Creek from the northeast corner of section 14 of T19N, R24E, where it is truncated by the Muleshoe fault, to Ghoul basin, where it is truncated by the younger Lemhi Pass fault (Plate 1). Fault K primarily cuts Precambrian quartzites, but it does cut the volcanic sequence at its eastern end. This fault has been interpreted as having a planar geometry, because it lacks a fold in its hanging wall. Fault K has 244 m of left separation where it cuts the volcanic sequence. Several small faults parallel to fault K die out in the Challis volcanic sequence. Because of this relationship, I assign a

TABLE 5. DESCRIPTION OF NORMAL FAULTS IN THE SOUTHEASTERN SALMON BASIN

Fault	Strike and dip	Episode of extension	Geometry used in cross-sections	Length (km) in study area	Amount of dip-slip displacement (km)	Heave (km)	Comments
Salmon basin(SBDF) detachment	166°/12°W* 140°/24°W†	3iii	planar	>7.0 km	>1.9 >2.0	>1.9 >2.0	Main detachment fault in study area
Lemhi Pass	107°/24°W† 105°/22°W†	3i	listric ?	>7.5 km	>1.3	>1.2	Offset by the SBDF
Agency - Yearian	204°/38°W† 194°/32°W† 189°/34°W† 189°/29°W† 186°/26°W† 230°/22°W† 207°/27°W† 237°/34°W† 221°/30°W† 202°/32°W† 237°/34°W†	2	listric plus ramp	>8.0 km	>1.1 6-7 km from Staatz (1979)	>0.9	Change in strike may reflect folding by the Warm Springs anticline. Fault H probably reactivated west-dipping portion
Beaverhead		4	planar	>3.0 km	?		Basin and Range fault; North end is arbitrarily placed at Agency Creek
Dan Patch	161°/45°E†	?	?	>2.5 km	>0.5	>0.3	modified from Staatz (1979)
Muleshoe	230°/24°W† 206°/31°W† 193°/21°W†	3iii	planar ?	7 km	>2.0	>1.7	Cuts fault C, main splay of the SBDF
A§	143°/34°E† 136°/56°E†	4?	planar ?	>7.5 km?	0.4	0.3	This fault has not been verified in the field.
B	156°/31°E† 126°/26°E†	4	planar ?	>5.3 km?	>0.4	>0.3	
C	104°/39°W† 179°/29°W† 146°/27°W†	3ii	listric ?	16.0 km	>1.5 >1.8	>1.3 >1.6	Merges with west dipping part of Agency-Yearian fault at its southeast end. Postdates the Warm Springs anticline, but is cut by the Muleshoe fault
D	149°/42°W† 109°/22°W†	3i	listric	5.7 km	1.8	1.3	Displaced strand of the Lemhi Pass fault
E	166°/39°W†	3i	listric	3.4 km	>0.3	>0.2	Displaced strand of the Lemhi Pass fault
F§	028°/79°E†	?	planar	3.0 km	>0.8	>0.1	A fault scarp developed in Qal at Baldy Creek.
G§	188°/21°W† 180°/23°W†	?	planar	10.0 km	3.5	3.3	uncertain geometry at northeast end
H	149°/32°W†	3iii	planar	6.5 km	220 m	0.2	Splay of Salmon basin detachment fault which reactivated the Agency-Yearian fault.
I	173°/44°W†	?	planar	2.0 km	200 m	0.01	
J	064°/63°E†	2	planar	4.5 km	210 m	95 m	Antithetic to the Agency part of the Agency-Yearian fault.
K	061°/76°E†	1	planar	6.5 km	300 m	70 m	
L	115°/65°W*	4	planar	2.0 km	?		

* = direct measurement
† = three point problems
§= Fault identified on aerial photographs. Existence has not been confirmed in the field.

syn–Challis age to fault K and its associated faults. Episode 1 was very minor in the southeast Salmon basin.

Other workers in east-central Idaho and southwest Montana have previously documented northeast-striking faults and assigned a middle to late(?) Eocene age to the faults (McIntyre et al., 1982; M'Gonigle et al., 1991; Janecke, 1992, 1995; VanDenburg, 1997; VanDenburg et al., 1998). These faults were active during Challis volcanism and faulting continued until shortly after volcanism in some areas (49.5 to 45 Ma), and document a period of northwest-southeast extension.

EPISODE 2 OF EXTENSION

The second episode of extension occurred along the north northwest-striking and west southwest-dipping Agency-Yearian normal fault. The Agency-Yearian fault can be divided into the northwest-dipping Agency portion and the southwest-dipping Yearian portion (Figure 1; Figure 8; Plate 1). These were initially mapped by Staatz (1979) as two separate faults, but are interpreted as one fault in this study. The Yearian portion of the fault may have been later reactivated in episode 3 by fault C, fault H, and the Salmon basin detachment fault.

The Agency-Yearian fault can be traced for at least 17 km overall, and it places middle Eocene volcanic rocks and overlying cobble to boulder conglomerates (Tcg3) onto Middle Proterozoic quartzites (Figure 8). Its trace extends from the southeastern edge of the map area east of Cow Creek to approximately 1.2 km east southeast of the Lucky Horseshoe mine where it is

truncated by a strand of the Lemhi Pass fault (Figure 8). This crosscutting relationship and the presence of conglomerates (Tcg3) in the hanging wall indicate that the Agency-Yearian fault was active after the end of middle Eocene Challis volcanism, but before the Lemhi Pass Fault, of middle Eocene to early Oligocene age (VanDenburg, 1997). These data indicate that slip on the Agency-Yearian fault occurred between middle Eocene and early Oligocene time.

Calculations from cross sections show a minimum of 1.12 km of dip-slip displacement, but it is probably greater along the Agency-Yearian fault on cross-section C-C' (Plate 2). Approximately 6-7 km of dip-slip displacement is consistent with cross-section A-A' of Staatz (1979), where correlative rocks are in both the hanging wall and footwall of the fault. Associated with the Agency-Yearian fault is fault J, which is probably a small antithetical fault in the hanging wall of the Agency segment of the Agency-Yearian fault (Figure 8; Plate 1).

The location of the offset portion of the Agency-Yearian fault in the footwall of the Lemhi Pass fault is uncertain, but the alignment of the Yearian segment of the Agency-Yearian fault and the Salmon basin detachment fault to the north-northwest suggests that the Agency-Yearian fault might continue further north as an older portion of the Salmon basin detachment fault. If this is the case, the Salmon basin detachment was active twice: first, during episode 2 and the deposition of the sedimentary rocks of Tendoy, and second, during episode 3iii and the deposition of the sedimentary rocks of

Sacajaweja. Further work north of the study area is required to confirm the possibility of recurrent movement along the Salmon basin detachment fault.

The Agency-Yearian fault may temporally correlate with the master detachment fault of the Eocene to Oligocene rift zone, the Muddy-Grasshopper detachment fault (Janecke et al., 1996a, 1996b; Perry and M'Gonigle, 1995), and the master detachment fault of the Eocene to Oligocene rift (Figure 1). Both the Muddy-Grasshopper detachment fault and the Yearian portion of the Agency-Yearian fault have similar strikes and dip directions and cut post-Challis sedimentary rocks (Figure 8; Janecke et al., 1996a, 1996b and in press). The Muddy-Grasshopper detachment fault was active during late middle Eocene to early Oligocene time (post 46 Ma and pre 27 Ma; Janecke et al., in press). The 46 Ma to post 31Ma (?) age of the syntectonic sedimentary rocks of Tendoy in the hanging wall of the Agency-Yearian fault suggests it may have been active at about the same time.

The strike of the Agency-Yearian fault changes from 237° to 186° from the northeast (near Flume Creek) to the southwest (east of Cow Creek) (Plate 1). This change in strike may be the result of the subsequent folding of the Agency-Yearian fault by the Warm Springs anticline, and will be discussed later. Overall this fault represents east-west extension. Both the Agency and Yearian faults were described by Staatz (1979) as being nearly vertical, but three-point analysis of the remapped fault trace shows it to be low angle with an average dip of 31° near the surface (Table 5). At depth, the Agency-Yearian fault is interpreted to flatten and then ramp more steeply beneath the Tendoy anticline and Pattee Creek syncline (cross-sections C-C', Plate 2).

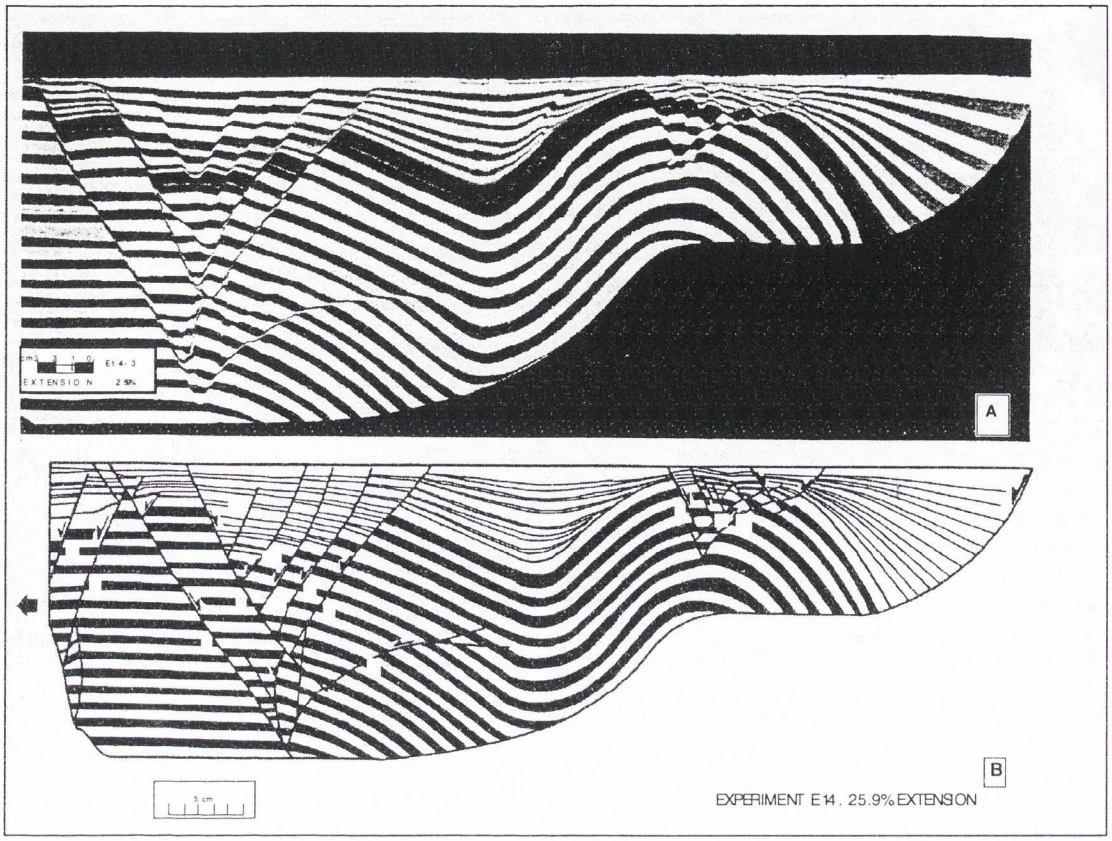

Figure 11. McClay (1989) analog model demonstrating the effect of the flat-ramp geometry of a normal fault on pretectonic (dark, thick layering) and syntectonic deposits (light, thin layering) in the hanging wall. The original figure was inverted to facilitate comparison with cross-section C-C', Plate 2.

The Tendoy anticline and Pattee Creek syncline are an anticline syncline pair in the hanging wall of the Agency-Yearian fault (Figure 10; Plate 1). The Tendoy anticline and Pattee Creek syncline are probably related to the Agency - Yearian fault, because the growth sedimentation patterns are consistent with those predicted by physical models of McClay (1989; Figure 11). The close parallelism of the fold axes to the strike of the fault also supports the interpretation that the anticline-syncline pair is related to the Agency-Yearian fault. The axes of the northern parts of the Tendoy anticline and the Pattee Creek north syncline are nearly parallel with the corresponding Agency portion of the Agency-Yearian fault. (The angles between the strike of the fault and trends of the folds are +17° for the Tendoy anticline and -18° for the Pattee Creek north syncline.) The axis of the Pattee Creek south syncline also nearly parallels the Yearian portion of the Agency-Yearian fault (22°).

The Tendoy anticline extends from the southern end of the study area between the Lemhi River and Cow Creek, north to the Lemhi Pass fault southeast of Pattee Creek (Figure 10; Plate 1). It folds Middle Proterozoic quartzites, Challis volcanic rocks, and the sedimentary rocks of Tendoy (cross-section C-C' Plate 2). At its north end, it plunges 02° toward 022°, has an interlimb angle of 106°, and an estimated maximum fold height of 2.2 km along cross-section F-F' (Plate 2). The normal fault associated with its formation is the Agency-Yearian fault, and the angle between the strike of the

fault and the fold axis is 16.6° at its northern end, making this a longitudinal fold. This anticline is not related to a plunging ridge in the underlying Lemhi Pass fault because the position of the ridge is not below the axial trace of the anticline, nor are sedimentation patterns consistent with this model (see below). A down-dip projection of the Lemhi Pass fault surface reveals that the axis of the Tendoy anticline does not coincide with the bend at the intersection of the Lemhi Pass fault and Salmon basin detachment fault (see point marked * in Section C-C'). The anticline's northwestern flank contains angular quartzite-clast-dominated conglomerates (Figure 12a) that may be derived from the core of the anticline, or from the footwall of the Lemhi Pass fault. The conglomerates on the southeastern flank of the anticline contain abundant volcanic clasts and are more rounded than the ones on the northwestern flank (Figure 12b). Conglomerates on the southeastern flank had two probable source areas 1) the footwall of the Agency-Yearian fault and 2) the core of the Tendoy anticline. The difference in the composition and character of the conglomerates on either side of the fold indicates that the Tendoy anticline was active during sedimentation and segmented the basin into subbasins.

The Pattee Creek syncline parallels the Tendoy anticline for its entire length of 11.8 km (Figure 10; Plate 1). It folds Middle Proterozoic metasedimentary rocks, Challis volcanic rocks, and the sedimentary rocks of Tendoy (cross-section C-C' Plate 2). The Pattee Creek syncline has been

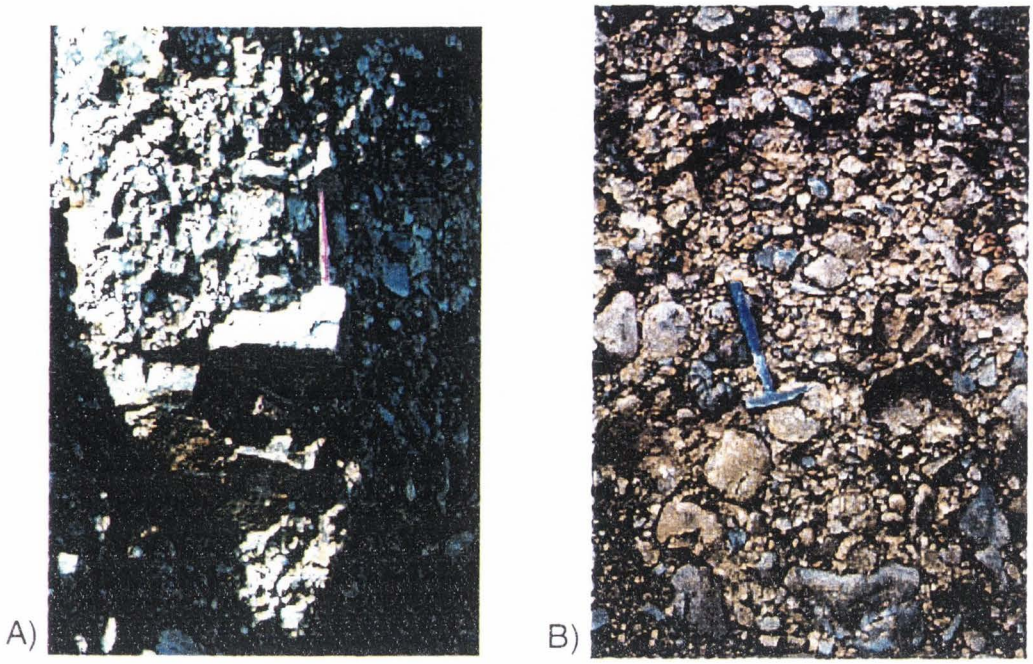

Figure 12. Photograph comparing conglomerates in the sedimentary rocks of Tendoy on the east and west flanks of the Tendoy anticline. (A) Pattee Creek east facies is from the northwest flank of the Tendoy anticline and is dominated by angular middle Proterozoic quartzite clasts. (B) Flume Creek facies is from the southeastern flank of the Tendoy anticline and has abundant volcanic clasts. Note the angular clast-supported character of the conglomerate in photo A, and the rounded clast-supported character of the conglomerate in photo B.

divided into a north and south section, because Quaternary cover along the Lemhi River does not allow for the continuous trace of the structure to be observed. The northern segment of the syncline plunges 21° toward 239°, and has an interlimb angle of 117°. The syntectonic sediment preserved on the northwest limb of the Pattee Creek north syncline is about 1400 m thick and on the southeast limb only about 400 m thick (cross-section C-C', Plate 2). The southern portion of the Pattee Creek syncline has a plunge and trend of 10°/010°, and an interlimb angle of 137°. The angle between the strike of the adjacent part of the Agency-Yearian fault and the trend of the Pattee Creek south syncline fold axis is 22°, and the fold and fault have an 18° angle between them in the northern portion. Although cross-sections do not show large changes in thickness of the sedimentary rocks across the southern portion of the Pattee Creek syncline (cross-section H-H', Plate 2) like that observed across the northern half of the syncline, there is a major change in the type of sedimentary rock across the fold (Figure 6). The west-northwestern limb of the Pattee Creek south syncline has a thick sequence of conglomerates (Tcg3) whereas the east-southeastern limb of the syncline does not (cross-section H-H', Plate 2). The presence of Basin and Range faults at the southern end of the syncline may have faulted out part of the Tertiary section, and changed the apparent thickness of the sedimentary rocks on opposite limbs of the Pattee Creek south syncline.

Physical models of fault-bend extensional folds by McClay (1989; Figure 11) match the fault and fold geometries and syntectonic sedimentation patterns around the Agency-Yearian fault, Tendoy anticline, and Pattee Creek syncline. Because the model closely matches the field observations, the Tendoy anticline and Pattee Creek syncline are interpreted as forming above of a longitudinal ramp and flat in the underlying Agency-Yearian fault. The Tendoy anticline is interpreted as a rollover fold above the listric east part of the Agency-Yearian fault, whereas the Pattee Creek syncline is interpreted as forming above a deeper ramp in the fault. This interpretation is consistent with the thickness variation in the syntectonic sedimentary rocks preserved in the Pattee Creek north syncline and the change in the character of the conglomerates on the two flanks of the Tendoy anticline (see below).

EPISODE 3 OF EXTENSION

The third episode of extension represents the largest amount of extension in the field area, is characterized by northwest-striking faults, and has at least three distinct subphases of faulting. The faults associated with this event are the Lemhi Pass fault, fault D, fault E, the Salmon basin detachment fault, and fault C (Figure 8; Table 5; Plate 1). This episode of extension allowed for the preservation of the volcanic sequence, sedimentary rocks of Tendoy and Sacajaweja, and structurally completed the formation of the Salmon basin. The three subphases were identifed on the

basis of cross-cutting relationships, but all accommodate roughly east-northeast to west-southwest extension.

The first phase (3i) of faulting associated the third episode of extension occurred along the Lemhi Pass fault (Figure 8; Plate 1). This is a large west-northwest-striking southwest-dipping normal fault in the Agency Creek and Goldstone Mountain quadrangles that places middle Proterozoic quartzites, volcanic rocks, and syn-Challis cobble- to boulder-conglomerates (Tcg2) against Middle Proterozoic quartzites. The Lemhi Pass fault probably also postdates folded conglomerates (Flume Creek facies of Tcg3) in its hanging wall. This fault has a minimum of 1.2 km of heave and 1.3 km of dip-slip displacement shown along cross-section D-D' (Plate 2). The Lemhi Pass fault is exposed along the northern boundary of Ghoul basin and its trace extends from its intersection with the Muleshoe fault near Pattee Creek southeast to the eastern edge of the map area 3 km east of the confluence of Agency Creek and Flume Creek (Figure 8). A fault line scarp along strands of the Lemhi Pass fault is apparent looking west northwest from Lemhi Pass across Ghoul basin. In Ghoul basin, fault rocks are exposed near the northeast corner of section 8, T19N, R25E. These fault rocks are brecciated and deform younger(?) quartz-sanidine ash-flow tuff in the hanging wall of the Lemhi Pass fault. The Lemhi Pass fault extents east southeast into the Horse Prairie basin of southwest Montana, where it is overlain by the sedimentary rocks of Everson Creek which contain Arikareean (29-20.5 Ma)

vertebrate fossils (VanDenburg, 1997). Altogether the Lemhi Pass fault is at least 18 km long. The overlapping Arikareean sedimentary rocks and the angular unconformity at their base led VanDenburg (1997) to assign a middle Eocene to early Oligocene age to the Lemhi Pass fault.

Previous workers interpreted the Lemhi Pass fault to be a steep fault that was first active prior to Challis volcanism and was then reactivated after Challis time (Staatz, 1979; Hansen, 1983). VanDenburg (1997) argued against multiple episodes of extension along the Lemhi Pass fault and a steep geometry. This study agrees with VanDenburg's (1997) interpretation of the Lemhi Pass fault as a listric low-angle structure. Three-point analyses in the Agency Creek quadrangle yielded southwest dips of 24° and 22° along the fault's trace (Table 5; cross-section D-D', Plate 2), which agree with VanDenburg's determination of a 24° dip along the fault in the Horse Prairie basin. The low angle of the fault may be the result of the fault's possible listric geometry.

Faults E and D are interpreted as the displaced western continuations of the Lemhi Pass fault (Figure 8; Plate 1). They have been displaced to the right 1.9 km along the younger Muleshoe fault. Several lines of evidence suggest that faults D and E correlate with the Lemhi Pass fault. They both have northwest strikes, although the northern ends of faults D and E have strikes that are more northerly than the Lemhi Pass fault. The amount of separation along Muleshoe fault between faults D and E and the Lemhi Pass

fault is nearly identical to the amount of right separation produced by the Muleshoe fault when it cut fault C. In several places the Lemhi Pass fault separates into two strands with the same spacing (0.8 km) as faults D and E. The Lemhi Pass fault separates into three strands, once in sections 5 and 6 of T19N, R25W, and into two strands where the fault crosses Flume Creek. The northwest end of faults D and E cut sedimentary rocks (Tcg3) and are overlapped by younger sedimentary rocks (Tcg4). Almost identical cross-cutting relationships characterize the east end of the Lemhi Pass fault in the Horse Prairie basin (VanDenburg, 1997). The absence of Challis volcanic rocks in the footwall of fault E suggests that slip was broadly occurring at the same time as the deposition of the sedimentary rocks of Tendoy. Challis volcanic rocks once in the footwall of fault E were eroded after slip on faults D and E and before slip on the Salmon basin detachment fault. Had slip only occurred after the depositon of the sedimentary rocks of Tendoy and before slip on the Salmon basin detachment fault, part of the volcanic sequence would have been preserved in the footwall of fault E and in the hanging wall of the Salmon basin detachment.

The present level of erosion along the Lemhi Pass fault and along faults D and E may not be the same, because faults D and E are dropped down in the hanging wall of the younger Salmon basin detachment fault relative to the Lemhi Pass fault. Therefore the steeper dips of faults D and E relative to the Lemhi Pass fault may be due to different levels of exposure

along a listric Lemhi Pass fault. A decrease in slip across the Lemhi Pass fault to the northwest may also give faults D and E steeper dips.

Fault E has a trace length of 3.5 km and is exposed from Kenney Creek southeast to just north of Warm Spring road where it merges with fault D (Figure 8; Plate 1). This west-northwest-striking, southwest-dipping normal fault contains Challis volcanic rocks in its hanging wall and a breccia of Middle Proterozoic quartzites in its footwall. At the northwest end of fault E, just north of Kenney Creek, the fault is lapped by younger cobble to boulder conglomerates of the sedimentary rocks of Sacajaweja (Tcg4). The southeast end of the fault may be truncated by the younger Muleshoe fault and this results in 1.9 km of right separation. Cross-section B-B' shows a minimum of 250 m of dip-slip displacement across fault E, but slip was probably greater because correlative Tertiary rocks are lacking from the footwall.

Fault D is directly to the southwest of fault E and extends from the eastern end of the Warm Springs road in the study area to just north of Kenney Creek where it is overlain by Tcg4 (Figure 8, Plate 1). This west-northwest striking-southwest dipping normal fault has 1.8 km of dip-slip displacement and 1.35 km of heave (cross-section B-B'). Fault D contains conglomerates (Tcg3) in its hanging wall and volcanic rocks in its footwall. Fault D merges with fault E near Kenney Creek.

The Warm Springs anticline, a large rollover anticline in the hanging wall of fault D, is interpreted as a fault-bend fold in the hanging wall of the Lemhi Pass fault (Plate 1; cross-sections I-I', Plate 2). The Warm Springs anticline extends from Kenney Creek southeast to at least Pattee Creek. It, like the genetically related Lemhi Pass fault, is probably cut by the Muleshoe fault strand of the Salmon basin detachment, and continues southeast into the footwall of the Agency-Yearian fault (Figure 10). This large anticline folds Challis volcanic rocks and syntectonic sedimentary rocks (Tcg3, and Tsh; cross-section I-I', Plate 2). The Warm Springs anticline, in the area around the Warm Springs road, plunges 35° toward 123° and the mean fold spacing between it and the adjacent syncline to the northeast is 1.8 km. The associated normal faults are fault D and E (primarily D) and the angle between their strike and the trend of the fold is 14°. The south-east plunge of the fold near the Warm Springs road can be attributed to the position of the anticline on the northwest limb of the Pattee Creek syncline. This interference between the preexisting Pattee Creek north syncline and the Warm Springs anticline results in the 35° southeast plunge of the Warm Springs anticline in this area. If the Warm Springs anticline continues to the southeast in the footwall of the Muleshoe fault, then the pronounced change in strike between the Agency and Yearian parts of the Agency-Yearian fault, approximately 2 km east of the confluence of Agency Creek and Cow Creek, may be due to folding of the fault by the Warm Springs anticline. Stereogram

analysis of the plane of the Agency-Yearian fault as a folded structure shows a trend of 302° (Figure 13a). This trend is identical to the trend of the Warm Springs anticline on the northwest limb of the Pattee Creek north syncline (Figure 9; Table 4). Other evidence for the Warm Springs anticline between the Agency-Yearian and the Muleshoe faults includes bedding attitudes from Middle Proterozoic quartzites (from Staatz, 1979) showing rocks folded about a northwest-trending axis (Figure 13b), and cross sections showing Challis volcanic rocks folded into a southeast-plunging anticline (cross-section D-D', Plate 2)

The Campground syncline is immediately southwest of the southeastern portion of the Warm Springs anticline at Agency Creek (Plate 1). This broad syncline plunges 35° toward 121°, and has an interlimb angle of 140°. The Campground syncline folds a thick sequence of Tertiary lava flows, the tuff of Curtis Ranch, and the younger quartz-sanidine ash-flow tuff (cross-section D-D', Plate 2). This fold could be associated with the Agency-Yearian fault or the Lemhi Pass fault. If the Agency-Yearian fault is responsible for its formation, it is a transverse fold and possibly a displacement-gradient fold. It may also be a longitudinal fold that formed in the hanging wall of the Lemhi Pass fault. This is the preferred interpretation because of its parallelism with the southeastern portion of the Warm Springs anticline.

The next phase of faulting occurred along the northwest-striking and

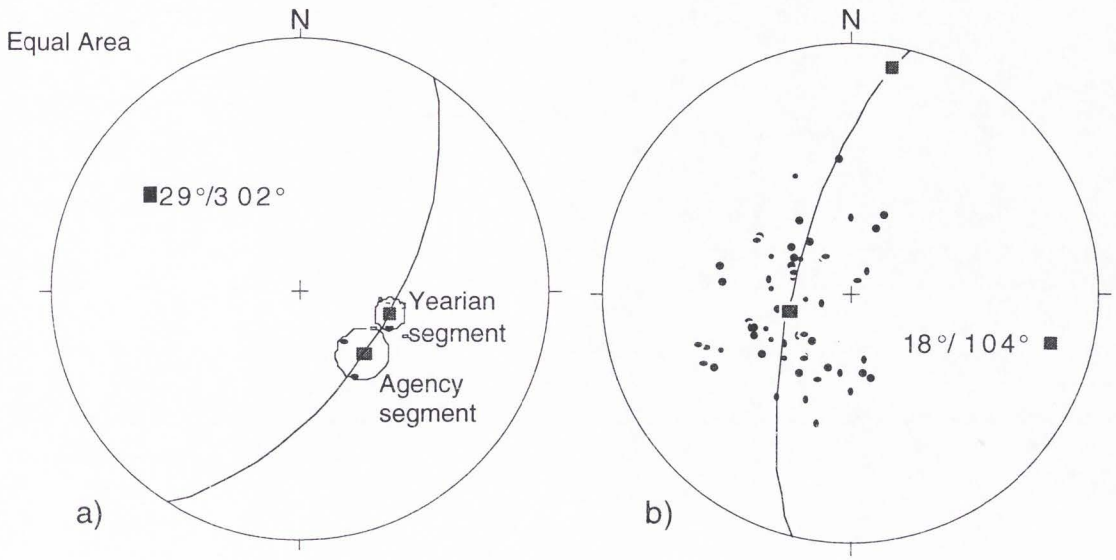

Figure 13. a) Stereogram of poles to the plane of the Agency-Yearian fault. Mean vectors with alpha 95% confidence cone are shown for each limb, and the cylindrical best-fit fold axis of the data is shown. b) Stereogram of the poles to bedding in middle Proterozoic quartzites in the core of the northeast-trending Tendoy anticline. A cylindrical best fit of the data show a fold axis with a trend and plunge of 104°/18°. The data are compiled from Staatz (1979).

southwest-dipping fault C (Plate 1). Fault C has a map trace 16 km long, and extends from 3 km northeast of the confluence of Kenney Creek and the Lemhi River to Cow Creek. The fault has 1.8 km of dip-slip displacement and 1.6 km of heave (Table 5; Figure 8). Fault C is interpreted as having a listric geometry, and soling into the proto-Salmon basin detachment fault, because of the presence of the Alkali anticline in the hanging wall of Fault C. This fault places cobble conglomerates (Tcg3) and shales (Tsh) against Challis volcanic rocks. The relative age of fault C can be determined because it cuts the large rollover anticline (Warm Springs anticline) produce by the Lemhi Pass fault (especially faults D and E), and it is cut by the Muleshoe splay of the Salmon basin detachment fault near Pattee Creek resulting in 1.9 km of right separation. These relationships indicate that fault C formed after the Lemhi Pass fault and before the Muleshoe splay of the Salmon basin detachment.

The Alkali syncline parallels fault C and is located in its immediate hanging wall (Figure 10; Plate 1). This syncline plunges 18° toward 128° and has an interlimb angle of 142° (Table 4). The Alkali syncline extends from Kenney Creek southeast to Pattee Creek and folds shales (Tsh), sandstones (Tss), and conglomerates (Tcg3). It is interpreted as a fault-drag fold because of its close proximity to fault C. Its southeast plunge is probably due to its position on the northwest limb of the Pattee Creek north syncline.

The Alkali anticline is a poorly exposed fold interpreted as having formed during phase 3ii, and being related to fault C. Lying in the hanging wall of fault C between the boundary of T20N and T19N and Agency Creek

approximately 1 km northeast of the Lemhi River, the Alkali anticline folds Tertiary siltstones and shales (Plate 1). The Alkali anticline is a longitudinal fold approximately 2 km southwest of fault C, which plunges 5° toward 179° and has an interlimb angle of 170°. This fold is interpreted as a rollover anticline in the hanging wall of fault C.

The final phase of faulting during episode 3 steps back into the footwall of faults D and E, and occurs along the Salmon basin detachment fault (Figure 8; Plate 1). This fault is responsible for forming much of the Salmon basin, and extends from the Salmon River north of North Fork, Idaho, southeast to Poison Gulch Spring just east of Pattee Creek, giving the fault a total trace length of 59 km. The Salmon basin detachment is interpreted as the youngest fault of episode 3 because it cuts conglomerates (Tcg4) which lap older faults (faults D and E), and because the Muleshoe splay of the Salmon basin detachment fault cuts the Lemhi Pass fault and fault C.

The Salmon basin detachment fault is well exposed along Kenney Creek where it was described by Tucker and Birdseye (1989). Tucker (1983) described the fault rocks as being cohesive crush rocks with veins of pseudotachylite that formed at the base of a overthrust plate in a mylonite zone. This study documented that the fault zone in Kenney Creek is a 3.5-m thick cataclasite zone that is cut by small faults, with relatively few slickenlines. Locally exposed along the fault surface is a foliated cataclasite, and not a mylonite or pseudotachylite as described by Tucker and Birdseye (1989). Thin-sections show no plastic deformation of quartz grains, amorphous, glassy, or devitrified pseudotachylite and the matrix has been

altered to clays (Figure 14). The fault rocks are consistent with a shallow structural level during their formation (James P. Evans, oral comm.).

The Salmon basin detachment fault (Figure 15) is interpreted as a planar northwest-striking, southwest-dipping fault that has at least 2 km of dip-slip displacement and 1.95 km of heave associated with it, but dip-slip is probably greater (Table 5, cross-sections A-A', B-B', Plate 2). If faults D and E are offset portions of the Lemhi Pass fault, zone as hypothesized earlier, then the Salmon basin detachment fault cuts the Lemhi Pass fault, resulting in 1.9 km of right-slip separation. The Muleshoe strand of the Salmon basin detachment cuts fault C and the Warm Springs anticline resulting in 1.9 km of right separation. This study noted that the strike-slip faults mapped by Tucker (1975) between Sandy Creek and Poison Gulch spring did not exist, and the Salmon basin detachment fault, which strikes 166°, has a sinuous trace as the result of its low dip angle (12°). Slickenline analysis along small subsidiary faults, in the footwall of the Salmon basin detachment fault along the north side of Kenney Creek, show the slickenlines plunge 17° toward 238° (Figure 16). These data indicate pure dip-slip motion along the 12° southwest-dipping Salmon basin detachment fault along Kenney Creek. The Salmon basin detachment fault may have reactivated the western part of the Lemhi Pass fault and transfer slip to the Dan Patch fault, but the critical cross-cutting relationships to constrain the age of the Dan Patch fault are lacking.

The Salmon basin detachment fault has two splays at its southern end near Pattee Creek. These splays are the northeast-striking, northwest-dipping Muleshoe fault and the north-northwest-striking, southwest-dipping

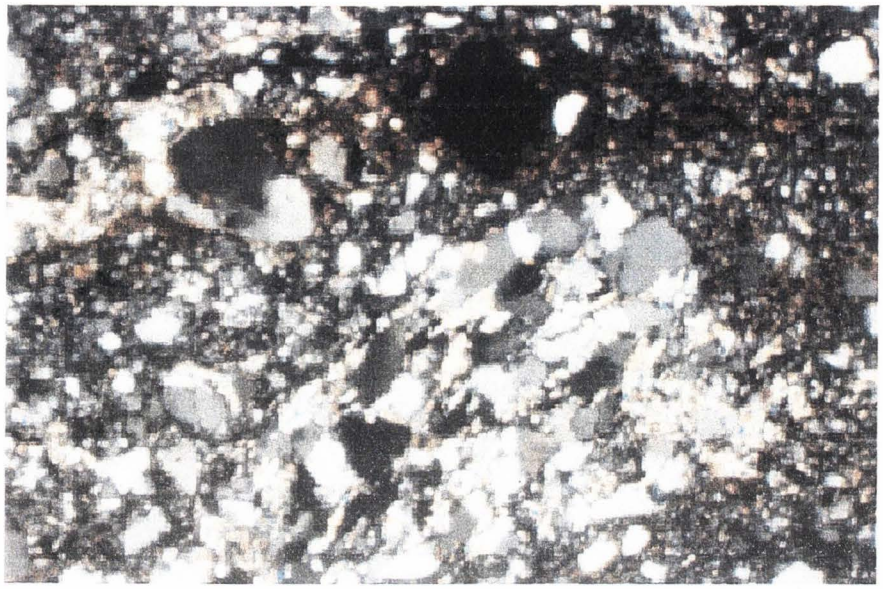

Figure 14. Photomicrograph of the foliated cataclasite along the fault plane of the Salmon basin detachment fault along Kenney Creek. Field of view is 3 mm across.

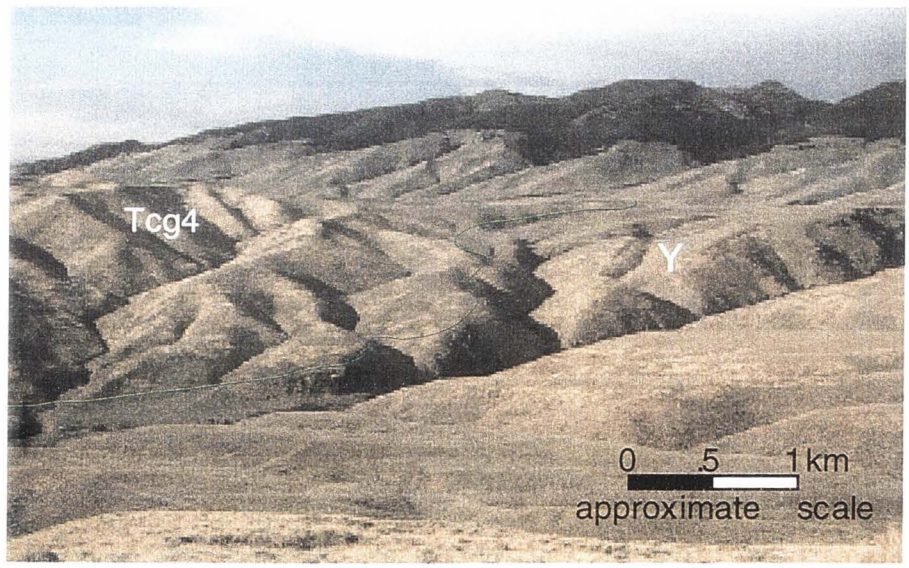

Figure 15. Photograph of the Salmon basin detachment fault looking north across Kenney Creek. Fault is outlined in green.

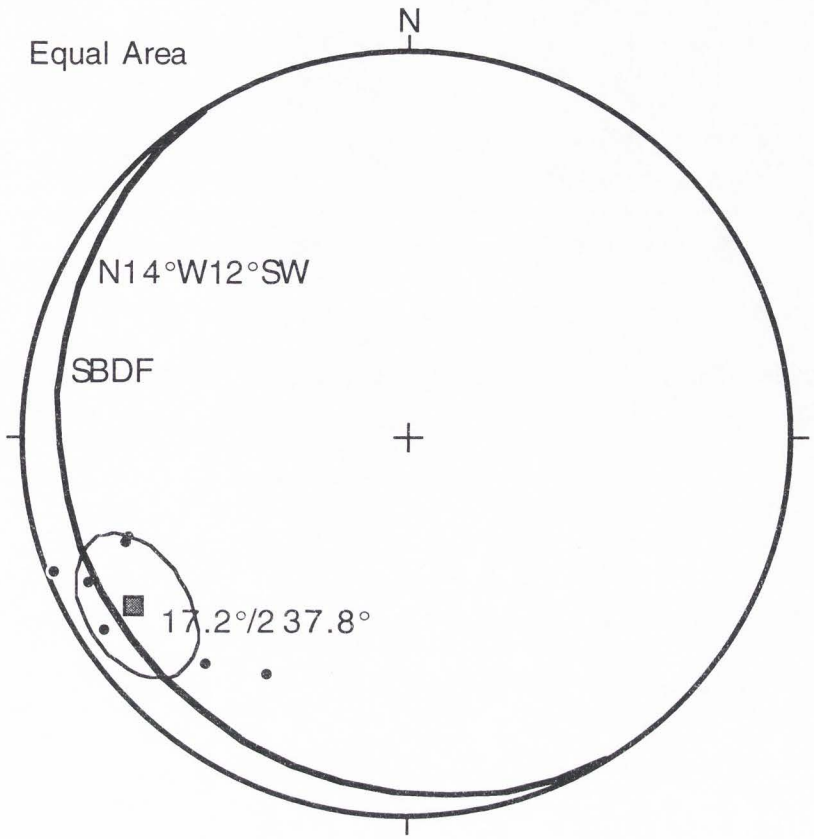

Figure 16. Slickenline data from small subsidiary faults in the footwall of the Salmon basin detachment fault, showing dip-slip movement on the Salmon basin detachment fault. Data were collected along Kenney Creek. Trend and plunge of the mean vector of the data are show with the 95% confidence cone. SBDF=Salmon basin detachment fault.

fault H (Figure 8; Plate 1). The Muleshoe fault extends from Poison Gulch Spring near Pattee Creek southwest to at least Agency Creek. South of Agency Creek it is unclear whether the fault continues or if the younger Beaverhead fault is the only fault present. I assigned the gently northwest-dipping fault northeast of Agency Creek to the Muleshoe fault and the poorly exposed and probably steeper northwest-dipping fault south of Agency Creek to the Beaverhead fault. The Muleshoe fault places cobble-to-boulder conglomerates (Tcg3) against Middle Proterozoic quartzites and Challis volcanic rocks. The Muleshoe fault has a trace length of 7 km and 1.8 km of dip-slip separation (Table 5; cross-section E-E', Plate 2). As defined here, the Muleshoe fault cuts fault C between Pattee Creek and Agency Creek and shows 1.9 km of right separation. This separation is identical to the amount of right separation produced by the Salmon basin detachment on the Lemhi Pass fault. The northwest-dipping Muleshoe fault is interpreted as one of the youngest faults of episode 2 because of its continuity with the young southwest-dipping Salmon basin detachment fault to the north, and because of the cross-cutting relationships detailed above. The anomalous northwest-dip direction of the Muleshoe fault may be due to an underlying ramp of the Agency-Yearian fault, into which the Muleshoe fault may sole.

Fault H is a small normal fault that extends for 6.5 km, from the southern tip of the Salmon basin detachment fault at Poison Gulch Spring near Pattee Creek, to 2 km east of the confluence of Agency Creek and Cow

Creek, where it merges with and may reactivate the Agency-Yearian fault (Plate 1). Fault H places middle-Eocene volcanic rocks against Middle Proterozoic quartzites, and has a curving southwest-dipping geometry. This fault has 180 m of dip-slip displacement and 150 m of heave along section E-E' (Plate 2).

The third episode of extension in the southeastern Salmon basin correlates with the third phase of extension documented in the Horse Prairie basin by VanDenburg (1997). The third episode of extension also correlates with extension in the rift zone of Janecke (1994). These correlations were made on the basis of fault orientation (north-northwest strikes) and the presence of the Lemhi Pass fault which extends into the Horse Prairie basin where VanDenburg (1997) assigned it to his phase three of deformation. Faults formed at this time also cut the entire volcanic sequence and the sedimentary sequence, and represent a period of east northeast/west southwest extension.

The presence of the sedimentary rocks of Tendoy in the hanging wall of the Lemhi Pass fault suggests that faulting during episode 3 initiated after their deposition (possibly post 31Ma). The correlation of the sedimentary rocks of Sacajaweja with the sedimentary rocks of Everson Creek indicate that the Lemhi Pass fault was active before 31-25 Ma.

Cross-cutting relationships loosely constrain the age of other faults that were active during episode 3. Since fault C cuts the Warm Springs

anticline which formed above the Lemhi Pass fault, faulting along it was either contemporaneous with or after faulting along the Lemhi Pass fault. Fault C and the Lemhi Pass fault are cut by the Salmon basin detachment, suggesting that this was the last fault to be active during episode 3. The end of faulting along the Salmon basin detachment fault is hard to pin down but was prior to the deposition of QTg. Temporal correlation of the Salmon basin detachment fault and the Maiden Peak fault (Figure 1) would indicate that faulting had ceased by late-middle Miocene (VanDenburg, 1997). Overall, episode 3 was active between late Eocene to early Miocene time.

EPISODE 4 OF EXTENSION

Episode 4 is characterized by northwest-striking Basin and Range normal faults, and includes fault A, fault B, and the Beaverhead fault (Figure 8, Table 5; Plate 1). All of the Basin and Range faults in the field area are in the southwestern portion of the field area. Faults B and A may be splays of the Beaverhead fault (Janecke, personal comm.), and further mapping south of the field area may clarify their origin. These three faults have been grouped on the basis of 1) similar orientation (northwest-striking, southwest-dipping); 2) apparent steep dips; and 3) apparent cutting of some of the youngest rocks (QTg) in the study area. Overall the Basin and Range faults represent a period of northeast-southwest extension.

The Beaverhead fault is a large north-northwest-striking Basin and Range fault that has a 151 km long trace with Holocene and late Pleistocene fault scarps, and can be divided into six segments (Crone and Haller, 1991).

The Beaverhead fault in the study area is probably part of the Lemhi segment of the Beaverhead fault which has a low slip rate and has no scarps in upper Quaternary alluvium (Crone and Haller, 1991). In the study area the Beaverhead fault is covered by Quaternary alluvium. It extends from Agency Creek (2.6 km southeast of the town of Tendoy) where the Muleshoe fault merges with it, to the southern edge of the field area (Figure 8; Plate 1). This fault is interpreted as having a steep (> 45°) dip angle and a planar geometry, based on an analogy with the Lost River fault (Richins et al., 1987), a similar Basin and Range fault exposed to the southwest. Because faults A and B appear to merge with the Beaverhead fault to the south, they are also assigned to episode 4.

Fault B is a northwest-striking normal fault that extends from 1.5 km west of the confluence of McDevitt Creek and the Lemhi River southeast to the Lemhi River 1.5 km north of the southern edge of the map area (Figure 8; Plate 1). This gives the fault a trace length of 5.3 km. The fault has 400 m of dip-slip displacement and 300 m of heave, and cuts late Cenozoic (?) conglomerates(QTg) (Table 5; cross-section H-H', Plate 2). Since this fault is interpreted as being a Basin and Range fault, it is interpreted as having a planar geometry.

Fault A is a large southwest-dipping normal fault that extends from McDevitt Creek along the southwestern edge of the study area southeast to the edge of the field area 1.5 km west of the Lemhi River (Figure 8; Plate 1). This fault has been mapped using aerial photographs and field reconnaisance and appears to duplicate a thick section of northeast-dipping

lava flows. The trace length of the fault is 7.5 km, but it is probably greater because it may merge with the Beaverhead fault south of the study area. This fault has 0.6 km of dip-slip displacement and 0.5 km of heave (Table 5; cross-section H-H', Plate 2). Fault A places conglomerates against volcanic rocks, and the base of the Challis volcanic sequence between McDevitt Creek and Muddy Creek shows 1.5 km of right separation. It is interpreted as having a planar geometry like the other Basin and Range faults in the region (Richins et al., 1987).

Initiation of Basin and Range faulting in the southeastern Salmon basin is hard to pin down since some of the faults may reactivate older faults of episode 3. The parallelism of Basin and Range faults in the southeast Salmon basin with other active northwest-striking normal faults in the region (Lost River fault, Lemhi fault, and Red Rock fault) suggests a strong temporal correlation between the faults. The presence of Quaternary scarps to the south along the Beaverhead fault and recent activity along the Lost River fault indicate that Basin and Range faults are still active (Crone and Haller, 1991).

NORMAL FAULTS OF UNCERTAIN AGE

Although fault G has only been mapped on aerial photographs (by S. U. Janecke), it appears to be a major northwest-dipping normal fault, with two strands that merge with or cut fault C at its northeastern end. It has a trace length of a least 10 km and is located in the northwestern part of the study area between Haynes Creek and Baldy Creek, extending northeast to Kenney Creek (Figure 8; Plate 1). The base of the volcanic rocks shows 1.2

km of left separation along fault G, and cross-section C-C' (Plate 2) shows 3.5 km of dip-slip separation. Mapping done with aerial photographs suggests that the fault cuts conglomerates assigned to the sedimentary rocks of Tendoy (Tcg3). If fault G does in fact cut Tcg3, then fault G is younger than most synvolcanic northeast-striking normal faults in this region and may have formed during episode of extension younger than episode 3, but before episode 4. If fault G is part of episode 2, it has an anomalous northeast-strike. Younger northeast-striking faults were documented by VanDenburg (1997) as forming during his phase 4, and fault G may be related to these northeast-striking normal faults. Future work may confirm the geometry and determine the age of fault G.

Fault F also has an orientation (northeast-striking and southeast-dipping) which is in contrast with other latest Cenozoic normal faults in the area and may be associated with fault G (Figure 8; Plate 1). The fault may have formed during a Miocene episode of extension (VanDenburg's phase 4). The fault appears to cut Quaternary alluvial deposits at Baldy Creek, but since it has only been mapped on aerial photographs north of Baldy Creek, a conclusive interpretation cannot be made. Future work may resolve this issue.

Fault L is a northwest-striking, southwest dipping fault that is exposed along Muddy Creek (Figure 8; Plate 1). The overall length of fault L is difficult to determine because it is only exposed north of Muddy Creek, but it is at least 2 km long. This fault may be a splay of the Beaverhead fault, but the sense of slip across the fault is difficult to determine. The Muddy

monocline may be associated with this fault, and if so, the orientations of the two structures indicate that the fault may have experienced reverse slip.

THRUST FAULTS

Only two possible thrust faults were identified in the study area. One possible thrust is along Warm Springs road in section 34, T 20 N, R 24 E, and the other possible thrust is north of Muddy Creek and south of McDevitt Creek in the southern portion of the study area (Plate 1). Both of these faults appear to be relatively minor structures and are probably related to extension. The possible thrust north of Muddy Creek may be associated with the formation of the Muddy monocline.

OTHER FOLDS

Longitudinal synclines are common in the hanging wall of many of the faults in the Salmon basin (Figure 8; Figure 10; Faults- G, C, D, and the Agency portion of the Agency-Yearian fault). The synclines are parallel with the normal faults for distances of up to 7 km along strike. Three possible mechanisms may be responsible for the formation of these synclines 1) fault-drag due to frictional resistance along the normal faults, 2) fault-bend folding above a rigid footwall block, and 3) fault-propagation folding. Fault-drag is the preferred interpretation, because if fault-bend folding were responsible, only a small portion of the hanging wall would display a syncline, and it is unlikely that erosion is at the same level at all locations where the synclines occur. Also, axial surfaces should dip steeply toward the associated normal fault if the mechanism is fault-bend folding, and should be subparrallel to the

associated normal fault for fault-drag folding. The synclines typically occur close to the associated normal fault, which is an observation consistent with the fault-drag mechanism. If the mechanism was fault-bend folding, the distance between the fault and the associated normal fault would depend on the size and geometry of the fault-bend. It is difficult to distinguish between fault-drag and fault-propagation folds, because fault-drag folds may have initiated as fault-propagation folds.

The Muddy monocline is a small but well-exposed structure that is noteworthy because it is a monocline with overturned beds (Figure 17). This monocline is directly north of Muddy Creek and south of McDevitt Creek(Figure 10; Plate 1). The Muddy monocline plunges 11° toward 292° and has an interlimb angle of 129°. It folds tuffaceous siltstones, shales, and lignites. The Muddy monocline appears to be a longitudinal fold because of its parallelism to fault L. Fault L cuts the steep to overturned limb of the Muddy monocline, strikes 115° and dips 65° SW, but its sense of slip is unclear because correlative marker beds are absent. The odd cut-off angle with subvertical beds in the footwall of fault L suggests that it may cut a preexisting fold. Because the fold may be related to slip along fault L, which might be a Basin and Range fault, the Muddy monocline is potentially the youngest fold in the study area.

The Flume Creek syncline is located at the confluence of Flume Creek and Agency Creek (Figure 10; Plate 1). At its northern end it is plunging 27° toward 153° and has an interlimb angle of 141°. The plunge and trend reverses near the Agency-Yearian fault at its southern end, where the White

Figure 17. Photograph of the Muddy monocline. Photograph was taken looking northwest across Muddy Creek toward the structure.

Creek and Flume Creek synclines intersect. The youngest rocks affected by the Flume Creek syncline are coarse cobble to boulder conglomerates of the Flume Creek facies of the middle conglomerate (Tcg3), and the fold is located in the hanging walls of the Lemhi Pass, Agency-Yearian, and the Dan Patch faults. The syncline is oblique to the Lemhi Pass fault, transverse to the Agency-Yearian fault, and subparallel to the Dan Patch fault (Table 4; Figure 9; Figure 10). The map trace of the axial surface and proximity to the Lemhi Pass fault of the Flume Creek syncline indicate that it may be a continuation of the syncline in the hanging wall of faults D and E (the western

segments of the Lemhi Pass fault). The map traces of the hingelines of both synclines indicate that the axial surfaces of both synclines are inclined. The exact mechanism responsible for the formation of the Flume Creek syncline cannot be pinned down because of its proximity to three large faults, but it was probably the result of multiple episodes of folding. This type of fold is called a compound fold (Janecke et al., 1998).

Several other folds were mapped in the study area but poor exposure and insufficient bedding attitudes preclude a detailed analysis. These folds include a possiable broad rollover anticline (anticline V) into the Salmon basin detachment. The anticline is east of a south-plunging anticline-syncline pair (anticline T, and syncline U) in the hanging wall of the merged faults D, E, and G between Kenney and Sandy Creeks. Another large anticline (anticline W) was identified on aerial photographs near Baldy Creek (Figure 10) where it parallels fault G and fault F.

Fold trains are located in two parts of the study area. The area between Pattee and Agency Creeks contains two small fold trains (trains X and Y), and the second area at the confluence of Flume Creek and Agency Creek contains a small fold train that parallels the Flume Creek syncline (train Z; Figure 10). Train Z is probably a subsidiary structure to the larger Flume Creek syncline.

DISCUSSION OF FOLDS AND FAULTS

The southeast Salmon basin has abundant folds, and these folds are related to the normal faults occurring in the area. Overall, extensional folds in

the study area are longitudinal folds with interlimb angles between 106° and 170° (open to gentle folds; Figure 9; Table 4). The angle between the axial plane of the folds and their associated normal fault ranges from 50° to 87°, and the bisecting surfaces of folds are close to vertical (89° to 75°) for folds with two limbs (Figure 9; Table 4). Most of the extensional folds in the study area are interpreted as fault-bend folds, and it is the recognition of extensional folds in the study area that has lent insights to the subsurface geometry of the associated normal faults.

Although many of the faults in the study area are interpreted as having a planar or listric geometry, the Agency-Yearian fault is interpreted as having a flat and ramp geometry because this geometry can explain the anticline-syncline pair in its hanging wall. The formation of this anticline-syncline pair has influenced sedimentation during the second episode of extension and during the deposition of the sedimentary rocks of Tendoy. The Lemhi Pass fault also has a listric geometry which has produced the Warm Springs anticline rollover fold. Superimposed folds produced dome and basin features within the study area, which has complicated the recognition of faults responsible for their formation.

BASIN EVOLUTION

The southeastern Salmon basin has four distinct evolutionary periods which resulted in the superposition of four distinct unconformity-bounded depositional sequences. The first period predates the development of the modern Salmon basin and is characterized by a large east-trending paleovalley and emplacement of up to 1.4 km of volcanic rocks. During the second period of development, most of the Salmon basin formed, and most of the sedimentary rocks in the study area were deposited. The geometry of the basin was modified during the third period, and erosional processes dominated in the final period. Normal faulting accompanied the second and third period.

Harrison (1985) hypothesized that the Salmon basin experienced evolving depositional systems during a single episode of extension. Harrison (1985) was led to this conclusion because she did not document angular unconformities in the depositional sequence, and lacked structural data, and an accurate geologic map. She suggested that initially a lake developed as a result of damming by Challis volcanics, then braided stream-dominated systems developed, and finally the fluvial system changed to mix-load stream channels (Harrison, 1985). This study did not confirm Harrison's interpretation, because it identifies at least three unconformity-bounded sequences of sedimentary rocks that were not identified by Harrison, and not one but several distinct episodes of extension.

METHODS

Pebble counts were conducted at 23 different cemented-conglomerate exposures within the field area (Table 6). At each site the composition of 50 clasts was recorded. Clasts included gray quartzite, white quartzite, red quartzite, granite, and volcanic rocks. The sources of the various quartzites were the Yellowjacket, Apple Creek, and Gunsight Formations for the gray quartzites clasts, the Swauger Formation for red quartzites clasts, and the Ordovician Kinnikinic Quartzite or quartz veins from Middle Proterozoic quartzites for the white quartzite clasts. No clasts of the Carmen stock were observed. Volcanic rocks were differentiated between tuff and lava where possible. To avoid a counting bias, the pebble counts were conducted by starting at a central clast and counting every clast in a spiral away from the central cast. Pebble count data, along with the detailed description of the outcrop that the count was taken from, were used to make paleogeographic reconstructions and to interpret depositional environments.

Pebble counts were plotted on maps and used with sediment-distribution maps to determine the paleogeography of the southeastern Salmon basin (Figure 18; Figure 19). Three types of sediment distribution maps were made. The first grouped sedimentary rocks of the same type together (conglomerate vs. sandstone vs. shale/siltstone) (Figure 6). This map was constructed to discriminate between basin-margin and basin-center facies. The second map shows compositions of conglomerates in the basin, and distinguishes between conglomerates with volcanic clasts, Middle Proterozoic quartzites clasts, or a mixture of volcanic and quartzite clasts

TABLE 6. PEBBLE COUNT DATA FROM THE SOUTHEASTERN SALMON BASIN

Count #	Percent gray quartzite	Percent white quartzite	Percent red quartzite	Percent total quartzite	Percent volcanic (lava)	Percent tuff	Percent total volcanic	Maximum clast size (cm)	Map unit
1	66%	17%	17%	100%	0%	0%	0%	150	Tcg1
2	34%	0%	3%	37%	63%	0%	63%	17	Tcg3
3	37%	3%	0%	40%	60%	0%	60%	15	Tcg3
4	53%	10%	0%	63%	27%	10%	37%		Tcg3
5	60%	33%	0%	93%	7%	0%	7%	10	Tcg3
6*	60%	40%	0%	100%	0%	0%	0%	6	Tsh
7*	--	--	--	60%	0%	40%	40%	5	Tsh
8	--	--	--	36%	16%	0%	64%	100	Tcg3
9*	--	--	--	36%	64%	0%	64%	5	Tsh
10*	--	--	--	38%	62%	0%	62%	15	Tsh
11	--	--	--	98%	2%	0%	2%	13	Tcg4
12*†	--	--	--	88%	12%	0%	12%	8	Tsh
13	--	--	--	88%	12%	0%	12%	2	Tss
14†	--	--	--	58%	42%	0%	42%	2	Tss
15	--	--	--	76%	24%	0%	24%	2	Tss
16	46%	24%	30%	100%	0%	0%	0%	8	Tcg3
17	54%	22%	24%	100%	0%	0%	0%	8	Tcg3
18	--	--	--	62%	38%	0%	38%		Tcg3
19	--	--	--	4%	96%	0%	96%	50	Ts
20	98%	2%	0%	100%	0%	0%	0%	5	Tcg3
21	98%	2%	0%	100%	0%	0%	0%	15	Tcg3
22	--	--	--	70%	30%	0%	30%	15	Tcg3
23	0%	0%	0%	0%	100%	0%	100%	20	Tcg3

Notes: Count number corresponds to count numbers on Figure 4.
* Denotes debris flow deposit into shale unit.
† Denotes count where tuff was observed but not differentiated from lava clasts.

Figure 18. Simplified map of the study area showing the distribution of conglomerates from the sedimentary rocks of Tendoy and sedimentary rocks of Sacajaweja, and Quaternary Tertiary gravels. Compositional differences between the conglomerates are shown in color and pattern changes. Pebble counts are indicated with dots, and numbers correspond with data in Table 5.

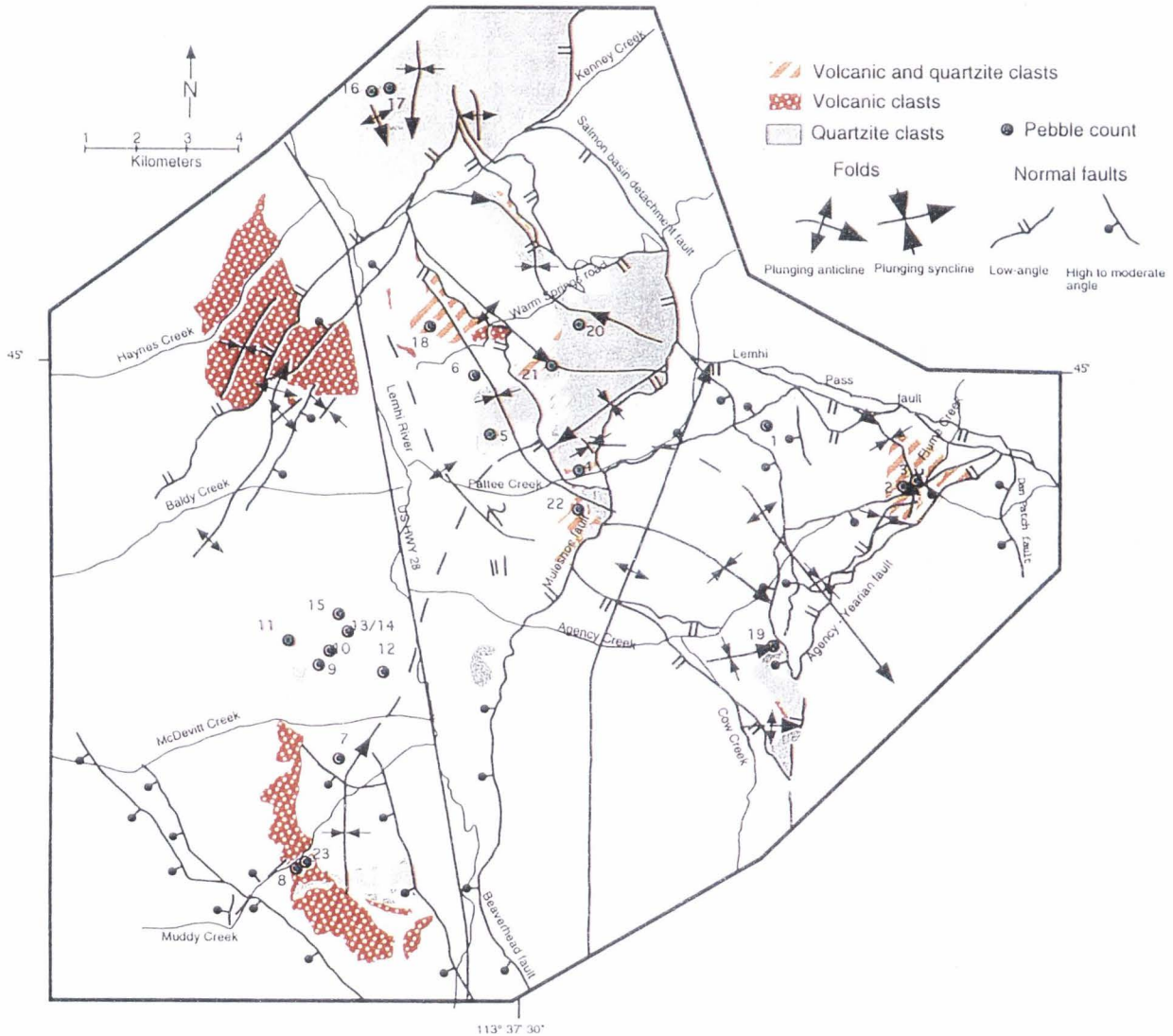
N
1 2 3 4
Kilometers
Volcanic and quartzite clasts
Volcanic clasts
Quartzite clasts
Pebble count
Folds
Normal faults
Plunging anticline
Plunging syncline
Low-angle
High to moderate angle
Kenney Creek
Salmon basin detachment fault
Warm Spring Creek
Haynes Creek
Baldy Creek
Lemhi River
Fallee Creek
Muldrow fault
Agency Creek
McDevitt Creek
Muddy Creek
Beaverhead fault
Cow Creek
Agency-Yearian fault
Dan Patch fault
Lemhi Pass fault
Burnt Knife Creek
Lemhi Pass
45°
113° 37' 30"
16
17
18
6
20
21
5
4
22
15
11
13/14
10
12
9
7
23
8
1
2
3
19

Figure 19. Simplified map of the study area showing the distribution of conglomerates with pie diagrams showing clast compositions obtained from pebble counts. Numbers in pie diagrams correspond with data in Table 5.

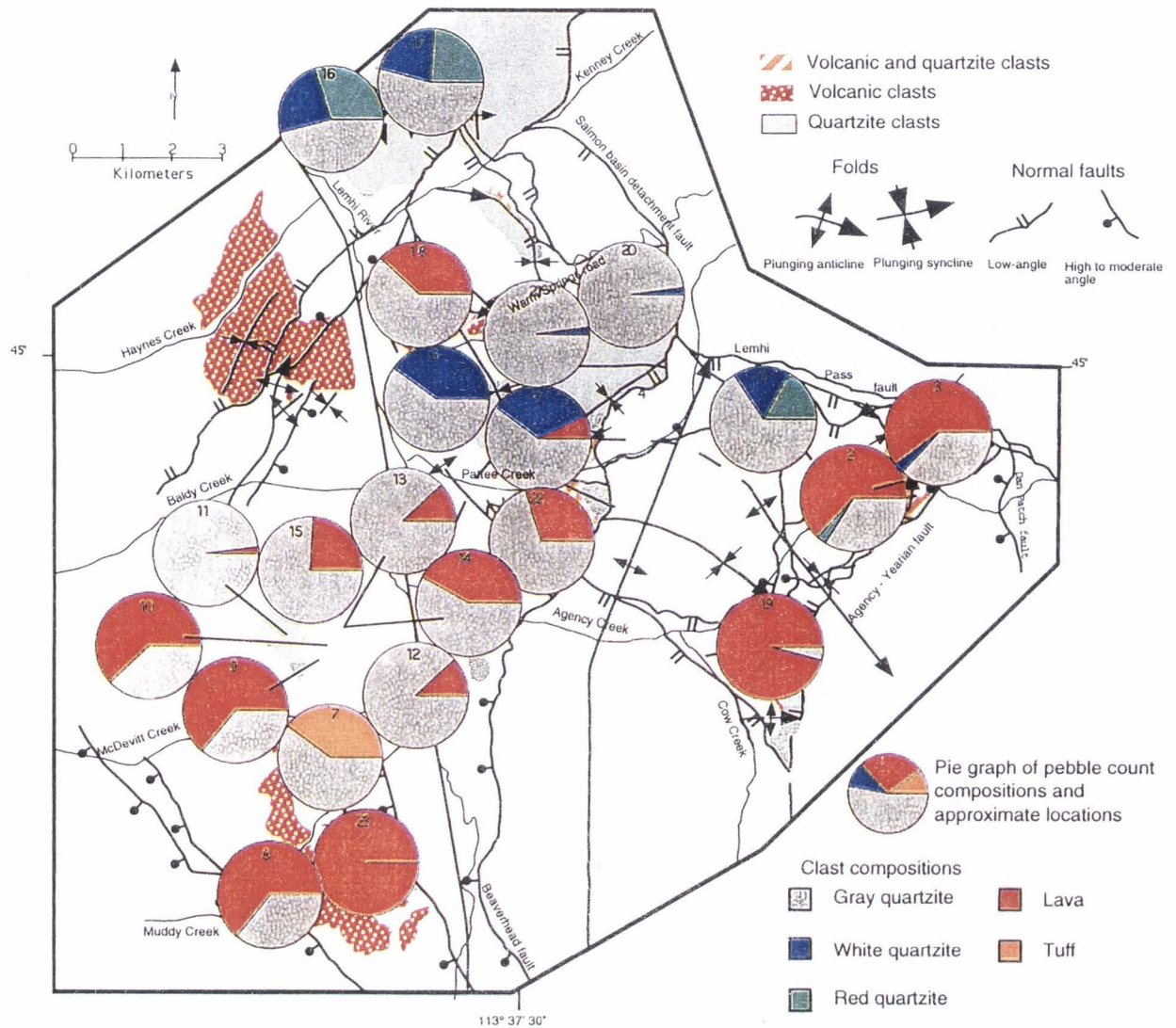
Volcanic and quartzite clasts
Volcanic clasts
Quartzite clasts
Folds
Normal faults
Plunging anticline
Plunging syncline
Low-angle
High to moderate angle
N
0 1 2 3
Kilometers
Kenney Creek
Salmon basin detachment fault
Lemhi River
Haynes Creek
Warm Spring Creek
Lemhi Pass fault
Baldy Creek
Parker Creek
Agency Creek
Agency - Yearian fault
Pan Tetch fault
McDevitt Creek
Cow Creek
Muddy Creek
Beaverhead fault
45°
113° 37' 30"
Pie graph of pebble count compositions and approximate locations
Clast compositions
Gray quartzite
White quartzite
Red quartzite
Lava
Tuff

(Figure 18; Figure 19). The third map grouped the sediment by age and type. This map helped to determine how the basin geometry evolved over time (Figure 5).

SYN-CHALLIS PALEOGEOGRAPHY

Challis volcanic rocks are widespread in the southeastern Salmon basin, but the quartzite-bearing ash-flow tuff, the granite-clast conglomerate, and the older quartz-sanidine ash-flow tuff are confined to a narrow northwest-southeast trending zone. The southwestern margin of the zone extends from northeast of Baldy Creek southeast to the northeast corner of section 15 of T19N, R24E, along Pattee Creek. The southern boundary is also preserved east of the Tendoy anticline in sections 18 and 19 of T19N, R24E, where the quartzite-bearing ash-flow tuff (Tqt) pinches out to the south (Plate 1). North of the pinchout of the quartzite-bearing ash-flow tuff, in the northern half of section 18 of T19N, R24E, the granite-clast conglomerate (Tcg2) and older quartz-sanidine ash-flow tuff (Tqs1) pinch out to the south (Plate 1). The northern boundary of this narrow zone cannot be defined in the study area, because it has been eroded from the footwall of the Lemhi Pass fault, but was probably no more than 2 km to the north of the Lemhi Pass fault based on relationships to the east in the Horse Prairie basin (VanDenburg, 1997). The presence of the quartzite-bearing ash-flow tuff just southeast of Kenney Creek indicates that the zone persisted at least this far north.

The quartzite-bearing ash-flow tuff, the granite-clast conglomerate, and older quartz-sanidine ash-flow tuff are interpreted as filling of an east-southeast trending paloeovalley (Janecke, pres. com., 1996). This paleovalley, termed the Lemhi Pass paleovalley by VanDenburg et al. (1998), has been traced over a distance of greater than 80 km from the Salmon River Mountains west of Salmon, Idaho, to the northern Tendoy Range, Montana, and probably initially developed during the late Cretaceous. The units confined to the paleovalley pinch out rapidly along strike to the north and south, and are interpreted as paleocanyon fills (Janecke, pers. comm., 1996; VanDenburg, 1997). A major river flowed in this paleovalley toward the foreland.

The apparent inset relationships in the Agency Creek-Ghoul basin area between the quartzite-bearing ash-flow tuff, granite-clast conglomerate, and older quartz-sanidine ash-flow tuff where younger units are more restricted in their distribution than the underlying one are consistent with a cut-and-fill evolutionary sequence. The river which occupied the Lemhi Pass paleovalley must have reestablished itself after the deposition of the quartzite-bearing ash-flow tuff in the valley bottom. The presence of large boulders (> 2.5m) of rapikivi granite in the granite-clast conglomerate indicates that this stream had considerable competence. Similar cut-and-fill relationships were observed by VanDenburg (1997) to the east in an adjacent segment of the Lemhi Pass paleovalley.

Overlying the three paleovalley-fill units are lava flows 490 m thick, the tuff of Curtis Ranch, and the younger quartz-sanidine ash-flow tuff, which

have a widespread distribution in the study area. The widespread distribution of these two units indicates that the topography was subdued in the study area after the deposition of the older quartz-sanidine ash-flow tuff. Some small normal faults were active at this time (fault K), but no depositional basins formed.

TENDOY BASIN

The Tendoy basin formed during a second period of evolution in the southeastern Salmon basin. This period of sedimentation was in response to initial large-scale rifting (episode 2), and it is recorded by a thick sequence of conglomerates, shales, sandstones, and some interbedded megabreccias of the sedimentary rocks of Tendoy (Tcg3, Tsh, Tss, Ts, and Tmb). Conglomerate deposits (Tcg3) of the sedimentary rocks of Tendoy display the greatest amount of variability within the basin and were divided into six separate facies (Flume Creek facies, Pattee Creek northeast and west facies, Sandy Creek facies, and Haynes Creek facies). The six different facies of conglomerates deposited in the Tendoy basin can be distinguished from one another using five criteria: 1) degree of rounding; 2) clast composition; 3) amount of sand interbedded with the conglomerates; 4) proportion of matrix; and 5) structural setting (relation to structures). Because the rocks of the Tendoy basin occur in the hanging wall of the Agency-Yearian fault and are cut by fault C, they are interpreted as being deposited during phase 2 of extension in the Salmon basin. Because movement along the Lemhi Pass fault and faults D and E are interpreted as occurring soon after movement

along the Agency-Yearian fault, uplifts in their footwalls faults D and E may have contributed sediment to the Tendoy basin, but overall their contribution was probably minor. This also relates their deposition to movement along the Agency-Yearian fault and possibly to early movement along the Salmon basin detachment fault.

Movement along the Agency-Yearian fault produced the Tendoy anticline and the two adjacent synclines. The deepest parts of the two subbasins of the Tendoy basin coincide with these two synclines and formed on the flanks of the Tendoy anticline. One basin is on the east southeastern flank (Flume Creek subbasin), and the other on the west northwestern flank of the anticline (Pattee Creek subbasin; Figure 8). These two basins are identified based on their position relative to the Tendoy anticline and the compositions of conglomerates deposited in them. Two lines of evidence show that the two subbasins were forming contemporaneously with the Agency-Yearian fault and its associated structures: 1) the presence of growth strata in the northeastern part of the Pattee Creek subbasin (Plate 2, cross-section C-C'), and 2) the differences in depositional environment and clast composition of conglomerates on opposite flanks of the Pattee Creek syncline and Tendoy anticline (Figure 18; Figure 19; Table 6).

Flume Creek subbasin

The Flume Creek subbasin is a relatively narrow basin that was confined to an elongate region between the Agency-Yearian fault and the Tendoy anticline. This subbasin probably widened over time as the basin

filled. In the study area, units deposited in the Flume Creek subbasin are the Flume Creek facies of Tcg3, sedimentary rocks of Sharky Creek (Ts), megabreccias (Tmb), and fine-grained tuffaceous sedimentary rocks mapped by Staatz (1979). Conglomerates of the Flume Creek facies are well-rounded and clast-supported, and have a greater abundance of volcanic clasts than Middle Proterozoic quartzite clasts. Near Sharky Creek, volcanic-clast conglomerates (Figure 19; Table 6; counts 2, 3, and 19) occur in the immediate hanging wall of the Agency-Yearian fault. The abundance of volcanic clasts in sedimentary rocks in the Flume Creek subbasin indicates that they must have had a source area separate from the one which provided abundant Middle Proterozoic quartzite clasts to the conglomerates in the northeast end of the Pattee Creek subbasin. Both the Tendoy anticline and the footwall of the Agency-Yearian fault could have been a source area for the volcanic clasts. Determining whether the source area for the volcanics was the footwall of the Agency-Yearian fault or the crest of the Tendoy anticline is difficult in the absence of paleocurrent indicators, because identical rock types would have been uplifted by both structures. I infer that both areas contributed clasts to the basin.

Although the conglomerates along Sharky Creek contain almost entirely volcanic clasts, associated megabreccias are 100% Middle Proterozoic metasedimentary rocks. South of the study area, immediately along strike of the Flume Creek subbasin, S. U. Janecke (unpublished mapping) has identified other megabreccias of Middle Proterozoic metasedimentary rocks and Challis volcanic rocks. The megabreccias have

been reinterpreted from Staatz (1979), who initially mapped them as in-place outcrops of Middle Proterozoic metasedimentary rocks and Challis volcanic rocks. The Flume Creek subbasin must have had rugged topography along its margins to allow for the deposition of these megabreccias.

Since the Flume Creek conglomerate facies is replaced southward by finer grained deposits of the sedimentary rocks of Sharky Creek, the Flume Creek subbasin is interpreted as having small alluvial fans along its eastern and western flanks, a braided stream system along its axis (along the present day Agency Creek and Cow Creek), and a lake to the south (Figures 5, 6, 20). The conglomerates of the Flume Creek facies have a high degree of rounding and are clast supported, which was probably achieved through fluvial transport. Alluvial fans were shed from the adjacent highlands. The eastern margin was fault-bounded and had considerable topographic relief. This provided a source area for large rock avalanches. Evidence for a lacustrine environment exists in this fault-bounded rift basin at the south end of the study area with the presence of limestone, bentonite beds, and siltstones and shales, and south of the study area where Staatz (1979) has mapped fine-grained tuffaceous Tertiary sedimentary rocks that contain the late Eocene (?) Cow Creek flora (Axelrod, unpublished data).

Pattee Creek subbasin

The Pattee Creek subbasin was larger and more complex than the Flume Creek subbasin. The Pattee Creek subbasin contains thick sequences of conglomerates and shales, with some interbedded sandstones

Figure 20. Facies model for the southeastern Salmon basin during the deposition of the sedimentary rocks of Tendoy (episode 2) and before the deposition of the sedimentary rocks of Sacajaweja (episode 3). Compare with Figure 11.

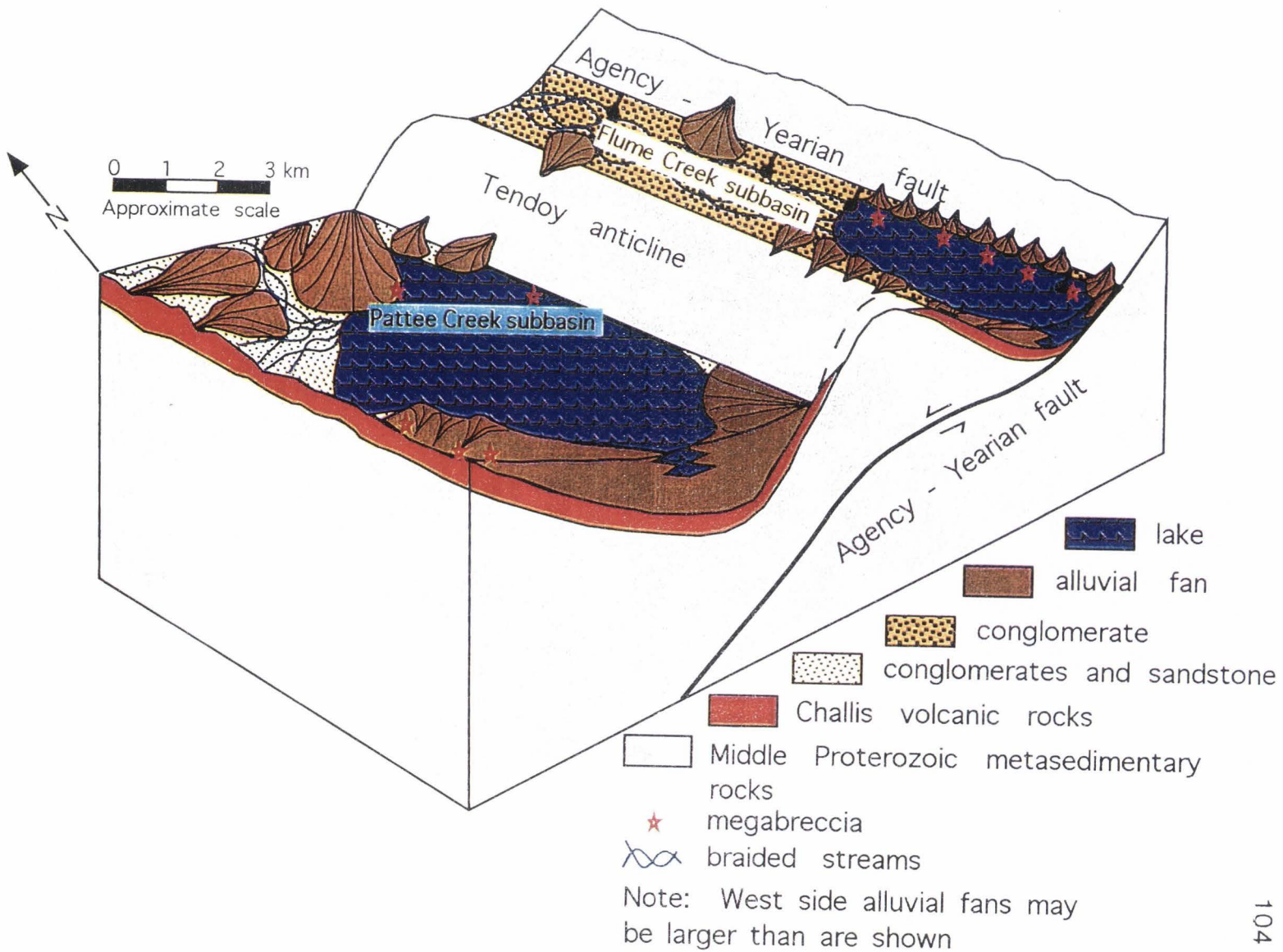
Agency - Yearian fault
Flume Creek subbasin
Tendoy anticline
0 1 2 3 km
Approximate scale
N
Pattee Creek subbasin
Agency - Yearian fault
lake
alluvial fan
conglomerate
conglomerates and sandstone
Challis volcanic rocks
Middle Proterozoic metasedimentary rocks
megabreccia
braided streams
Note: West side alluvial fans may be larger than are shown

(units Tcg4, Tss, and Tsh; Figure 5; Figure 6). Sedimentary rocks deposited in this subbasin are located east and west of the Lemhi River, along Muddy Creek, McDevitt Creek, Baldy Creek, Sandy Creek, Kenney Creek, Warm Springs road, Pattee Creek, and Agency Creek (Figure 5). Sedimentary rocks north and south of Haynes Creek are probably part of this subbasin too. The sedimentary rocks in the Pattee Creek subbasin can be divided into conglomeratic basin margin facies (Tcg3) and shaley bentonitic lacustrine facies (Tsh) from the basin's center. Conglomeratic basin-margin facies were further divided into the Pattee Creek northeast and west facies, Sandy Creek facies, and Haynes Creek facies (Figure 20).

The syntectonic conglomerates along the margin of the Pattee Creek subbasin have different clast compositions on the east and west side of the subbasin. The Pattee Creek northeast facies, located on the northwestern flank of the Tendoy anticline and east of the Lemhi River, contains angular to subrounded, clast-supported conglomerates that are typically dominated by Middle Proterozoic quartzites, although volcanic clasts are present near the base and the northwestern edge of the sequence (Figure 19; Table 6; counts 4, 5, 6, 18, 20, 21, and 23). Present in the Pattee Creek northeast facies are large coherent megabreccias of volcanic rocks. The presence of angular clasts and megabreccias may record steep topography and probably rapid uplift of the Tendoy anticline along the eastern margin of the subbasin. The lack of volcanic clasts on the eastern margin indicates that volcanic rocks exposed by the uplift of the Tendoy anticline were rapidly eroded to expose

Middle Proterozoic quartzites. The conglomerates of the Pattee Creek northeast facies are interpreted as alluvial fan deposits.

To the north, the Pattee Creek northeast facies is replaced by the sand-rich Sandy Creek facies, which consists of interbedded sandstone (> 60%) and conglomerates (< 40%). The conglomerates of the Sandy Creek facies are well rounded, poorly to well sorted, clast to matrix-supported, with clasts consisting entirely of Middle Proterozoic quartzites (Figure 19; Table 6; counts 16 and 18). The interbedding of the pebbley sandstones and conglomerates is interpreted as a near-shore or shore environment with fluvial systems extending onto the near-shore or shore environment. This facies may also represent deltaic deposits.

Pattee Creek west facies is on the west and southwestern flank of the Tendoy basin and consists of moderately rounded, matrix-supported, and volcanic-clast conglomerate (Figure 19; Table 6; counts 8 and 23). East of and up section from the Pattee Creek west facies are conglomerate deposits interbedded in the shale and sandstone facies. These conglomerate beds may be dominated by either quartzite clasts or volcanic clasts (Figure 19; Table 6; counts 7, 9, 10, 12, 13, 14, and 15). These conglomerates are interpreted as debris flows and debris-flow fans along the western margin of the Pattee Creek subbasin. The presence of conglomerates interbedded with fine-grained sedimentary rocks indicates subaqueous deposition of debris flows. Coarse clastics on the northeast side of the Pattee Creek basin may extend farther into the basin (~ 2 km) than coarse clastics on the western, hanging wall side (~ 1.5 km). The presence of large debris fans on

both the eastern and the western margin fits with neither end-member model for sedimentation in a half-graben basin (Leeder and Gawthorpe, 1987; Friedmann and Burbank, 1995).

Directly north of the Pattee Creek west facies is the Haynes Creek facies, which appears to be dominated by angular, clast-supported (?), boulder-sized, volcanic-clast conglomerate. Field reconnaisance indicates that the Haynes Creek facies is similar to the Pattee Creek west facies, in that they both are dominated by volcanic clasts. This facies may be a continuation of the Pattee Creek west facies, or it may be a younger conglomerate related to the sedimentary rocks of Sacajaweja (Tcg4). Future work may determine the age and significance of this package of sedimentary rocks.

The center of the Pattee Creek subbasin is characterized by a thick sequence of tuffaceous siltstones and shales. These fine-grained, thinly bedded sedimentary rocks are interpreted as having been deposited in a lake. In some places, these shales lie directly on the volcanic sequence (section 25 of T19N, R23E), and on Middle Proterozoic quartzite (section 28 of T19N, R24E). The absence of basin margin facies in these locations may be the result of the relief and topography along the basin's margin, or spaced fan deltas along the margin of a lake. The shale unit is located where the deepest portion of the basin is predicted. This is based on the location of the structurally deepest part of the Pattee Creek syncline where the syncline's plunge reverses. Gravity data compiled by McCafferty (1995) and Bankey

and Kleinkopf (1988) show that the deepest part of the southeast Salmon basin coincides with the shales in the center of the Pattee Creek subbasin.

Overall the Pattee Creek subbasin was complex with at least three active depositional systems. The margins of the basin were dominated by alluvial fan complexes (Pattee Creek northeast and west facies, and Haynes Creek facies) which graded into fluvial and near-shore or beach environments to the north (Sandy Creek facies). A lake occupied the center of the basin and transitions between the basin-margin facies and the lake facies were rapid especially on the east and northeast side. Intermediate facies (sandstones) are subordinate, indicating that considerable topography was present.

SACAJAWEJA BASIN

Superimposed on the Pattee Creek subbasin of the Tendoy basin is the Sacajaweja basin. The conglomerates of Kenney Creek (Tcg4), which have a limited distribution in the field area, were deposited in the Sacajaweja basin. The thickest section of Tcg4 is north of Kenney Creek in the hanging wall of the Salmon basin detachment fault. Because these conglomerates occur in the hanging wall of the Salmon basin detachment fault and lap the fault D (which is correlated to the Lemhi Pass fault), the Sacajaweja basin formed during episode 3iii of extension and has a probable age of late Oligocene to early Miocene.

The conglomerates of Kenney Creek are dominated by Middle Proterozoic quartzite clasts, but volcanic clasts are present is some beds

(Tucker and Birdseye, 1989). Clasts range from angular to subrounded, and sandstone lens are locally present. The base of the sequence is a sedimentary breccia deposit of very angular Middle Proterozoic quartzite clasts that overlies a fault block of Middle Proterozoic quartzite. This breccia is interpreted as a paleotalus deposit. This study agrees with Tucker and Birdseye's (1989) interpretation of the conglomerates as alluvial fan deposits, but not that they were synvolcanic. Instead, the deposition of this thick sequence of conglomerates reflects movement along the Salmon basin detachment fault during episode 3iii of extension. The footwall of the Salmon basin detachment fault was probably the source area for the Middle Proterozoic quartzite clasts in the sedimentary rocks of Sacajaweja.

It is difficult to reconstruct the paleogeography of the Sacajaweja basin, because exposures are limited to a 9-km^2 area in the immediate hanging wall of the Salmon basin detachment fault. The available exposures along Kenney Creek indicate that large alluvial fans were present in this basin. Future work in the region may provide more insights to the depositional process active in this basin.

LATE CENOZOIC EVOLUTION

The Late Cenozoic evolution of the southeast Salmon basin was dominated by erosional processes. Downcutting of the Lemhi River has exposed many sections of the sedimentary rocks of Tendoy, but in the process has completely stripped most of the conglomerates of Kenney Creek (except along Kenney Creek). Scattered outcrops of quartzite-clast-

dominated gravel in terraces occur throughout the study area and these may be the remains of Pliocene (?) to Pleistocene alluvial fans and river terraces.

SUMMARY OF THE BASIN EVOLUTION

The southeastern Salmon basin has undergone a complex basin evolution, which can be divided into four evolution periods. The first evolutional period was dominated by a large paleovalley that was filled by Challis volcanic and synvolcanic sedimentary rocks. By late Eocene (?) time, faulting along the Agency-Yearian fault created the Tendoy basin, which was divide into two subbasins by the north-trending Tendoy anticline. The formation of the Tendoy anticline and Pattee Creek syncline lead to the deposition of growth strata in the Pattee Creek subbasin. The growth strata show 400 m of sedimentary deposition on the southeastern flank of the Pattee Creek north syncline and 1400 m of sedimentary deposition on the northwestern flank of the syncline. During the Oligocene, faulting along the Salmon basin detachment fault created the Sacajaweja basin, which was dominated by large alluvial fan complexes. This completed the structural development of the Salmon basin and by Pliocene (?) to Pleistocene (?) time, erosional processes began to excavate the Tertiary deposits in the basin.

DISSCUSSION

The southeastern Salmon basin is a complex half-graben that has undergone four temporally distinct episodes of extension during Cenozoic time. The extension direction in the study area, as inferred from the strikes of normal faults, has changed from northwest-southeast (episode 1), to east west (episode 2), to east northeast-west southwest (episode 3), to northeast-southwest (episode 4; Figure 4). Multiple episodes of extension have been recognize in adjacent basins (Vandenburg, 1997; Janecke 1992, 1995), but were not previously documented in the Salmon basin. Harrison (1985) interpreted the northern Salmon basin as forming in one continuous sequence. Two lines of evidence indicate that Harrison's (1985) interpretation is incorrect. First, this study has documented multiple episodes that can be determined from cross-cutting relationships along the faults of different ages. Second, at least two angular unconformities have been identified bounding the sedimentary basin fill of the southeastern Salmon basin. The possible absence of the sedimentary rocks of Sacajaweja and quartzite-clast gravel (QTg) north of the study area, perhaps due to subsequent erosion, may have led Harrison (1985) to her interpretation. Future work may resolve this issue.

In basins adjacent to the southeastern Salmon basin, in east-central Idaho and in southwest Montana, the earliest episode of extension documented by other workers is an episode of pre-volcanic northeast-southwest extension that was not documented in this study. This early

episode of extension was attributed to gravitational collapse of the Sevier fold and thrust belt (Skipp, 1987, 1988; Janecke et al., in press). This interpretation was made because prevolcanic faults parallel Mesozoic structures, and their timing closely follows and may be contemporaneous with contractional deformation (VanDenburg, 1997).

The earliest episode (episode 1) of extension experienced in the southeastern Salmon basin occurred along northeast-striking normal faults. Because faults related to this early episode of extension do not completely cut the Challis volcanic sequence, they must have been active during the middle Eocene (49.5 to 46 Ma; Figure 21). Other workers have observed similar relationships along middle-Eocene northeast-striking faults in adjacent basins (McIntrye et al., 1982; Janecke, 1992, 1995; VanDenburg, 1997). Faults of this episode of extension correlate to VanDenburg's (1997) phase 2. This episode was very minor in the southeastern Salmon basin and produced only about 100 m of extension.

It was prior to and during episode 1 that a thick sequence of volcanic rocks (Challis volcanic rocks) was deposited in the Lemhi Pass paleovalley. The angular unconformity identified by Staatz (1979) in the volcanic sequence was not identified in this study and the volcanic rocks appear to have been deposited in more or less one continuous sequence. Because the quartzite-bearing ash-flow tuff, the older quartz-sanidine, and younger quartz-sanidine have strikingly similar lithologies, and resemble tuffs in the caldera identified by Ruppel et al. (1993) north of the study area near

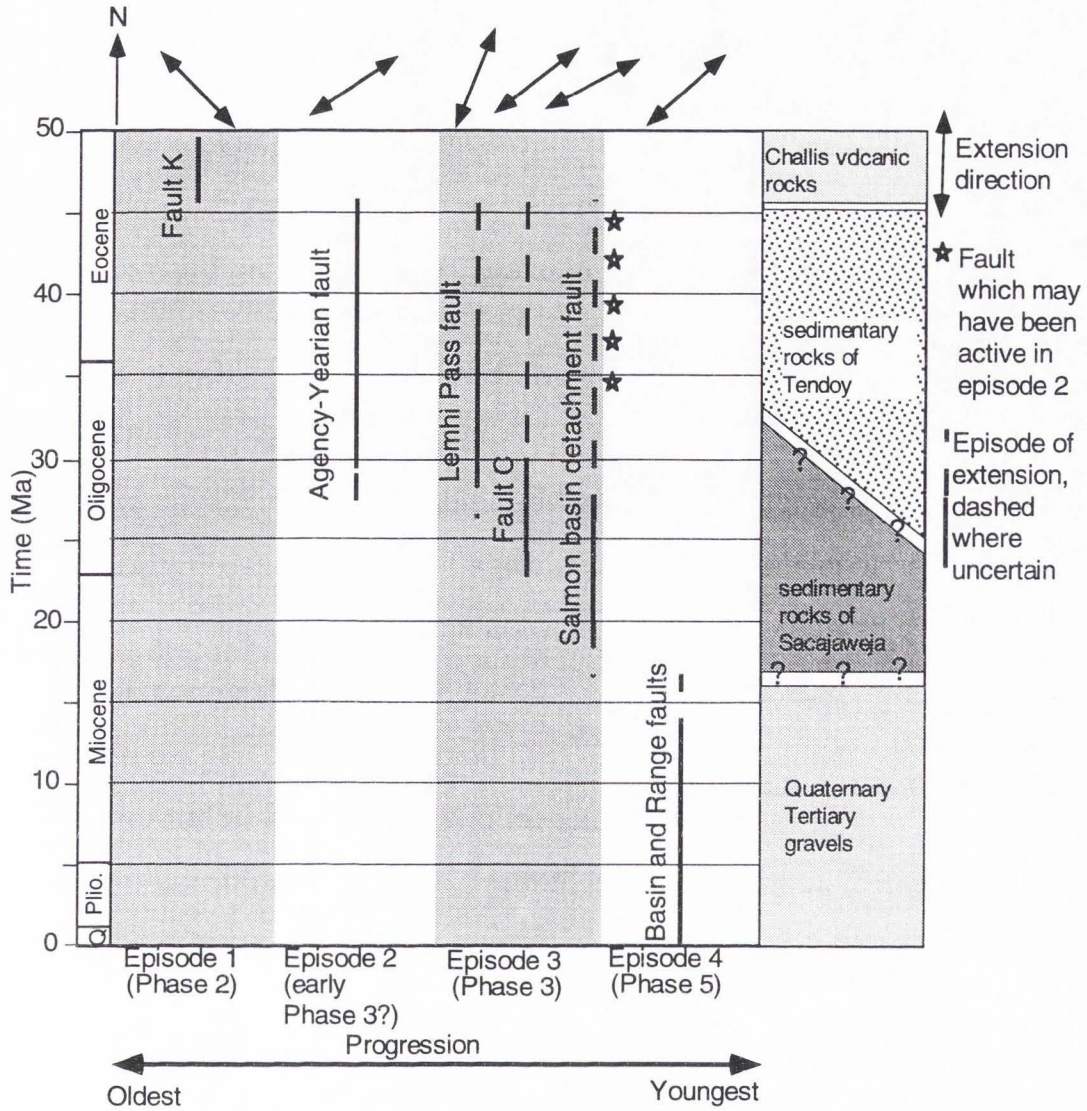

Figure 21. Graph showing faults active and rock units deposited during each of the four episodes of extension in the southeastern Salmon basin. Extension direction for each of the episodes of extension is given at the top of the graph. VanDenburg's (1997) phases of extension are in parentheses below the corresponding episode of extenson this study.

Withington Creek, this caldera is interpreted as being the source caldera for the tuffs.

The next episode (episode 2) of extension was the largest in the study area, and it was active after 46 Ma. Deformation may have continued until as late as about 27 Ma, but most of the slip probably occurred before 31 Ma (Figure 21). This episode of extension occurred along the north-northwest-striking and west-southwest-dipping Agency-Yearian fault. This episode of extension was responsible for the formation of much of the Salmon basin and deposition of the sedimentary rocks of Tendoy. Movement along the Agency-Yearian fault during this episode of extension led to the formation of two large fault-bend folds, the Tendoy anticline and Pattee Creek syncline. The rise of the Tendoy anticline divided the proto-Salmon basin into two subbasins, with one to the west of the Tendoy anticline (Pattee Creek subbasin), and another to the east of Tendoy anticline (Flume Creek subbasin; Figure 20). This episode of extension was probably coeval with slip on the Muddy-Grasshopper fault system, the master detachment and breakaway fault for the rift zone of Janecke (1994).

The north-northwest strike of the Agency-Yearian fault closely parallels the strike of many of the thrust faults in the region, and may reflect a return to gravitational collapse of the Sevier fold-and-thrust belt during late middle Eocene to Oligocene time. The Agency-Yearian fault is south of the Miner-Beaverhead Divide reverse or thrust fault. No thrusts have been mapped in

the footwall of the Agency-Yearian fault; therefore, the Agency-Yearian fault may not reactivate a thrust fault at upper crustal levels. The subsequent collapse of the thickened crustal wedge produced by these thrusts may have driven extension during episode 2, and reactivation of the structures may be reflected in the complex normal fault geometries in the southeast Salmon basin.

The third episode (episode 3) of extension reflects continued gravitational collapse along southwest-dipping normal faults, which include the Lemhi Pass fault (including faults D and E), fault C, and the Salmon basin detachment fault. Active between late Eocene and early Miocene (?) times, the strikes of normal faults during this episode of extension change from west-northwest to northwest as the episode progressed (Figure 8; Figure 22). VanDenburg (1997) documented similar complex relationships in the Horse Prairie, east of the Salmon basin. During the correlative episode of extension (his phase 3), he documented two rather than three subphases. The reorientation of normal faults during a single episode of extension can be explained in three ways: 1) the stress field rotated; 2) the relative magnitudes of stresses changed; and 3) the stress field was three-dimensional. With the exception of the Lemhi Pass fault, this episode of extension contains faults with dominantly north-northwest strikes.

The Warm Springs anticline also formed during episode 3. This large anticline is interpreted as a rollover anticline in the hanging wall of the Lemhi

Pass fault (Cross-section I - I', Plate 2). This large fold (episode 3i) folds the Pattee Creek north syncline, the north end of the Tendoy anticline, and the Agency-Yearian fault, and it is cut by fault C (episode 3ii). The presence of the Warm Springs anticline in the hanging wall of the Lemhi Pass fault suggests that movement along the Lemhi Pass fault was mostly dip-slip. The third episode of extension allowed for the preservation of the sedimentary

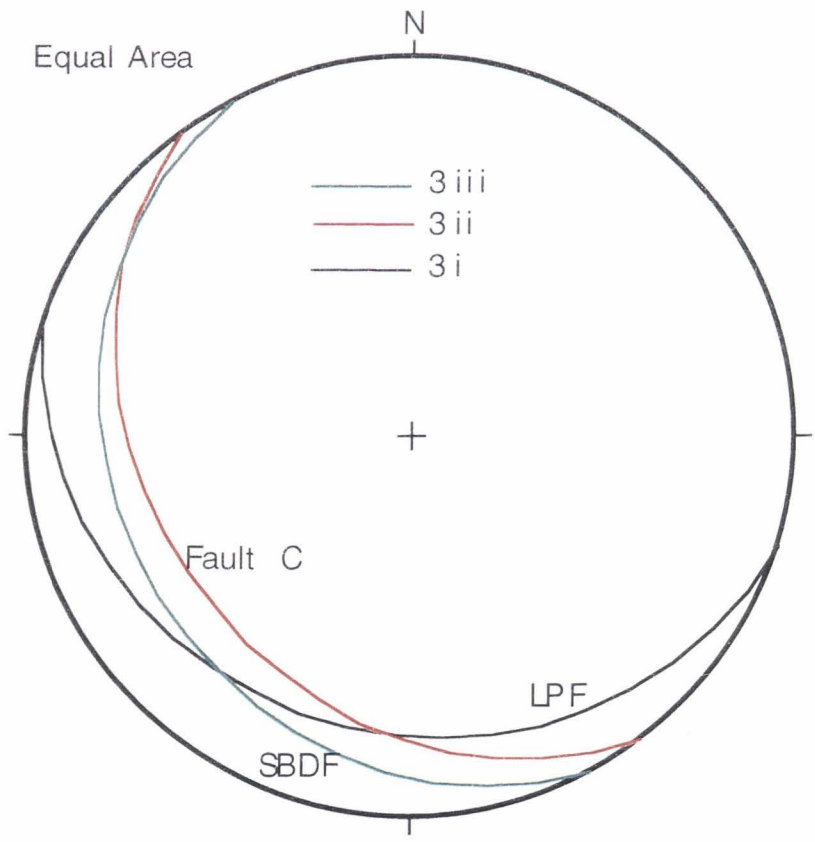

Figure 22. Stereogram comparing the orientations of the faults formed during episode 3. Fault orientations change from west-northwest-striking [Lemhi Pass fault (LPF)] to northwest-striking [(fault C and Salmon basin detachment fault (SBDF)] as the episode progressed.

rocks of Tendoy, the deposition of the sedimentary rocks of Sacajaweja, and completed the formation of the Salmon basin.

Episodes 2 and 3 correlate to VanDenburg's (1997) phase 3. Both this study's episodes 2 and 3, and VanDenburg's (1997) phase 3 are interpreted to be driven by gravitational collapse and to lie in a narrow Eocene to Oligocene rift zone (Janecke, 1994). This study supports the rift hypothesis in timing, geometry, and location, but multiple episodes of deformation along faults with a range of strikes were not predicted by Janecke's (1994) model. This study has identified the Agency-Yearian fault and the Salmon basin detachment as major detachments within the narrow Eocene to Oligocene rift zone of Janecke (1994). These two faults extend the hanging wall of the Muddy-Grasshopper fault, the breakaway and sole fault for the rift zone. All three faults may connect at depth, but lack of geophysical data in the Salmon basin hinder this interptation. The timing relationships determined here, when combined with those from adjacent areas (VanDenburg, 1997; Janecke et al., 1998), show complex time and space patterns of extension. Simple westward younging of deformation as predicted by the rolling hinge model (Buck, 1988; Wernicke and Axen, 1988) did not characterize this region during the Paleogene.

The final episode (episode 4) of faulting occurred along northwest-striking Basin and Range faults, and was active from the early Miocene (?) to the present (Figure 21). This final episode of extension occurs along the

Beaverhead fault and faults A and B. The Beaverhead fault remains active (Crone and Haller, 1991). Although no Quaternary scarps were observed along the Beaverhead fault in the study area, there is a scarp along the northeast striking and incompletely mapped fault F. Episode 4 has outlasted extension predicted by gravitational collapse. An active mantle may be driving continued extension in the northern Basin and Range Province (Liu and Shen, 1998). Episode 4 correlates to phase 5 of VanDenburg (1997). Normal faults of VanDenburg's phase 1 and 4 were not identified in the southeast Salmon basin.

This study has documented that the southeastern Salmon basin has long history of crustal thinning, which continues today. The earliest normal faults in the study are synChallis and represent a short period of northwest-southeast extension (49.5 to 46 Ma). The basin-bounding normal faults in the study area have a low-angle geometry with greater than 2 km of dip-slip separation, and may have as much as 5 to 10 km of dip-slip separation. Slip across the Salmon basin detachment may be even greater.

EXTENSIONAL FOLDS

Because the southeast Salmon basin has undergone multiple episodes of extension along normal faults with varying geometries, there are many (> 9) extensional folds in the basin. Extensional folds in the Salmon basin have three general trends: north-south, northwest-southeast, and northeast-southwest; and represent at least two generations of extensional

folds. The folds are open to gentle with bisecting surfaces that are near vertical (Figure 9; Table 4). Most folds are longitudinal folds and the angle between the axial plane of the folds and the plane of the associated normal faults ranges between 50° and 87° (Figure 9; Table 4). The mechanism responsible for forming extensional folds is closely tied to the geometry of the controlling fault, so identification of the controlling fault is critical to understand the mechanism responsible for producing an extensional fold. The most common mechanism responsible for folding in the southeastern Salmon basin is fault-bend folding, and the recognition of this mechanism has provided insight to the subsurface geometry of many of the faults in the southeast Salmon basin.

Although extensional folds have been recognized in a wide range of extensional settings throughout the world (Janecke et al., 1998), folds in the southeastern Salmon basin are unusual because of their great abundance and large size. The reactivation of preexisting thrust faults by normal faults may have produced normal faults with complex geometries, and may explain why an abundance of extensional folds occur in the southeast Salmon basin. Ongoing and future work may lend insights into the geometries of the preextension thrust faults of the region, and may determine whether thrust faults were reactivated as normal faults. Transtension and transpression along unrecognized strike-slip faults or normal-oblique slip faults in the region may have also influenced the formation of folds in the basin. Future work is needed to verify the presence or absence of strike-slip faults or normal-oblique slip faults.

The recognition of extensional folds is important because they may have important economic significance. The recognition of folds in extensional settings may open up new previously unexplored regions to petroleum and groundwater exploration (Janecke et al., 1998).

MODELS FOR SEDIMENTATION

The complex fault geometries in the southeastern Salmon basin have led to the development of complex sedimentation patterns that are not predicted by existing models of sedimentation in extensional half-grabens. Rift basin models by Leeder and Gawthorpe (1987) assumed simple high-angle fault geometries, and models of Friedmann and Barbank (1995) assumed simple low-angle geometries. Complex flat-ramp geometries are not addressed by either of the two models.

Friedmann and Burbank's (1995) model of superdetachment basins predicts that large alluvial fans from the footwall extend far into the hanging wall, and are dominated by mass wasting processes. In contrast, Leeder and Gawthorpe (1987) predict small alluvial fans near steeper basin-bounding faults. Structurally, the Tendoy basin is a superdetachment basin. However, the presence of small alluvial fans and proximal lacustrine deposits in the Flume Creek subbasin deters this interpretation. Because the Leeder and Gawthorpe (1987) model applies to rift basins with steep basin-bounding faults, it does not work structurally for the southeastern Salmon basin.

Physical models of normal faults with flat-ramp geometries produced a large anticline-syncline pair, with growth relationships in the syntectonic

sedimentary rocks (McClay, 1989; Figure 11). These physical models also show sedimentation taking place in two subbasins forming in the hanging wall of a normal fault with a flat ramp geometry (McClay, 1989; Figure 11). This study interprets the Tendoy anticline and Pattee Creek syncline as forming above a ramp-flat in the Agency-Yearian fault. The rise of the Tendoy anticline produced an interbasin high, and formed two subbasins in the hanging wall of the Agency-Yearian fault. This is a relationship that is not predicted by existing models for sedimentation in half-graben basins, but has been shown in physical models of extensional folds (McClay, 1989).

This model for sedimentation allows for hanging-wall rocks to be eroded, then redeposited in the hanging wall. The erosion of the core of the Tendoy anticline probably provided a source for the quartzite clasts in the conglomerates along the margins of the Pattee Creek syncline. The McClay (1989) model also predicts sedimentation patterns which occur in the Pattee Creek syncline, where ~ 1400 m of sediment was deposited on the northwestern flank of the syncline and only ~ 400 m of sediment was deposited on the southeastern flank.

Future work to the north and south of the study area may determine the full extent of extension during episode 2, and if the Salmon basin detachment fault was active at this time. Work in progress by Karl Evans may clarify the pre-Tertiary structure and stratigraphy of the region and lend insights on the role of preexisting structures on the Tertiary deformation of the Salmon basin.

In summary, I show that the Salmon basin has undergone a least four distinct episodes of extension. The largest episode of extension was episode

2, and it was during this episode that the sedimentary rocks of Tendoy were deposited in two distinct subbasins (Pattee Creek subbasin and Flume Creek subbasin). Extension during episode 2 was accommodated along the Agency-Yearian fault, a previously unrecognized regional detachment fault. The Salmon basin detachment is another major regional detachment fault that was identified in the study. Active during episode 3, the Salmon basin detachment fault was responsible for the deposition of the sedimentary rocks of Tendoy. Extensional folds are abundant in the southeast Salmon basin and their occurrence is related to complex geometries of the faults which are responsible for their formation. Overall, this study supports the rift hypothesis in timing, geometry, and location.

REFERENCES CITED

Anderson, A. L., 1956, Geology and mineral resources of the Salmon quadrangle, Lemhi County, Idaho: Idaho Bureau of Mines and Geology Pamphlet 106, 102 p.

Anderson, A. L., 1957, Geology and mineral resources of the Baker Quadrangle, Lemhi County, Idaho: Idaho Bureau of Mines and Geology Pamphlet 112, 71 p.

Anderson, A. L., 1959, Geology and mineral resources of the North Fork Quadrangle, Lemhi County, Idaho: Idaho Bureau of Mines and Geology Pamphlet 118, 92 p.

Anderson, A. L., 1961, Geology and mineral resources of the Lemhi Quadrangle, Lemhi County, Idaho: Idaho Bureau of Mines and Geology Pamphlet 124, 111 p.

Armstrong, R. L., 1975, The geochronometry of Idaho: Isochron West, v. 14, p. 1-50.

Axelrod, D. I., 1968, Tertiary floras and topographic histrory of the Snake River Basin, Idaho: Geological Society of America Bulletin, v. 79, p. 713-734.

Axelrod, D. I., 1998, The Oligocene Haynes Creek Flora of Eastern Idaho: Universtiy of California Publications Geological Sciences, v. 143, 99 p.

Bankey, V., and Kleinkopf, M. D., 1988, Boulder gravity anomaly map and four derivative maps of Idaho: U.S. Geological Survey Geophysical Investigations Map GP-978, scale1: 1,000,000, 3 sheets.

Buck, W. R., 1988, Flextural rotation of normal faults: Tectonics, v. 7, p. 959-794

Burchfiel, B. C., Cowen, D. S., and Davis, G. A., 1992, Tectonic overview of the Cordilleran orogen in western United States, *in* Burchfield, B. C., Zoback, M. L., and Lipman, P. W., eds.,The Geology of North America, v. G-3, The Cordilleran Orogen: Conterminous U.S., Geological Society of America, Boulder Colorado, p. 407-480.

Constenius, K. N., 1996, Late Paleogene extensional collapse of the Cordilleran foreland fold and thrust belt: Geological Society of America Bulletin, v. 108, p. 20-39.

Crone, A. J., and Haller, K. M., 1991, Segmentation and coseismic behavior of Basin and Range normal faults: Examples from east-central Idaho and southwestern Montana, U.S.A.: Journal of Structural Geology, v. 13, p. 151-164.

Cooke, M., and Pollard, D., 1997, Bedding plane slip in the initial stages of fault-related folding: Journal of Structural Geology, v. 19, p. 567-581.

Davis, G. H., and Reynolds, S. J., 1996, Structural geology of rocks and regions: New York, John Wiley and Sons, Inc., 532 p.

Evans, K. V., 1981, Geology and geochronology of the eastern Salmon River Mountains, Idaho, and implications for regional Precambrian tectonics [Ph.D. Diss.]: University Park, Pennsylvania State University, 179 p.

Evans, K., and Zartman, R. E., 1988, Early Paleozoic alkalic plutonism in east-central Idaho: Geological Society of America Bulletin, v. 100, p. 1981-1987.

Evans, K. V., and Zartman, R. E., 1990, U-TH-Pb- and Rb-Sr geochronology of middle Proterozoic granite and augen gneiss, Salmon River Mountains east-central Idaho: Geological Society of America Bulletin, v. 102, p. 63-73

Fisher, F. S., McIntyre, D. H., and Johnson, K. M., 1992, Geological map of the Challis 1°x2° Quadrangle, Idaho: U. S. Geological Survey I-1819, 39 p.

Friedmann, S. J., and Burbank, D. W., 1995, Rift basins and supradetachment basins: Intracontinental extensional end-members: Basin Research, v. 7, p. 109-127.

Fritz, W. J., and Harrison S., 1985, Early Tertiary volcaniclastic deposits of the northern Rocky Mountains, *in* Flores, R. M., and Kaplan, S. S., ed., Cenozoic paleogeography of the West Central U. S.: Denver, Colorado, Rocky Mountain Section SEPM p. 383-402.

Fritz, W. J., and Sears, J. W., 1993, Tectonics of the Yellowstone hotspot wake in southwestern Montana: Geology, v. 21, p. 427-430

Hansen, P. M., 1983, Structures and stratigraphy of the Lemhi Pass Area, Beaverhead Range, southwest Montana and east-central Idaho [M. S. thesis]: University Park, Pennsylvania State University 112 p.

Harlan, S. S., Geissman, J. W., Lageson, D. R., and Snee, L. W., 1988, Paleomagnetic and isotopic dating of thrust-belt deformation along the eastern edge of the Helena salient, northern Crazy Mountains Basin, Montana: Geologic Society of America Bulletin, v. 100, p. 492-499.

Harrison, S., 1985, Sedimentology of Tertiary rocks near Salmon Idaho [Ph.D. dissertation]: Missoula,University of Montana 175 p.

Janecke, S. U., 1992, Kinematics and timing of three superposed extensional systems, east-central Idaho: Evidence for an Eocene tectonic transition: Tectonics, v. 11, p. 1121-1138.

Janecke, S. U.,1994, Sedimentation and paleogeography of an Eocene to Oligocene rift zone, Idaho and Montana: Geological Society of America Bulletin, v. 106, p. 1083-1095.

Janecke, S. U. 1995, Eocene to Oligocene half grabens of east-central Idaho: Structure, Stratigraphy, Age, and Tectonic: Northwest Geology, v. 24, p. 159-199.

Janecke, S. U., and Snee, L. W., 1993, Timing and episodicity of Middle Eocene volcanism and onset of conglomerate deposition, Idaho: Journal of Geology, v. 101, p. 603-621.

Janecke, S. U., M'Gonigle, J. W., MacIntosh, W. C., VanDenburg, C. J., Perry, W. J. Jr., Good, S. C. and Nichols, R, 1996a, Sedimentation patterns in the Muddy Creek, Medicine Lodge/Horse Prairie and Grasshopper supra-detachment basins, MT: Geological Society of America Abstracts with Programs, v. 28, no. 7, p. 444.

Janecke, S. U., Perry, W. J. and M'Gonigle, 1996b, Scale-dependent reactivation of pre-existing structures by an Eocene-Oligocene detachment fault, southwestern Montana: Geological Society of America Abstracts with Programs, Cordilleran Section, v. 28, p. 78.

Janecke, S. U., McIntosh, W., and Good, S., in press, Structure and stratigraphy of an Eocene-Oligocene supra-detachment basin, Muddy Creek half grabben, southwest Montana: Testing supradetachment basin models: Basin Research.

Janecke, S. U., VanDenburg, C. J., and Blankenau, J. J., 1998, Geometry, mechanisms, and significance of extensional folds from examples in the Rocky Mountain Basin and Range provence, U.S.A.: Journal of Structural Geology, v. 20, p. 841-856.

John, B. E., 1987, Geometry and evolution of a mid-crustal extensional fault system: Chemehuevi Mountains, southeastern California: Continental Extensional Tectonics, v. 28, p. 313-336.

Kilroy, K. C., 1984, $^{40}Ar/^{39}Ar$ geochronology and structural relationships of some intermediate intrusions in the northern Beaverhead Mountains, Idaho-Montana: Geological Society of America Abstracts with Programs, v. 16, no. 4, p. 126.

Leeder, M. R., and Gawthorpe, R. L., 1987, Sedimentary models for extensional tilt-block/half-graben basins, *in* Coward, M. P., Dewy, J. F., and Hancock, P. L., eds., Continental extensional tectonics: Geological Society of London, Special Publication No. 28, p. 139-152.

Link, P. K., Christie-Blick, N., Devlin, W. J., Elston, D. P., Horodyski, R. J., Levy, M., Miller, J. M. G., Pearson, R. C., Prave, A., Stewart, J. H., Winston, D. , Wright, L. A., and Wrucke, C. T., 1993, Middle and late Proterozoic stratified rocks of the western U. S. Cordillera, Colorado Plateau, and Basin and Range provence, *in* Reed, J. C., Jr., Bickford,

M. E., Houston, R. S., Link, P. K., Rankin, D. W., Sims, P. K., and Van Schmus, W. R., eds., Precambrian: Conterminous U. S.: The Geology of North America: Boulder, Colorado, Geological Society of America, p. 463-595.

Liu, M., and Shen, Y., 1998, Crustal collapse, mantle upwelling, and Cenozoic extension in the North American Cordillera: Tectonics, v. 17, p. 311-321.

McCafferty, A. E., 1995, Assessing the presence of a buried meteor impact using geophysical data, south central Idaho [M. S. Thesis]: Golden, Colorado School of Mines, 224 p.

McClay, K. R., 1989, Physical models of structural styles during extension, *in* A. J., and Balkwill, H. R., eds., Extensional tectonics and stratigrahphy of the North Atlantic margins, Tankard: American Association of Petroleum Geologists Memoir 46, p. 95-110.

McIntyre, D. H., Ekren, E. D., and Hardyman, R. F., 1982, Stratigraphic and structural framework of the Challis volcanic rocks in the eastern half of the Challis 1° x 2° quadrangle, Idaho, *in* Bonnichsen, B. and Breckenridge, R. M., eds., Cenozoic geology of Idaho: Idaho Bureau of Mines and Geology Bulletin 26, p. 3-22.

M'Gonigle, J. W., and Dalrymple, G. B., 1993, $^{40}Ar/^{39}Ar$ ages of Challis volcanic rocks and the initiation of Tertiary sedimentary basins in southwestern Montana: Mountain Geologist, v. 30, p. 112-118.

M'Gonigle, J. W., and Dalrymple, G. B., 1996, $^{40}Ar/^{39}Ar$ ages of some Challis volcanic group rocks and the initiation of Tertiary sedimentary

basins in southwestern Montana: U.S. Geological Survey Bulletin 2132, 17 p.

M'Gonigle, J. W., Kirschbaum, M. A., and Weaver, J. N., 1991, Geologic map of the Hansen Ranch quadrangle, Beaverhead County, southwest Montana: U.S. Geological Survey Quadrangle Map GQ-1704, scale 1:24,000.

Patton III, T. L., 1984, Normal-fault and fold development in sedimentary rocks above a preexisting basement normal fault [Ph.D. diss.]: College Station, Texas A&M University, 224 p.

Patton III, T. L., and Fletcher, R. C., 1995, Mathematical block-motion model for deformation of a layer above a buried fault of arbitrary dip and sense of slip: Journal of Structural Geology, v. 17, p. 1455-1472.

Perry, W. J. Jr., and M'Gonigle, J. W., 1995, Neogene extensional events, northern Tendoy Mountains and adjacent Medicine Lodge basin, southwest Montana: Geological Society of America Abstracts with Programs, v. 27, no. 4, p. 51.

Ramsay, J. G., and Huber, M. I., 1987, The techniques of modern structural geology: New York: Academic Press, v. 2, 700 p.

Richins, W. D., Pechmann, J. C., Smith, R. B., Langer, C. J., Goter, S. K., Zollweg, J. E., and King, J. J., 1987, The 1993 Borah Peak Idaho earthquake and its aftershocks: Bulletin of the Seismic Society America, v. 77, p. 694-723.

Ross, C. P., 1962, Stratified rocks in south-central Idaho: Idaho Bureau of Mines and Geology Pamphlet 125, 126 p.

Ross, C. P., 1963, Geology along U.S. highway 93 in Idaho: Idaho Bureau of Mines and Geology Pamphlet 130, 80 p.

Ruppel, E. T., 1975, Precambrian and lower Ordovician rocks in east-central Idaho: U. S. Geological Survey Professional Paper 889, 34 p.

Ruppel, E. T., 1978, Medicine Lodge thrust system, east-central Idaho and south west Montana: U.S. Geological Survey Professional Paper 1031, 23 p.

Ruppel, E. T., 1982, Cenozoic block uplifts in east-central Idaho and southwest Montana: U.S. Geological Survey Professional Paper 1224, 24 p.

Ruppel, E. T., and Lopez, D. A., 1984, The thrust belt in southwest Montana and east-central Idaho: U.S. Geological Survey Professional Paper 889, p. 1-23.

Ruppel, E. T., O'Neil, J. M., and Lopez, D. A., 1993, Geologic map of the Dillon 1°x2° Quadrangle, Idaho and Montana: U.S. Geological Survey Miscellaneous Investigations I-1803-H, scale 1:250,000.

Schlische, R. W., 1996, Geometry and origin of fault-related folds in extensional settings: American Association of Petroleum Geologists Bulletin, v. 79, p. 1661-1678.

Skipp, B., 1987, Basement thrust sheets in the Clearwater orogenic zone, central Idaho and western Montana: Geology, v. 15, p. 220-224.

Skipp, B., 1988, Cordilleran thrust belt and faulted foreland in the Beaverhead Mountains, Idaho and Montana, *in* Schmidt, C. J., and Perry, W. J., Jr., eds., Interaction of the Rocky Mountain foreland and

Cordilleran thrust belt: Geological Society of America Memoir 171, p. 237-266.

Snider, L. G., 1995, Stratigraphic framework, geochemistry, geochronology, and eruptive styles of Eocene volcanic rocks in the White Knob Mountains area, southeastern Challis volcanic field, central Idaho [Master's thesis]: Pocatello, Idaho State University, p. 212.

Staatz, M. H., 1979, Geology and mineral resources of the Lemhi Pass Thorium District, Idaho and Montana: U. S. Geological Survey Professional Paper 1049-A, 90 p.

Tucker, D. R., 1975, Stratigraphy and structure of Precambrian Y (Belt?) metasedimentary rocks and associated rocks, Goldstone Mountains quadrangle, Lemhi County Idaho, and Beaverhead County, Montana: Miami University 245 p.

Tucker, D. R., 1983, Structural analysis of a detachment zone in east-central Idaho: Northwest Geology, v. 12, p. 57-62.

Tucker, D. R., and Birdseye, R. U., 1989, An Eocene synvolcanic alluvial fan complex in east-central Idaho: Stratigraphic relationships and structural implications: The Mountain Geologist, v. 6, p. 23-30.

Twiss, R. J., and Moores, E. M., 1992, Structural geology: New York, W. H. Freeman and Company, 532 p.

Tysdal, R. G., 1996a, Geologic map of the Lem Peak quadrangle, Lemhi County, Idaho: U.S. Geological Survey Quadrangle Map GQ-1777, scale 1:24,000.

Tysdal, R. G., 1996b, Geologic map of adjacent areas in the Hayden Creek and Mogg Mountain quadrangles, Lemhi County, Idaho: U.S. Geological Survey Miscellaneous Investigations Series Map I-2563, scale 1:24,000.

Tysdal, R. G., and Moye, F. J., 1996, Geologic map of the Allison Creek quadrangle, Lemhi County, Idaho: U.S. Geological Survey Quadrangle Map GQ-1778, scale 1:24,000.

VanDenburg, C. J., 1997, Tectonic and paleogeographic evolution of the Horse Prairie half graben, southwest Montana [Master's thesis]: Logan, Utah State University, 152 p.

VanDenburg, C. J., and Janecke, S. U., 1996, Tertiary paleogeographic and tectonic evolution of the upper Horse Prairie Basin, southwest Montana: Geology of the crook in the Snake River Plain, Twin Falls and vicinity, Idaho p. 122-123.

VanDenburg, C. J., Janecke, S. U., and Nichols, R., 1996, Multiple episodes of Tertiary extension in the west-central Horse Prairie Basin, southwestern Montana: Geological Society of America Abstracts with Programs, Cordilleran Section, v. 28, p. 120.

VanDenburg, C. J., Janecke, S. U., and McIntosh, W. C., 1998, Three-dimensional strain produced by >50 m. y. of episodic extension, Horse Prairie rift basin, SW Montana, U.S.A., Journal of Structural Geology, v. 20, p. 1747-1767.

Wernicke, B. P., and Axen, G. J., 1988, On the role of isostasy in the evolution of normal fault systems: Geology, v. 16, p. 848-851.

Wolfe, J. A., and Wehr, W., 1987, Middle Eocene dicotyledonous plants from Republic norteastern Washington: U. S. Geological Survey Bulletin 1597, 25 p.

Xiao, H., and Suppe, J., 1992, Origin of rollover: American Association of Petroleum Geologists Bulletin, v. 76, p. 509-529.

APPENDICES

Appendex A.

Age spectrum graphs

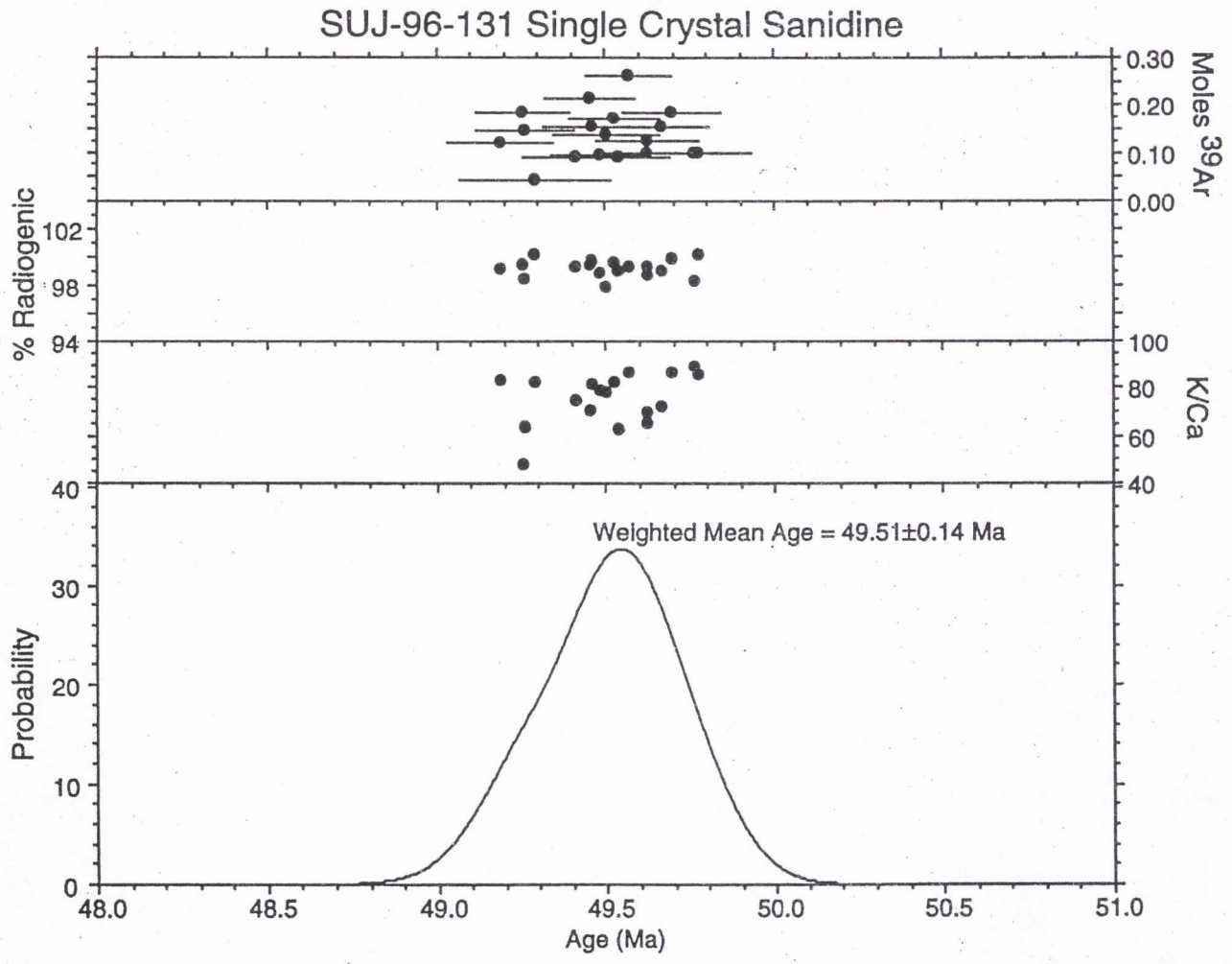

Figure A1. Age spectrum graph of sample SUJ96-131. Sample has a weighted mean age of 49.51±0.14 Ma.

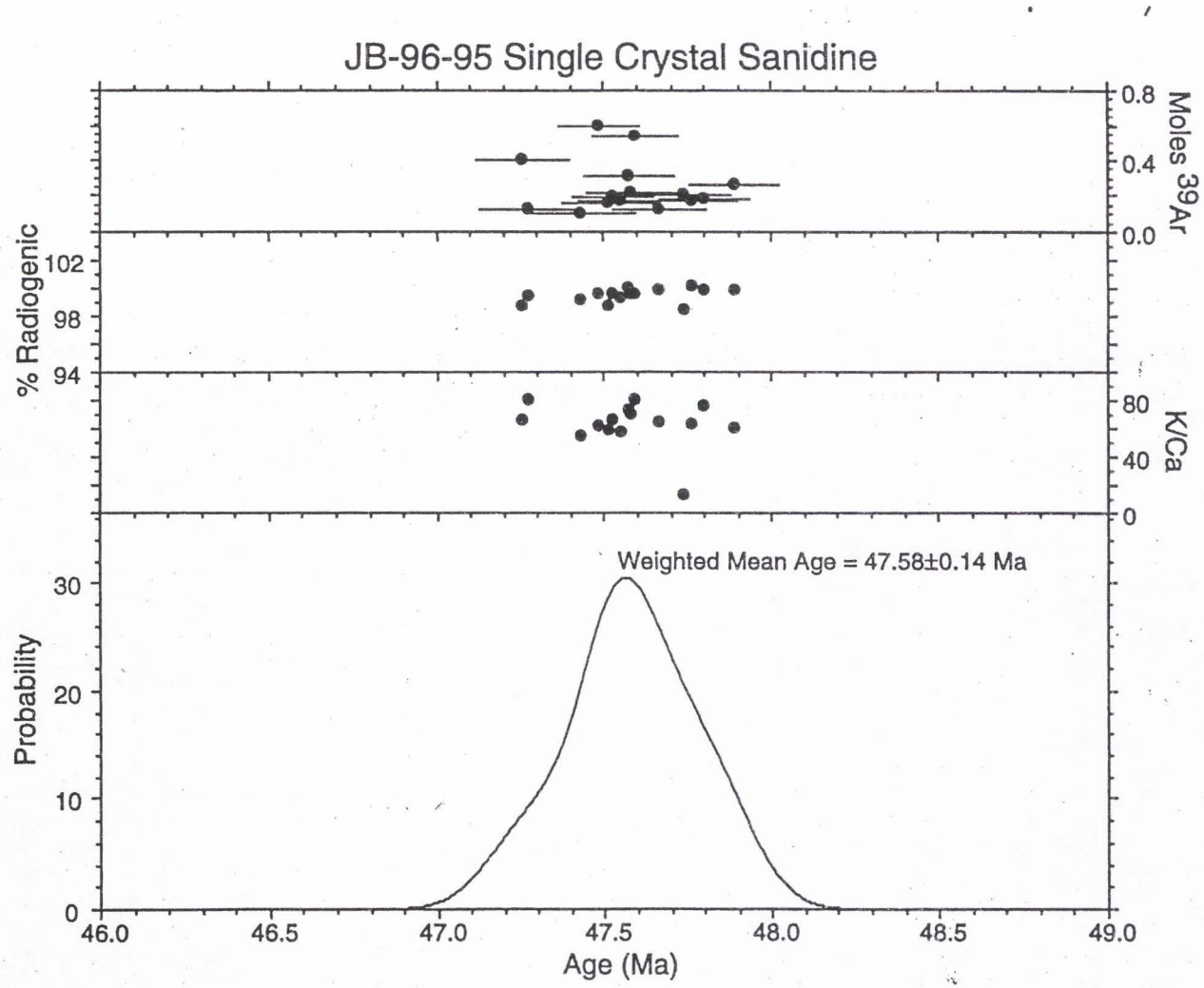

Figure A2. Age spectrum graph of sample JB96-95(Tcr). Sample has a weighted mean age of 47.58±0.14 Ma.

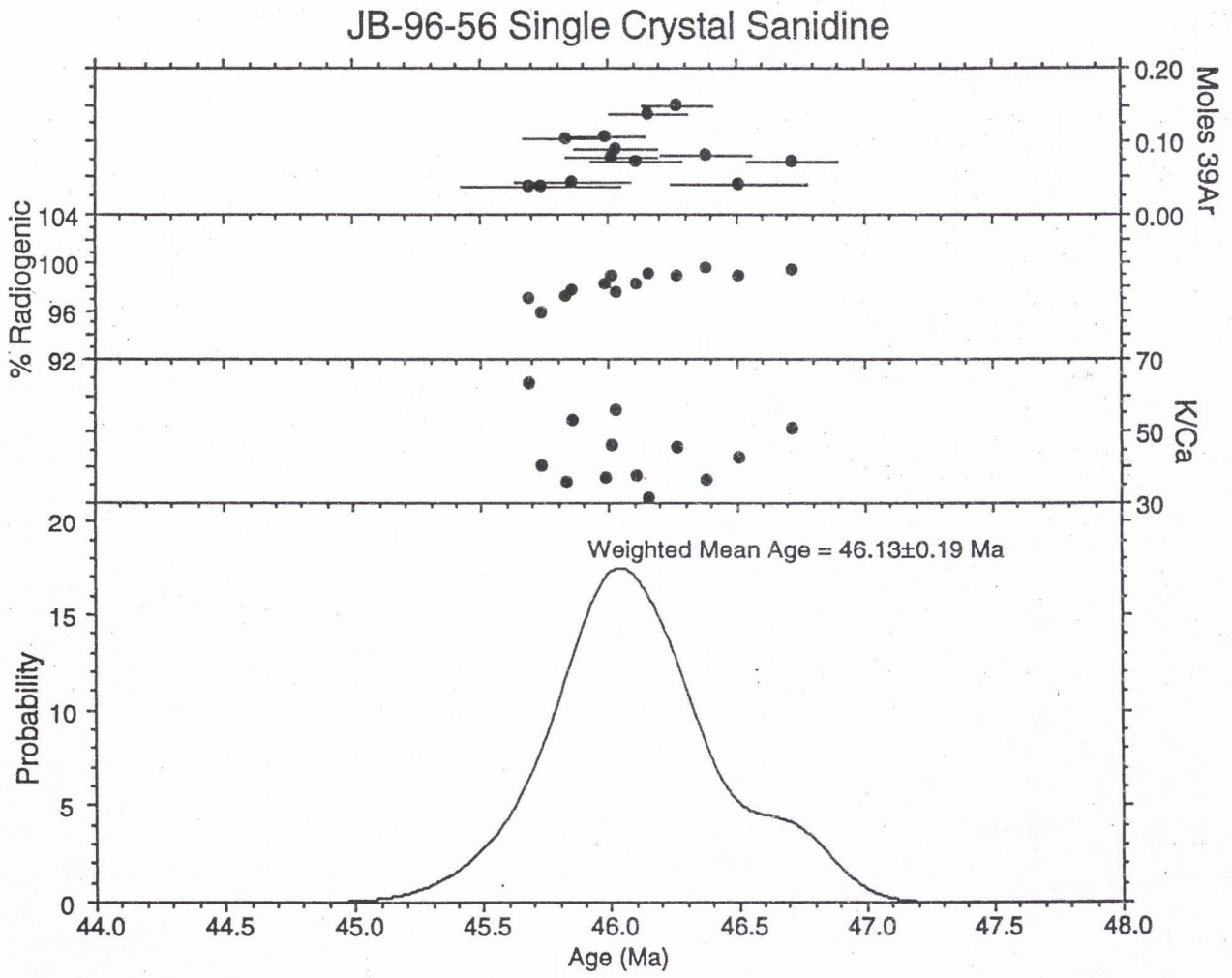

Figure A3. Age spectrum graph of sample JB96-56(Tqs). Sample has a weighted mean age of 46.13±0.19 Ma.

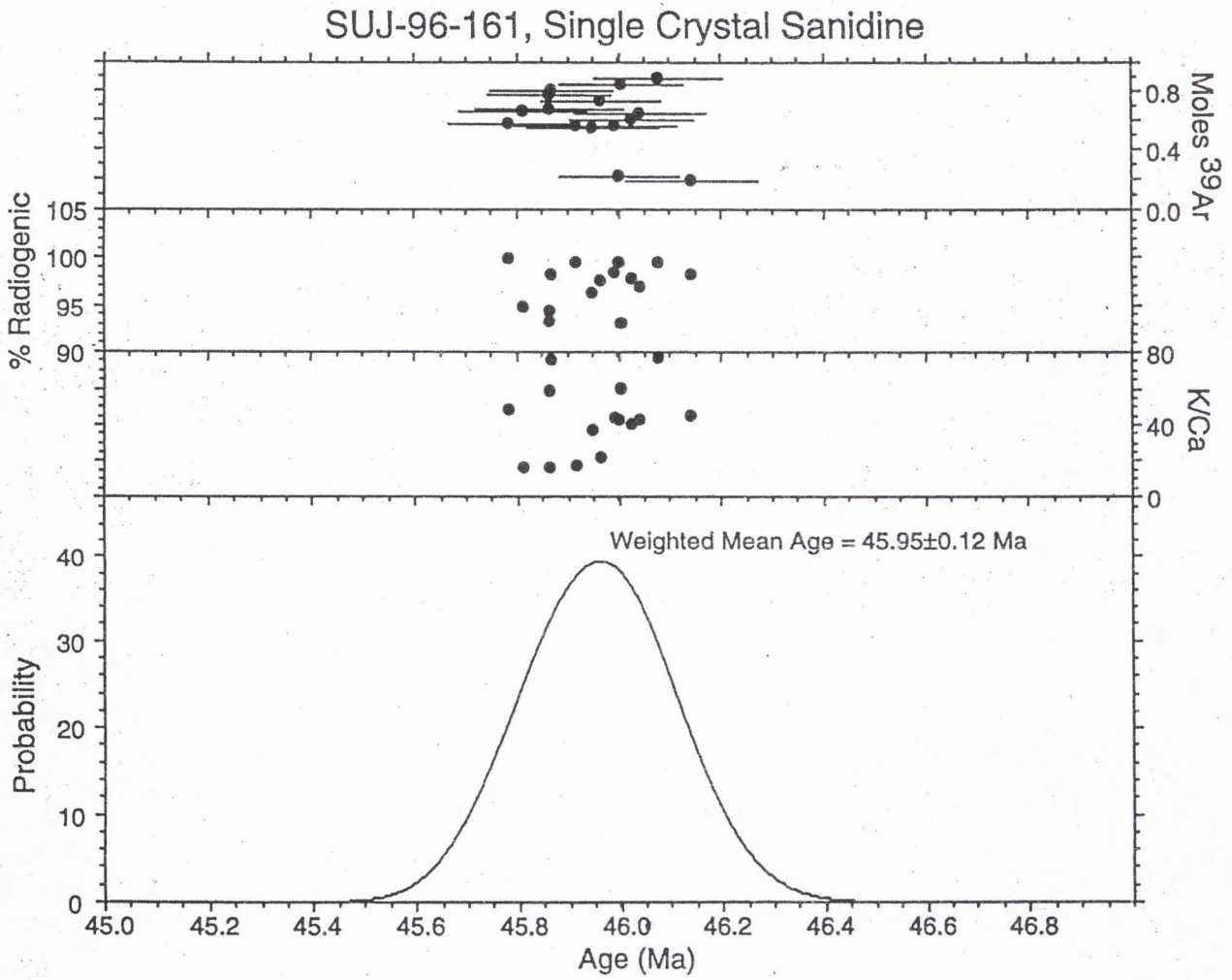

Figure A4. Age spectrum graph of sample SUJ69-161 (Tqs). Sample has a weighted mean age of 45.95±0.12 Ma.

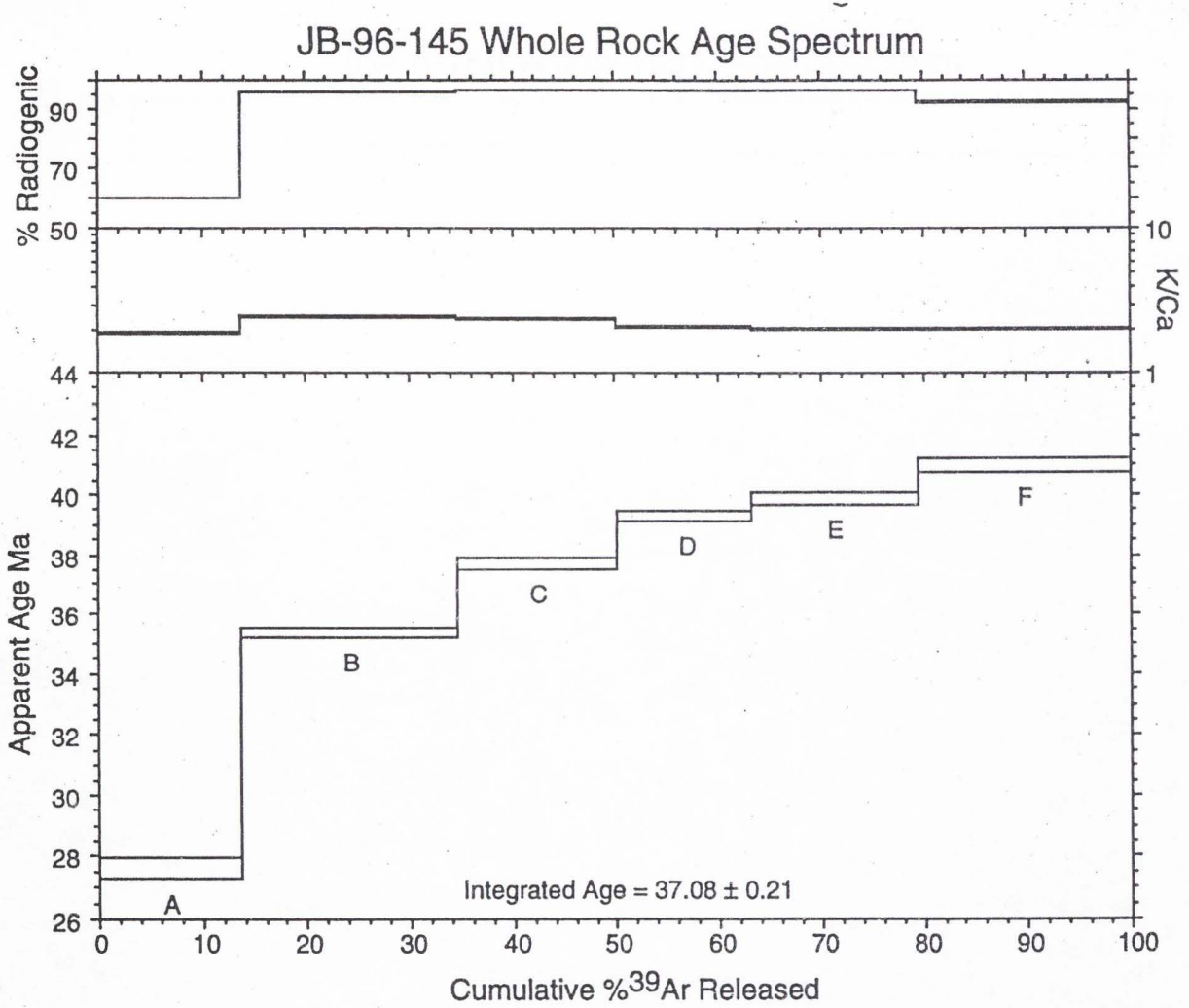

Figure A5. Age spectrum graph of sample JB96-145 (Ti). Sample is highly disturbed and has an integrated age of 37.08±0.21 Ma.

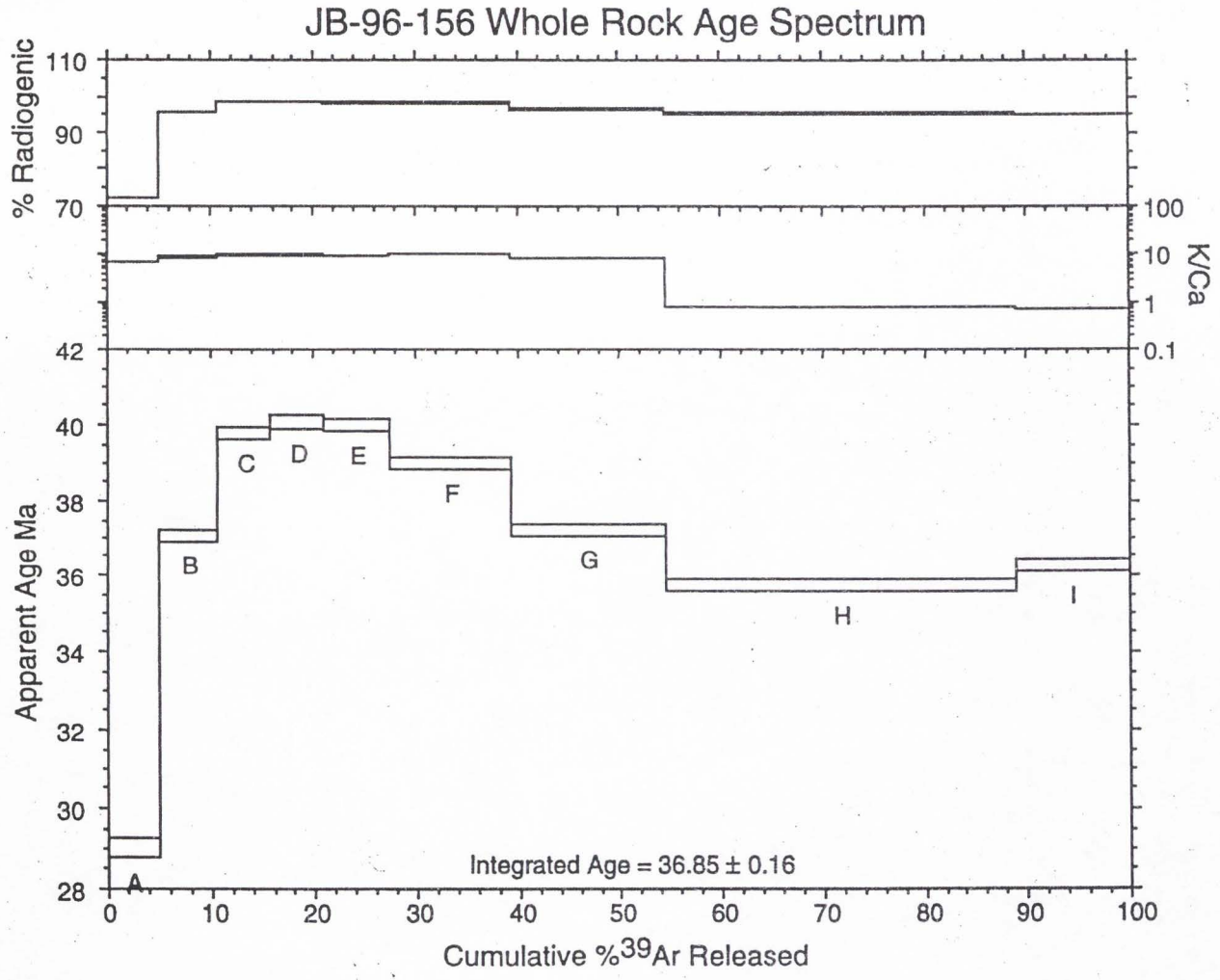

Figure A6. Age spectrum graph of sample JB96-156 (Tl). Sample is highly disturbed and has an integrated age of 36.85±0.16 Ma.

Appendix B

Aerial photographs used in the study

TABLE B1. AERIAL PHOTOGRAPHS USED IN THE STUDY

Flight number	Roll number	Exposures	Project	Agency	Scale	Date
2	13B	1-4	ID-93-AC	BLM	1:23,000	7-28-93
3	10A	1-5	ID-93-AC	BLM	1:23,000	7-29-93
3	11A	5-12	ID-93-AC	BLM	1:23,000	7-29-93
3	11B	1-2	ID-93-AC	BLM	1:23,000	7-29-93
4	10	8-10	ID-93-AC	BLM	1:23,000	7-30-93
18	12B	2-8	ID-93-AC	BLM	1:23,000	7-15-93
18	13A	8-11	ID-93-AC	BLM	1:23,000	7-15-93
18	14A	11-13	ID-93-AC	BLM	1:23,000	7-15-93
589*		240-245	6020 152,86	USDA	1:40,000	9-1-89
689*		7-17	6020 152,86	USDA	1:40,000	9-1-89
689*		240-244	6020 152,86	USDA	1:40,000	9-4-89

* Denotes black and white aerial photographs

Plate 1. Geologic map of the southeastern Salmon Basin, east-central Idaho.

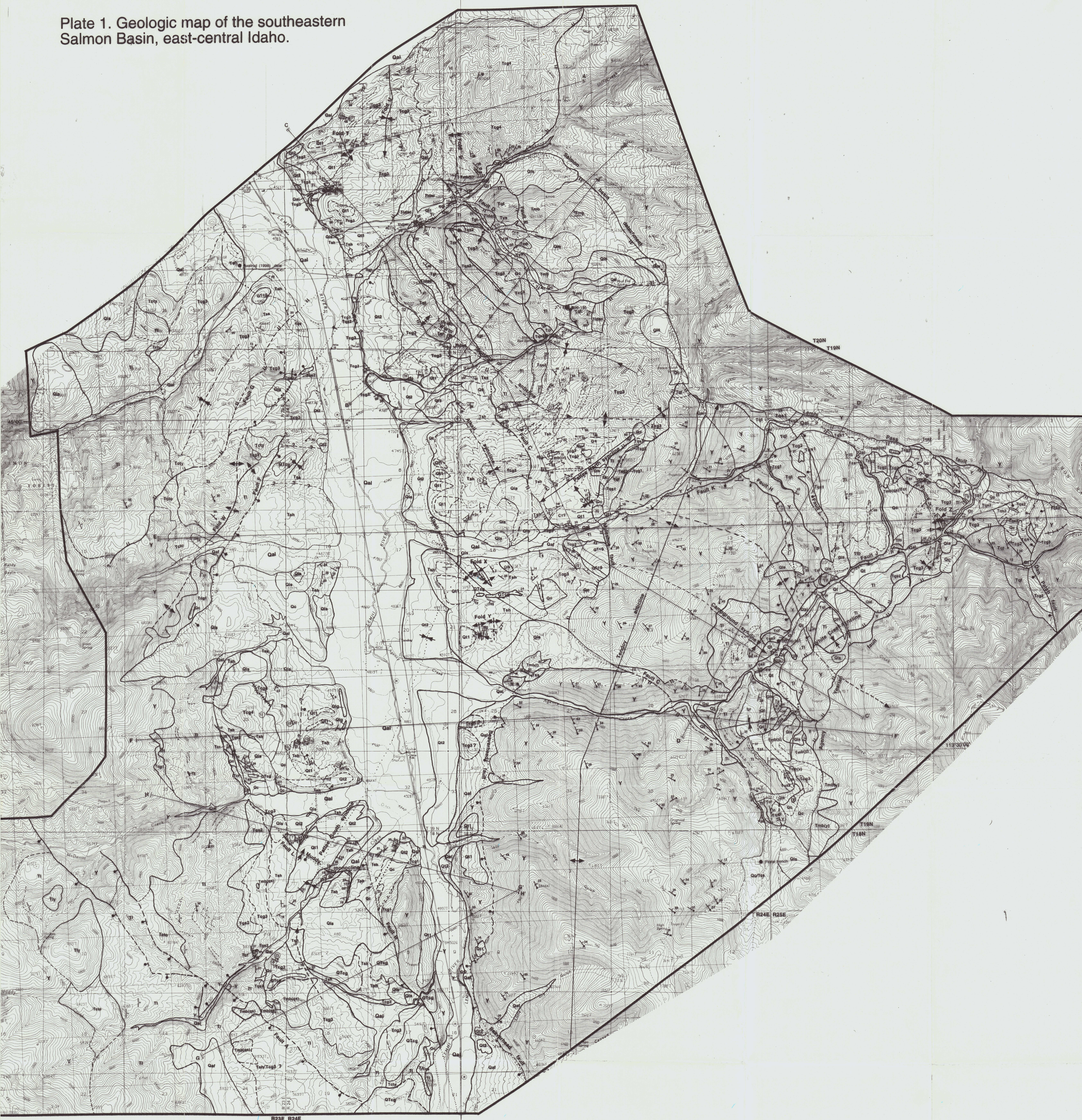

Plate 2. Geologic cross-sections of the Southeastern Salmon basin

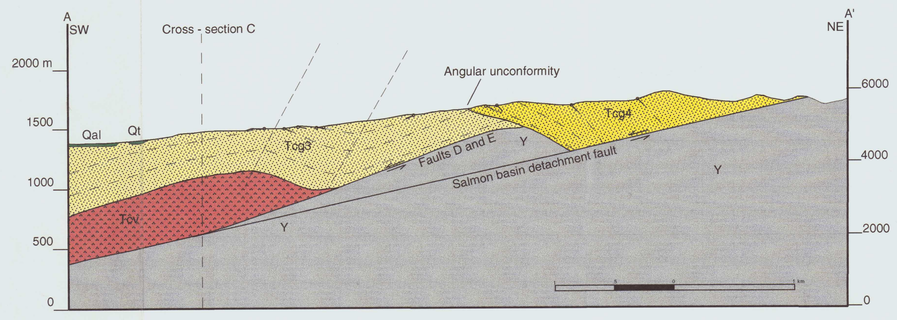

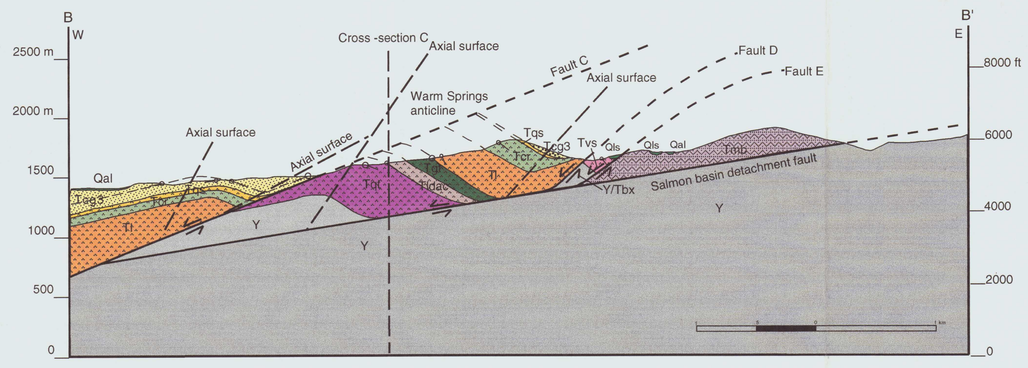

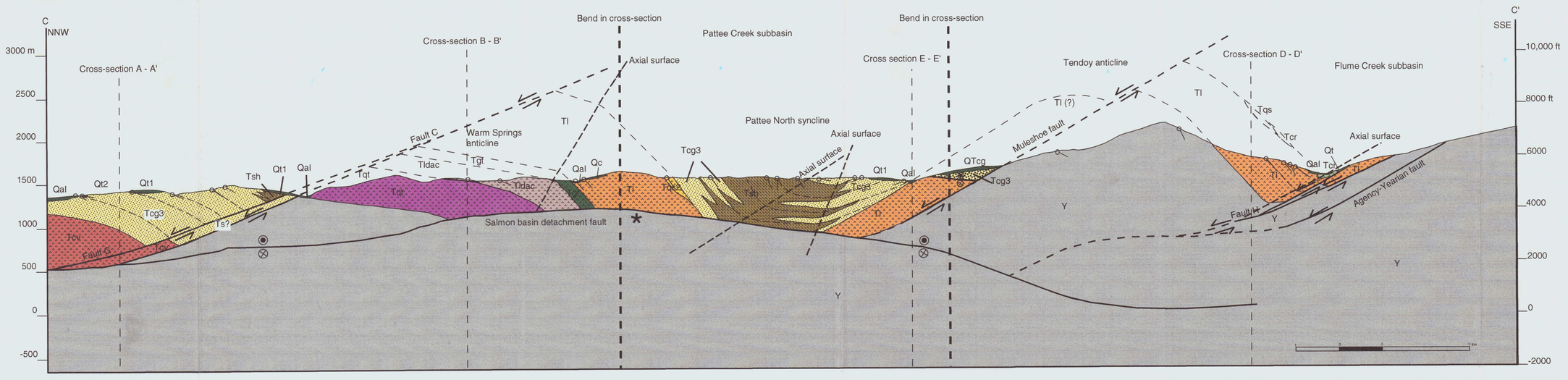

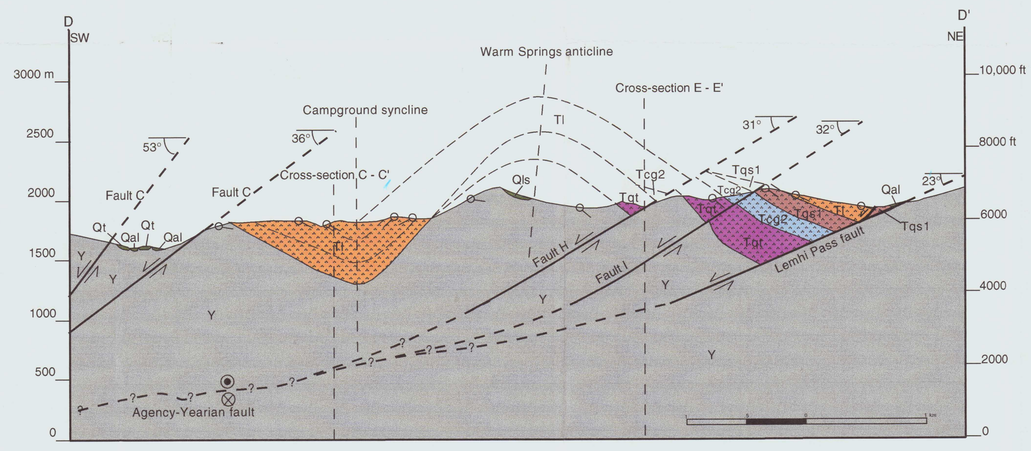

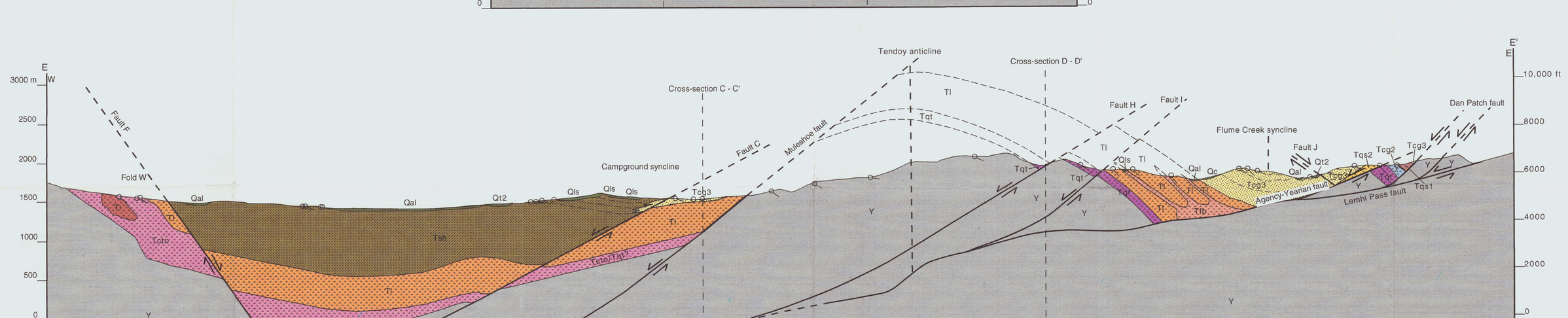

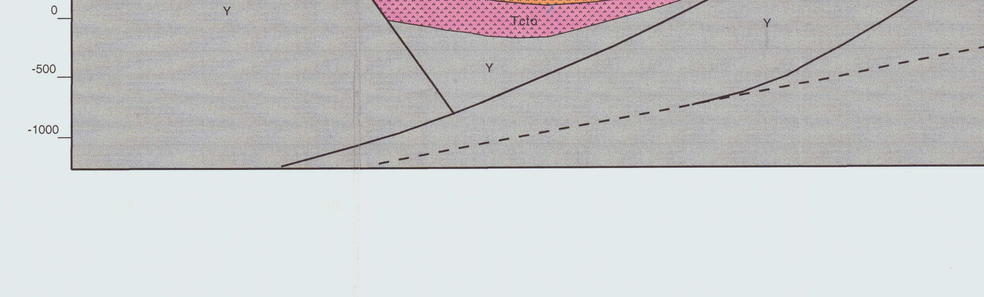

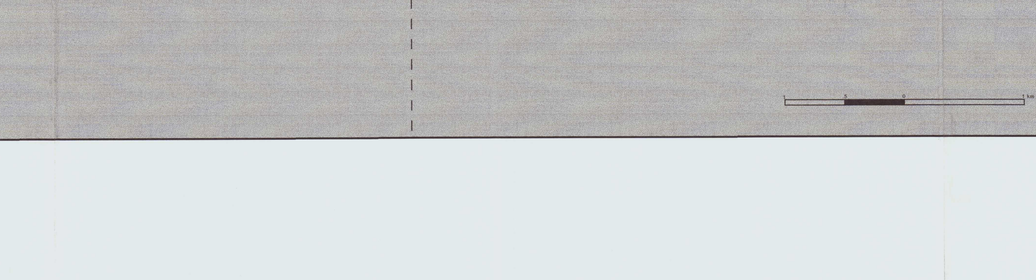

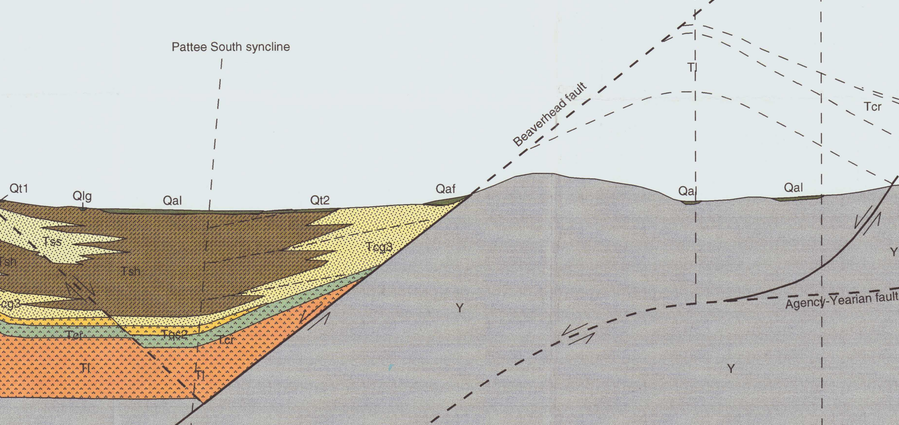

Plate 3. Legend for the geologic map and cross-sections.

Stratigraphy

Quaternary deposits

- Qal — Alluvium
- Qc — Colluvium
- Qt — Terrace of uncertain age
- Qt2 — Youngest Terrace
- Qt1 — Oldest Terrace
- Qls — Landslide Deposit
- QTcg — Quaternary-Tertiary Conglomerate

Sedimentary rocks of Sacajaweja (middle Oligocene (?) to Miocene)

- Tcg4 — Conglomerate of Kenney Creek - cobble to boulder conglomerate

Sedimentary rocks of Tendoy (late middle Eocene to Oligocene)

- Tss — Sandstone - moderate to well-sorted lithic arenite
- Tsh — Shale unit - tan to white tuffaceous shale
- Tcg3 — Middle conglomerate - cobble to boulder, angular to well rounded conglomerate
- Ts — Sediment of Sharky Creek - undifferentiated limestone, bentonite, tuff, and conglomerate
- Tmb(y) — Megabreccia - Megabreccia with fragments of Precambrian quartzite
- Tmb(qs) — Megabreccia - Megabreccia with fragments of quartz-sanidine welded tuff

Challis volcanic group (middle Eocene)

- Tly — Younger Challis lava, undifferentated
- Tcty — Younger Challis tuffs, undifferentiated
- Tqs2 — Younger quartz-sanidine welded tuff - White to white green, or gray green, with euhedral chatoyant sanidine and smoky quartz in a fine ash matrix.
- Tcr — Tuff of Curtis Ranch - White to greenish white tuff containing abundant biotite, and lesser amounts of smoky quartz, plagioclase, and angular volcanic and quartzite lithics. Pumice is abundant to rare.
- Tcs — Challis sandstone - Tan, poorly cemented, coarse-grained volcaniclastic sandstone
- Tt — White tuff - White fine grain biotite tuff.
- Tfb — Flow breccia - Hematitic red to green, flows consisting of subangular lava clasts (< 75 cm), in a angular sand to pebble lava clast and red ash matrix.
- Tl — Lava flows- Black to dark gray-green, or dark brown-black aphanitic to vesicular, or porphyritic andesitic lava flows.
- Tgt — Green tuff - Green to light green biotite tuff, containing abundant euhedral biotite, smoky quartz, minor sanidine (subhedral), and pumice in a white to light green ash matrix. Coarse sections also contains lithics of volcanic clasts (3 mm) and a few quartzite clasts.
- Tldac — Lava/dacite lava - Purple to purple gray, or dark brown dacite and lava flows containing phenocrysts of euhedral biotite, hornblende, and plagioclase along with minor amounts of quartz, and augite(?) in a fine crystalline matrix.
- Tlt — Lithic-rich tuff - White to pinkish white, poorly to moderately welded ash flow tuff containing volcanic and quartzite lithics, along with biotite, and smoky quartz.
- Taf — Air-fall tuff - White to pink, rhythmically layered, fine grained tuff. Present in some areas where the granite-clast conglomerate is absent.
- Tcg2 — Granite-clast conglomerate - Poorly sorted, well rounded, cobble and boulder gravel, dominantly consisting of quartzite clasts and lesser amounts of large boulders (<2.5m) of porphyritic rapakivi granite.
- Tqs1 — Older quartz-sanidine welded tuff - Tan-orange, to light-pink welded tuff containing euhedral to subhedral crystals of sanidine and smoky quartz, along with pumice fragments in a fine crystalline matrix.
- Tqt — Quartzite-bearing ash-flow tuff - White, pinkish-red, white-gray, or pink-gray welded tuff containing abundant angular gray quartzite lithics, and lesser amounts of smoky quartz, and plagioclase. Confined to the Lemhi Pass paleovalley.
- Tcto — Older tuff - Undifferentiated Chalis volcanic tuffs.
- Tcg1 — Basal conglomerate - Sub- to well-rounded cobble to boulder, clast-supported conglomerate, with a fine white to gray ash matrix. Clasts are 100% quartzites.

Pre-Tertiary rocks

- Y — Precambrian metasedimentary rocks - Light gray micaceous and feldspathic quartzites, argillites, and some interbedded siltites.

Intrusions and fault rocks

- Tmb — Megabreccia - Fault breccia from movement along the Salmon basin detachment.
- Ti — Tertiary intrusion - Dark red to gray andesitic intrusion.

Map symbols

- Low-angle normal fault, dashed where uncertain, dotted where concealed. Double tick on downthrown side.
- High-angle normal fault, dashed where uncertain, dotted where concealed. Ball and bar on downthrown side.
- Thrust fault, dashed where uncertain, dotted where concealed. Triangles on upthrown side.
- Anticline; axial arrow indicates plunge direction.
- Syncline; axial arrow indicates plunge direction.
- Monocline
- Lithologic contact dashed where uncertain, dotted where concealed.
- Bedding traces
- Lineament
- A — A' Cross-section location
- Strike and direction of dip of bedding.
- Strike and direction of dip of bedding compiled from Staatz (1979) or Tucker (1975).
- Strike and direction of dip of bedding determined by three point solutions.
- Approximate strike and direction of dip of bedding, dertermined from bedding traces and aerial photographs.
- (1) Sample site for geochronology.
- [1] Pebble count site numbers correspond to sample site numbers in Table 6.

Cross-section symbols

- Fault trace, dashed where uncertain.
- Fault slip direction.
- Fault slip direction of fault coming out of page, dot indicate fault movement out of page, cross indicates fault movement into page.
- Axial surface of folds.
- Apparent dip of beds.

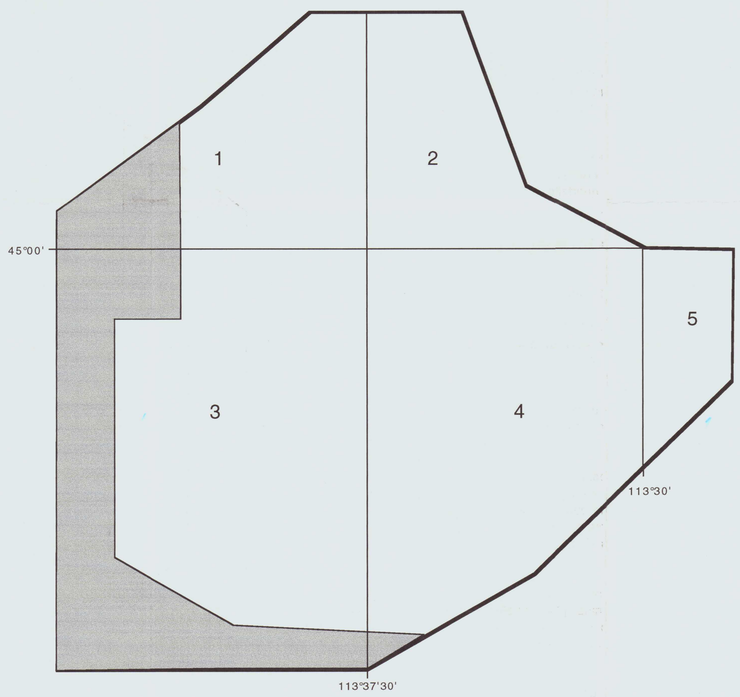

Index topographic bases for plate 1. (1) Baker quadrangle; (2) Goldstone Mountain quadrangle; (3) Tendoy quadrangle; (4) Agency Creek quadrangle; (5) Lemhi Pass quadrangle. Shaded region was mapped on aerial photographs.